Quantum Correlations in Information Theory

Davide Girolami

Thesis submitted to The University of Nottingham
for the degree of Doctor of Philosophy

June 2013

Abstract

The project concerned the study of quantum correlations (QC) in compound systems, i.e. statistical correlations more general than entanglement which are predicted by quantum mechanics but not described in any classical scenario. I aimed to understand the technical and operational properties of the measures of QC, their interplay with entanglement quantifiers and the experimental accessibility.

In the first part of my research path, after having acquired the conceptual and technical rudiments of the project, I provided solutions for some computational issues: I developed analytical and numerical algorithms for calculating bipartite QC in finite dimensional systems. Then, I tackled the problem of the experimental detection of QC. There is no Hermitian operator associated with entanglement measures, nor with QC ones. However, the information encoded in a density matrix is redundant to quantify them, thus the full knowledge of the state is not required to accomplish the task. I reported the first protocol to measure the QC of an unknown state by means of a limited number of measurements, without performing the tomography of the state. My proposal has been implemented experimentally in a NMR (Nuclear Magnetic Resonance) setting.

In the final stage of the project, I explored the foundational and operational merits of QC. I showed that the QC shared by two subsystems yield a genuinely quantum kind of uncertainty on single local observables. The result is a promising evidence of the potential exploitability of separable (unentangled) states for quantum metrology in noisy conditions.

Writing is good, Thinking is better

Cleverness is good, Patience is better

Acknowledgements

There is an endless list of people to thank, blame on me as I am going to forget some of them, I hope they will forgive me if one day will read these lines.

A special thank to my family, whose support has been and will always be essential.

I thank the crew of the School of Maths of Nottingham, an ideal place to study and develop science. I thank Slava Belavkin, who sadly left us last November. He offered me the opportunity to start this marvellous adventure and then shared with me some of his mastery of the quantum world. It has been an honour and a pleasure to be his student. I thank Madalin Guta for the valuable discussions during the group meetings. I also thank all my collaborators and whoever has talked about quantum physics with me, in particular Tommaso Tufarelli and Luis Correa. I enjoyed their friendship and sincerely admired their scientific brilliance and hard-working attitude. Also, I thank Stephen Scully, Michael White, Christina Cerny, Sebastian Hugot and Antony Lee, who made funnier the in-office but off-working hours. A thank has to be addressed to the many housemates I had in last three years.

There is a person who must be thanked for all the reasons mentioned above. Thanks Gerardo for everything, from the emails (and telephone calls!) in the middle of the night to our discussions about every single word of a paper, from our sloppy chats of friday afternoon to the gentle patience you showed whenever I did not get the point. Now I can tell that you were right, sometimes!

Finally, the most important thank to Alexandra, who makes my life the best I could wish for. This work is dedicated to her.

Contents

List of Figures

List of Tables

CHAPTER 0

Introduction and Scope

Quantum Mechanics is one of the most precious scientific gifts of the last century and the theoretical background of an impressive range of applications and peculiar phenomena in complex systems. Notwithstanding, it manifests in many complementary, sometimes elusive ways, so that a popular slogan claims that "nobody understands Quantum Mechanics"[1]. Yet, we are able to advance well-posed questions on it. For example, one of the most intriguing challenges for quantum physicists is to characterize the boundary between the classical and quantum worlds, finding out when and how quantum effects play a role in describing physical phenomena or enhancing the performance of information and communication tasks. The potential results of a better understanding of the transition between the classical and quantum regimes, and of how to harness quantum properties of macroscopic systems, would be tremendous. First, to make quantum information processing feasible, by exploiting the superposition principle to improve our ability to store, manipulate and transmit data. Also, to reach a deeper knowledge of the structure and behaviour of biological processes and complex systems overall.

The burgeoning field of Quantum Information provides the tools for challenging the resilience of the quantum postulates and, at the same time, for pushing technology over its inherent limits. The genuinely quantum speed-up in information processing and in energy transport mechanisms is believed to be due to

[1] Attributed to R. P. Feynman.

quantum entanglement, i.e. peculiar correlations described by quantum laws which are shared, for example, between the sender and the receiver of a message. However, it has been recently shown that entanglement is not the most general form of quantum correlations. Even unentangled states of compound systems have a quantum character, as their subsystems can share truly quantum correlations. This is an interesting result, as creation and protection of entanglement could be a too demanding condition to be satisfied in macroscopic biological systems and for engineering appliances, which have to deal with high temperature and high disorder regimes. Indeed, entanglement is typically fragile whenever the systems under scrutiny undergoes the detrimental interaction of an external environment. Therefore, it sounds compelling to verify the feasibility of large scale quantum technologies by making use of alternative resources, and to identify the roots of the tangible signatures of quantumness at the macroscopic scale.

The project aimed to investigate the theoretical framework of quantum correlations (QC[2]), devise how we may take advantage from them and benchmark their experimental accessibility and usefulness for technological applications. In particular, this thesis consists of the most of my contributions to research on bipartite QC in finite dimensional composite systems. Needless to say, I benefited from fruitful collaborations with senior fellows and students.

The manuscript is organized in chapters. The first page of each chapter outlines its content, while the last section summarises its main results. In the body of the work, the narrative voice is "we", as I repute it to be more suitable for the scientific exposition. The content of each chapter is the following:

- Chapter 1 is merely introductory. First, I review basic facts and terminology of Quantum Mechanics and Quantum Information. Then, I introduce and motivate the concepts of entanglement, classical correlations and QC. I clarify what these terms mean and fix notations and terminology adopted in the

[2]In this work, I call *quantum correlations* the statistical correlations not described by classical physics (entanglement included), and use the acronym QC whenever I specifically refer to general quantum correlations, but not to entanglement.

body of the work.

- In Chapter 2, I detail and exploit the theoretical toolbox for calculating bipartite QC in relevant case studies of finite dimensional systems. Essentially, I report the results obtained in the first part of my PhD.
- Chapter 3 is about my attempt, in spite of the theoretical flavour of the project, to answer to the quest for measuring the QC of an unknown state in laboratory. I both developed the theory and made the theoretical analysis of the experiment, which has been implemented in a Nuclear Magnetic Resonance system.
- A more mature, alternative point of view on QC is provided in Chapter 4. I highlight the interplay between global quantum effects as QC, and local ones, specifically the quantum uncertainty on *single* observables. Apart from the foundational relevance of the result, this suggests to exploit QC to guarantee the accuracy of phase estimation protocols.
- Finally, in Chapter 5 I briefly summarise the original contributions of the thesis and outline some of the potential future lines of investigations on QC which meet my personal interest. It is a collection of pilot studies, unpublished material and random discussions, which passed the stage of "sparse thoughts" but, to date, have not reached yet the stand of proper research work.

The most of the material presented here has been reported in various forms in these papers:

[DG1] D. Girolami, M. Paternostro, and G. Adesso, Faithful non-classicality indicators and extremal quantum correlations in two-qubit states, Journal of Physics A: Mathematical and Theoretical 44, 352002, (2011)

[DG2] D. Girolami and G. Adesso, Quantum discord for general two-qubit states: Analytical progress, Physical Review A 83, 052108, (2011)

[DG3] D. Girolami and G. Adesso, Interplay between computable measures of entanglement and other quantum correlations, Physical Review A 84, 052110

(2011)

[DG4] D. Girolami and G. Adesso, Observable Measure of Bipartite Quantum Correlations, Physical Review Letters 108, 150403 (2012)

[DG5] D. Girolami, R. Vasile, and G. Adesso, Theoretical insights on measuring quantum correlations, International Journal of Modern Physics B 27, 1345020 (2012)

[DG6] I. Almeida-Silva, D. Girolami, R. Auccaise, R. S. Sarthour, I. S. Oliveira, T. J. Bonagamba, E. R. deAzevedo, D. O. Soares-Pinto, and G. Adesso, Measuring Bipartite Quantum Correlations of an Unknown State, Physical Review Letters 110, 140501 (2013)

[DG7] D. Girolami, T. Tufarelli and G. Adesso, Quantum uncertainty on single observables, arXiv:1212.2214, submitted to Physical Review Letters.

During my PhD, I have also worked on the transposition to continuous variables and hybrid systems (qubits *vs* harmonic oscillators), in particular to Gaussian states of continuous variable systems (which are arguably the most relevant ones for quantum information processing), of the techniques developed for qudits. I furthermore co-authored a "News & Views" article on quantum optics experiments. My contributions on these topics are NOT included in the thesis, but have been published in:

[DG8] L. Mista, R. Tatham, D. Girolami, N. Korolkova, and G. Adesso, Measurement-induced disturbances and nonclassical correlations of Gaussian states, Physical Review A 83, 042325, (2011)

[DG9] G. Adesso and D. Girolami, Gaussian geometric discord, International Journal of Quantum Information 9, 1773 (2011)

[DG10] T. Tufarelli, D. Girolami, R. Vasile, S. Bose, and G. Adesso, Quantum resources for hybrid communication via qubit-oscillator states, Physical Review A 86, 052326 (20012)

[DG11] G. Adesso, S. Ragy, and D. Girolami, Continuous variable methods in rel-

ativistic quantum information: Characterisation of quantum and classical correlations of scalar field modes in non-inertial frames, Classical and Quantum Gravity 29, 224002 (2012)

[DG12] G. Adesso, D. Girolami, and A. Serafini, Measuring Gaussian quantum information and correlations using the Renyi entropy of order 2, Physical Review Letters 109, 190502 (2012)

[DG13] G. Adesso and D. Girolami, Quantum optics: Wave - particle superposition, Nature Photonics - News and Views 6, 579 (2012)

[DG14] T. Tufarelli, T. MacLean, D. Girolami, R. Vasile, and G. Adesso, The geometric approach to quantum correlations: Computability versus reliability, arXiv:1301.3526, submitted to Journal of Physics A: Mathematical and Theoretical.

All the numerical simulations and plots have been generated by employing the software *Mathematica* of the Wolfram Research.

Declaration of originality

I declare that the present thesis has been written by me and its content is my own work.

CHAPTER 1

Introduction to Quantum Correlations

Here I introduce the concept of general quantum correlations (QC), which has represented the theoretical substrate of my research project. The chapter is divided in three parts. First, I review some basic ingredients of Quantum Mechanics which will be useful in the following chapters. I do not refer to any specific reference, while my point of view has been certainly influenced by some of the countless excellent books on the topic, as [15, 16]. Then, I present the young and rapidly evolving discipline of Quantum Information. The reader should refer to the monumental opera of Nielsen and Chuang for a complete perspective [17]. Finally, I discuss the characterisation of quantum states of compound systems in entangled, unentangled but quantum correlated, and classical states. I show the QC of a state can be measured by the quantum discord. Some explicit examples are provided to clarify the main points.

1.1 Basics of Quantum Mechanics

1.1.1 States and Observables

We call *physical system* the portion of Universe we want to describe and refer to the *environment* as one or more other systems interacting with it. A *state* of the system is the available information on the properties of the system which are of our interest. Such information is accessible by measuring the value of appropriate physical quantities, called *observables*. For example, let us consider a system given by one particle: it may be useful to know its position in space. If this is all the information we wish to have, we just need to measure the value of the three observables which represent the spatial coordinates.

It is possible to associate mathematical objects with these physical concepts. In Quantum Mechanics, the conventional Dirac notation is largely employed, because it is surprisingly simple yet insightful. A state is represented by a complex unitary ray $|\psi\rangle$ in a complex vector space equipped with an inner product, which can be a finite as well as an infinite (countable or uncountable) dimensional space. The state $|\psi\rangle$ belongs then to a separable Hilbert space $\mathcal{H}$, and the vectors $|\psi\rangle$ and $e^{i\varphi}|\psi\rangle, \varphi \in [0, 2\pi]$, describe the same physical state. The dual space $\mathcal{H}^*$ of $\mathcal{H}$ is the space of continuos linear functionals from $\mathcal{H}$ to $\mathbb{C}$. Its elements are defined as

$$\langle\phi| : |\psi\rangle \longmapsto \langle\phi|\psi\rangle. \tag{1.1.1}$$

There exists an isomorphism between a Hilbert space and its dual:

$$\dagger : |\psi\rangle \longmapsto |\psi\rangle^\dagger = |\psi\rangle^{*t} = \langle\psi|. \tag{1.1.2}$$

In this way, by representing $|\psi\rangle$ as a column vector $\begin{pmatrix} \psi_1 \\ \vdots \\ \psi_d \end{pmatrix}$, it is immediate to identify $\langle\psi|$ as a row vector $\begin{pmatrix} \psi_1 \dots \psi_d \end{pmatrix}^*$. The inner product $\langle\varphi|\psi\rangle$ is linear in

the second term and anti-linear in the first one (mathematicians usually adopt the opposite convention):

$$\begin{aligned} |\phi\rangle &= a|\phi_1\rangle + b|\phi_2\rangle \\ |\psi\rangle &= c|\psi_1\rangle + d|\psi_2\rangle \\ \langle\phi|\psi\rangle &= a^* c\langle\phi_1|\psi_1\rangle + b^* c\langle\phi_2|\psi_1\rangle \\ &+ a^* d\langle\phi_1|\psi_2\rangle + b^* d\langle\phi_2|\psi_2\rangle. \end{aligned} \tag{1.1.3}$$

The vectors are normalized to 1, thus $\langle\psi|\psi\rangle = ||\psi||^2 = 1$.
A quantum observable is a self-adjoint operator with dense domain in $\mathcal{H}$. Its eigenvectors form an orthonormal complete basis of the Hilbert space. The observable K is represented by a square matrix whose elements (k_{ij}) are $k_{ij} = \langle i|K|j\rangle$. A system with d degrees of freedom, which are the physical properties we are interested to, is described by a set of d[1] commuting observables $\{K_i\}$:

$$[K_i, K_j] = K_i K_j - K_j K_i = 0, \qquad \forall i, j \in 1, \ldots, d. \tag{1.1.4}$$

An observable L commuting with all the $\{K_i\}$ is necessarily a function of them, as a vector in the space is linearly dependent on three spatial coordinates x, y, z: $L = f(K_1, \ldots, K_d)$ (in this sense, the set of observables is said to be complete). It is possible to diagonalize simultaneously the mutually commuting observables $\{K_i\}$, and the relative eigenspace is non-degenerate. The simultaneous eigenvector is $|k_1 \ldots k_d\rangle = \bigotimes_{i=1}^{d} |k_i\rangle$, where $\{k_i\}$ are the eigenvalues of a specific K_i, while $\{|k_i\rangle\}$ are the eigenstates:

$$K_i|k_1 \ldots k_i \ldots k_d\rangle = k_i|k_1 \ldots k_d\rangle. \tag{1.1.5}$$

[1] We only consider the case of a finite number of degrees of freedom.

As previously remarked, the set of all the simultaneous eigenvectors identifies an orthonormal complete basis of $\mathcal{H}$:

$$\sum_{k_i \in \mathrm{DS}} |k_1 \dots k_d\rangle\langle k_1 \dots k_d| = \mathbb{I}, \tag{1.1.6}$$

where DS is the spectrum of the discrete eigenvalues of the K_i (we do not take into account the continuous variables case). Obviously, the choice of the observables $\{K_i\}$ is arbitrary.

For limited operators, it is ensured the existence of the adjoint operator $K^\dagger$, such that $\langle K^\dagger i|j\rangle = \langle i|Kj\rangle$. In the non-limited case (infinite-dimensional Hilbert spaces), further conditions are required to guarantee the existence of $K^\dagger$, but caring about them is out of the scope of this brief review. Anyway, in Quantum Mechanics all the interesting Hermitian operators have self-adjoint extensions, therefore quantum observables are safely deemed to be Hermitian operators. If A is self-adjoint, then $K = K^\dagger$ and it is easy to prove that $\langle i|K|j\rangle = (\langle j|K^\dagger|i\rangle)^* = (\langle j|K|i\rangle)^*$.

We claimed that a physical state is represented by the ray $|\psi\rangle$. But this is just an ideal case, in which the full information content of the system is accessible. More generally, there is a certain (classical) probability c_1 that the system is in the state $|\psi_1\rangle$, a probability c_2 that it is described by $|\psi_2\rangle$, and so on. It is possible to introduce a more powerful formalism to take into account statistical ensemble of states, called mixed states. Indeed, the more general description of a physical state is given by a density operator ρ:

$$\rho = \sum_i c_i \Pi_{\psi_i} = \sum_i c_i |\psi_i\rangle\langle\psi_i|. \tag{1.1.7}$$

The operator ρ is physically meaningful if and only if it satisfies the properties:

$$\begin{aligned} \rho &= \rho^\dagger \\ \mathrm{Tr}[\rho] &= \sum_i c_i = 1 \\ \langle i|\rho|i\rangle &\geq 0, \qquad \forall |i\rangle \in \mathcal{H}. \end{aligned} \tag{1.1.8}$$

Ideal states, that we call pure states, are simply represented by $\rho = |\psi\rangle\langle\psi|$.
A pure state of a composite system AB, with subsystems A and B, called bipartite state, is described by a ray $|\psi\rangle_{AB}$ in a Hilbert space $\mathcal{H}_{AB} = \mathcal{H}_A \otimes \mathcal{H}_B$ such that

$$|\psi\rangle_{AB} = \sum_{ij} c_{ij} |i\rangle_A \otimes |j\rangle_B \,, \tag{1.1.9}$$

where $\{|i\rangle_A\}$ and $\{|j\rangle_B\}$ are bases of $\mathcal{H}_A$ and $\mathcal{H}_B$ respectively, while $\{|i\rangle_A \otimes |j\rangle_B\}$ is a basis of $\mathcal{H}_{AB}$. The density matrix of a mixed state reads accordingly:

$$\rho_{AB} = \sum_i c_i |\psi_i\rangle\langle\psi_i|_{AB}. \tag{1.1.10}$$

The marginal density matrix of the subsystem A is $\rho_A = \mathrm{Tr}_B[\rho_{AB}] = \sum_j \langle j|\rho_{AB}|j\rangle_B$, and for subsystem B it is: $\rho_B = \mathrm{Tr}_A[\rho_{AB}] = \sum_i \langle i|\rho_{AB}|i\rangle_A$.

1.1.2 Open Quantum Systems

At theoretical level, one could take in exam a quantum system S without dealing with the potential disturbance induced by the external environment E. In that case, the evolution of the system is assumed to be unitary, hence described by the Schrödinger equation. However, in the real experimental practice, it is unavoidable to have to consider the effects due to the interaction $S - E$. The theory of Open Quantum Systems[2] provides the theoretical tools to describe the quantum dynamics of open systems. For a complete perspective, see [18].
The initial global state is assumed to be factorized: $\rho_{SE}(0) = \rho_S(0) \otimes \rho_E(0)$. The evolution of ρ_S fails to be unitary because of the noise produced on the system by the environment, whilst the global system SE evolves unitarily. For a time-independent Hamiltonian, one has

$$\rho_{SE}(t) = U_{SE}(t)\rho_{SE}(0)U_{SE}^\dagger(t) = e^{-iHt}\rho_{SE}(0)e^{iHt}. \tag{1.1.11}$$

[2]Note that in thermodynamics a system is open if it exchanges matter and energy with the environment. Here, a system is open whenever its evolution is not unitary.

At any time t, the density matrix of the system must be physical, thus $\rho_S(t)$ is Hermitian, positive and of trace one. Then, the evolution of the system is described by a linear CPTP (completely positive and trace preserving) map Φ:

$$\begin{aligned} \frac{\mathrm{d}\rho_S(t)}{\mathrm{d}t} &= \Phi(t)\rho_S(0) \\ \mathrm{Tr}[\rho_S(t)] &= 1 \\ \rho_S(t) &> 0, \qquad (\Phi(t)\otimes \mathbb{I}_T)\rho_{ST}(t) > 0, \forall t. \end{aligned} \tag{1.1.12}$$

Note that the complete positivity ensures that even by adding a system T the global operation $\Phi(t)\otimes\mathbb{I}_T$ is still positive. In the Schrödinger picture, if the semigroup composition law holds:

$$\Phi(t+s) = \Phi(t)\circ\Phi(s), \qquad \forall t,s \geq 0, \tag{1.1.13}$$

then the evolution of the system is described by the Lindblad master equation:

$$\begin{aligned} \frac{\mathrm{d}\rho_S(t)}{\mathrm{d}t} &= \mathcal{L}(\rho_S) = -i[H,\rho_S] + \sum_{i=1}^{n^2-1} \gamma_i (L_i\rho_S L_i^\dagger - \frac{1}{2}\{L_i^\dagger L_i, \rho_S\}) \\ \rho_S(t) &= \Phi(t)\rho_S(0) = e^{\mathcal{L}t}\rho_S(0), \end{aligned} \tag{1.1.14}$$

where we distinguish the term $[H,\rho]$ due to reversible evolution, a dissipative component specified by the γ_i, which are positive constants determined by the dynamics, and the Lindblad (super)-operators L_i.
The most general method of describing the dynamics of an open quantum system is by means of the operator-sum representation [17]:

$$\rho_S(t) = \mathrm{Tr}_E[U_{SE}(t)\rho_{SE}(0)U_{SE}^\dagger(t)] = \sum_i M_{S,i}(t)\rho_S(0)M_{S,i}^\dagger(t), \tag{1.1.15}$$

where $\{M_i\}, \sum_i M_i^\dagger M_i = \mathbb{1}$[3] are called Kraus operators. In the case of unitary evolution of the system S, there trivially exists one Kraus operator (the unitary itself), while this representation allows us to describe any quantum process (as-

[3] A quantum map can be not trace-preserving: $\sum_i M_i^\dagger M_i < \mathbb{1}$, but the argument is out of the topic of the thesis.

suming that $\rho_{SE}(0)$ is factorized), quantum measurements and dissipative dynamics included.

1.1.3 Measurements

Two main theoretical frameworks have been developed to describe the measurement process in Quantum Mechanics, which is inherently probabilistic. The first one is the projective (von Neumann) measurement, which is defined by a set of positive Hermitian operators $\{\Pi_i\}$ such that $\sum_i \Pi_i = \mathbb{I}$ and $\Pi_i \Pi_j = \delta_{ij}\Pi_i$. A projective measurement maps a state ρ into a statistical ensemble of states $\{p_i, \rho_i\}$, where $\rho_i = \frac{\Pi_i \rho \Pi_i}{\mathrm{Tr}[\Pi_i \rho \Pi_i]}$ is the post-measurement state with probability $p_i = \mathrm{Tr}[\Pi_i \rho \Pi_i]$. If we focus on a local projective measurement on the subsystem A of a bipartite system in the state $\rho_{AB} \equiv \rho$, say $\{\Pi_i^A \equiv \Pi_{A,i} \otimes \mathbb{I}_B\}$, the state is then mapped into an ensemble of conditional states $\rho_{B|\Pi_i^A} = \frac{\Pi_i^A \rho \Pi_i^A}{\mathrm{Tr}[\Pi_i^A \rho \Pi_i^A]}$. Let us consider a system in a state $|\psi\rangle$, and suppose to measure the value of the physical quantity K in this state by a projective measurement $\{\Pi_{K,i} \equiv \Pi_{k_i}\}$. The output will be one of the eigenvalues k_i of K with a certain probability $p_\psi(k_i)$. This unpredictability is not epistemic, i.e. it does not depend of the accuracy and precision of the measurement, but it is a peculiar property of Quantum Mechanics. We remark that a quantum measuremeent of an observable K perturbs the physical system. Indeed, it changes the state of the system, sending $|\psi\rangle$ in one of the eigenstates $|k_i\rangle$ of K with probability $p_\psi(k_i)$. A successive measurement of the same operator would be deterministic, by producing the output k_i with probability $p_{k_i}(k_i) = 1$. Assuming that K takes only discrete values and the related eigenspace to k_i is non-degenerate, the probability of measuring k_i is given by

$$p_\psi(k_i) = |\langle k_i|\psi\rangle|^2 = \langle\psi|k_i\rangle\langle k_i|\psi\rangle = \langle\psi|\Pi_{k_i}|\psi\rangle = \langle\Pi_{k_i}\rangle_\psi, \tag{1.1.16}$$

where Π_{k_i} is the projector into the eigenspace of k_i. Since K is a self-adjoint operator with dense domain in the separable Hilbert space $\mathcal{H}$, its eigenvectors

form an orthonormal complete basis of $\mathcal{H}$:

$$\begin{aligned} K &= \sum_{k_i \in \text{Sp } K} k_i \Pi_{k_i} \\ \sum_{k_i \in \text{Sp } K} \Pi_{k_i} &= \mathbb{1} \\ \sum_{k_i \in \text{Sp } K} p_\psi(k_i) &= \langle\psi| \sum_{k_i \in \text{Sp } K} \Pi_{k_i} |\psi\rangle = 1, \end{aligned} \tag{1.1.17}$$

where Sp K is the spectrum of K. The mean value $\langle K \rangle_\psi$ is asymptotically achieved by performing ideal measurements of K on infinite identical systems in the state $|\psi\rangle$:

$$\begin{aligned} \langle K \rangle_\psi &= \sum_{k_i \in \text{Sp } K} k_i p_\psi(k_i) \\ &= \langle\psi| \sum_{k_i \in \text{Sp } K} k_i \Pi_{k_i} |\psi\rangle = \langle\psi|K|\psi\rangle. \end{aligned} \tag{1.1.18}$$

If we pick a basis $\{|i\rangle\}$ of $\mathcal{H}$ such that $\sum_i |i\rangle\langle i| = 1$, then

$$\begin{aligned} \langle\psi|K|\psi\rangle &= \sum_i \langle\psi|i\rangle\langle i|K|\psi\rangle = \sum_i \langle i|K|\psi\rangle\langle\psi|i\rangle \\ &= \text{Tr}[K|\psi\rangle\langle\psi|] = \text{Tr}[K\Pi_\psi], \end{aligned} \tag{1.1.19}$$

and the probability related to an eigenvalue corresponds to the mean value of its projector: $p_\psi(k_i) = \text{Tr}[\Pi_\psi \Pi_{k_i}]$.
In a mixed state, for every observable K, one obtains

$$\begin{aligned} \langle K \rangle_\rho &= \sum_i c_i \langle K \rangle_{\psi_i} = \sum_i c_i \langle\psi_i|K|\psi_i\rangle \\ &= \sum_i c_i \text{Tr}[K\Pi_{\psi_i}] = \text{Tr}[K\rho]. \end{aligned} \tag{1.1.20}$$

Immediately, we see that the probability to obtain an output k_j by measuring an observable K on a state ρ is

$$p_\rho(k_j) = \text{Tr}[\Pi_{k_j}\rho] = \sum_i c_i \langle\psi_i|\Pi_{k_j}|\psi_i\rangle = \sum_i c_i p_{\psi_i}(k_j). \tag{1.1.21}$$

We point out that there is a fundamental difference between the mixed state

$$\rho = \sum_i c_i |k_i\rangle\langle k_i|, \tag{1.1.22}$$

and a pure state being a superposition of other pure states:

$$|\psi\rangle = \sum_i d_i |k_i\rangle, \qquad |d_i|^2 = c_i. \tag{1.1.23}$$

Let us consider a second observable L, having eigenvalues $\{l_m\}$ and relative eigenvectors $\{|l_m\rangle\}$, which does *not* commute with K. In the mixed state case, the probability to have the eigenvalue l_m as the result of a measurement of L is

$$p_\rho(l_m) = \mathrm{Tr}[\rho \Pi_{l_m}] = \sum_i c_i |\langle l_m|k_i\rangle|^2, \tag{1.1.24}$$

while if the state is pure one has

$$\begin{aligned} p_\psi(l_m) &= |\langle l_m|\psi\rangle|^2 = \sum_j d_j^* \langle k_j|l_m\rangle \sum_i d_i \langle l_m|k_i\rangle \\ &= \sum_i |d_i|^2 |\langle l_m|k_i\rangle|^2 + 2\sum_{i\neq j} d_j^* d_i \langle k_j|l_m\rangle\langle l_m|k_i\rangle \\ &= p_\rho(l_m) + 2\Sigma_{i>j}\mathrm{Re}[d_j^* d_i \langle k_j|l_m\rangle\langle l_m|k_i\rangle]. \end{aligned} \tag{1.1.25}$$

The pure state is more informative than the mixed one: this supplemental information is stored in the interference (coherence) term. In the mixed state, the information about the relative phase β in the products $d_i d_j^* = |\alpha| e^{i\beta}$ is lost, as only the square modules $|d_i|^2 = c_i$ appear. Classically, also encouraged by our common sense, we can imagine neither a coin that is in a superposition of the states "head" and "tail" nor a Schrödinger's cat that is both "dead" and "alive" at the same time, while in the microscopic world quantum coherence is not only relevant but also necessary to provide a satisfactory description of physical phenomena.

The second, more general description of a quantum measurement is known as POVM (positive operator-valued measure). It is still defined as a set of Hermitian positive operators $\{F_i\}$ such that $\sum_i F_i = \mathbb{I}$, but they are not necessarily

orthogonal nor commuting with each other. A POVM $\{F_i\}$ is built as follows. The system under scrutiny is supposed to be in the state $|\psi\rangle_S$. Let us add an ancillary system in an arbitrary state $|\alpha\rangle_A$, such that the global state is now $|\psi\rangle_S \otimes |\alpha\rangle_A$, and the system SA undergoes a unitary evolution that couples system and ancilla: $|\Psi\rangle_{SA} = U_{SA}(|\psi\rangle_S \otimes |\alpha\rangle_A)$. Finally, we make a projective measurement $\{\Pi_i^A \equiv \mathbb{I}_S \otimes \Pi_{A,i}\}$ on the ancilla, thus the post-measurement state is an ensemble of components: $\rho_{S|\Pi_i^A} = \frac{1}{p_i}\Pi_i^A|\Psi\rangle\langle\Psi|_{SA}\Pi_i^A$. It has been shown that $\mathrm{Tr}_A[\rho_{S|\Pi_i^A}] = \frac{1}{p_i}M_{S,i}|\psi\rangle\langle\psi|_S M_{S,i}^\dagger, M_i M_i^\dagger = F_i, \sum_i F_i = \mathbb{I}$ (refer to [17] for technical details). As a result of this, a global unitary and a projective measurement on the ancilla correspond to a local POVM $\{F_i\}$ on the system. This abstract construction describes physical situations in which we do not know the post-measurement state of S because it is not uniquely determined by the outcomes of the measurement. For example, by detecting the position of a photon destroys the photon itself, thus a POVM is the appropriate description of the process. Indeed, the probability to obtain the i outcome is $p_i = \langle\psi|M_i^\dagger M_i|\psi\rangle_S = \langle\psi|F_i|\psi\rangle_S$, and it is verified for any M_i (and final state $M_{S,i}|\psi\rangle_S$) satisfying the equation $F_i = M_i M_i^\dagger$, which has infinite solutions. The final state of the system S is therefore undetermined.

1.1.4 Quantum Entanglement

There is an important criterion of classification for states of composite systems, related to a fundamental quantum fingerprint of Nature (in Schrödinger words, this is *the* characteristic trait of Quantum Mechanics [19]). The bipartite state of Eq. (1.1.9) is said to be *separable* if and only if it is factorized:

$$|\psi\rangle_{AB} = \sum_i a_i|i\rangle_A \otimes \sum_j b_j|j\rangle_B. \tag{1.1.26}$$

In general, by considering also mixed states Eq. (1.1.10), the density matrix of a separable state reads

$$\rho_{AB} = \sum_i p_i \rho_{A,i} \otimes \rho_{B,i}. \tag{1.1.27}$$

If a state is not separable, then it is said to be *entangled*. Entanglement is a truly quantum feature of a state. An entangled state describes a composite system whose subsystems are not in definite states. For example, let us consider a system of two (fair or unfair) coins which we are going to toss. The state of the system is obviously classical, i.e. it is represented by a classical probability distribution:

$$\rho_{\text{coins}} = \begin{pmatrix} p(h,h) & 0 & 0 & 0 \\ 0 & p(h,t) & 0 & 0 \\ 0 & 0 & p(t,h) & 0 \\ 0 & 0 & 0 & p(t,t) \end{pmatrix}, \tag{1.1.28}$$

where $p(h,t)$ is the probability to have "head" and "tail" as outcomes of the toss of each coin, and so on. On the other hand, the information on the spins of two particles could be not only encoded in the classical state of the form Eq. (1.1.28), but also in an entangled state, for example $\frac{1}{\sqrt{2}}(|01\rangle + |10\rangle)$, such that the subsystems are not in an eigenstate of any local observable (we will discuss in detail this point in Ch. 4). Hence, it is appropriate not to deem the entangled particles to be two different systems, but to form one single physical system.

Entanglement is the umbrella concept of deep and insightful discussions about validity and limitations of Quantum Mechanics. Referring to [20] for an extended review of the topic, we briefly introduce the concept of *non-locality*, and see how it is linked to entanglement.

One of the most exciting features of Quantum Mechanics has been discussed for the first time in the celebrated Einstein-Podolski-Rosen (EPR) paper [21]. They argue that a physical theory must satisfy three properties: realism, which

implies that an element of reality in a physical system is a quantity whose value can be known from the theory with certainty without perturbing the system itself; completeness, i.e. every element of the reality must be described by an object of the theory; and locality, which means that the outcomes of measurements made on a given system are independent of quantum operations on space-like separated systems. EPR pointed out that the quantum theory does not satisfy the three properties at the same time because it is not complete. Indeed, it paradoxically implies that incompatible physical quantities, mathematically represented by non-commuting observables, have simultaneous reality in the physical world. Let us suppose that the state of the system is $\frac{1}{\sqrt{2}}(|01\rangle_{AB} + |10\rangle_{AB})$. If a measurement on the basis $|0,1\rangle_A$ (say of the spin σ_z) on A has outcome 0, then it is known with certainty, without perturbing the system, that a second measurement on B on the same basis will have outcome 1. But we could instead make a local change of basis, and obtain $\frac{1}{2}(|{+}{+}\rangle_{AB} + |{-}{-}\rangle_{AB}), |\pm\rangle = \frac{1}{2}(|0\rangle \pm |1\rangle)$. Now, if a measurement on A in the basis $|+,-\rangle_A$ (of the spin σ_x) returns an outcome $+$, then the result of a second measurement on B has outcome $+$ with certainty. Hence, eigenstates of incompatible observables, i.e. the local spin components σ_z and σ_x, are both real at the same time, and this is in open contrast to the Heisenberg principle. In the 60's, J. Bell found that the three conditions of realism, completeness and locality impose that statistical correlations of spacelike-separated measurements must satisfy constraints known as Bell inequalities. He developed an extension of Quantum Mechanics which satisfies the three criteria (and then the inequalities) by introducing additional quantities (*hidden variables*), whose value is not uniquely defined by a quantum state [21]. On the contrary, Quantum Mechanics predicts that Bell inequalities are violated by entangled states, a condition known as non-locality. Pioneering experiments have been implemented by Aspect and collaborators in early 80's [22], and still nowadays Bell tests feed a flourish research line. To date, Quantum Mechanics is the most effective theory for explaining the results of all the experiments carried out. Indeed, Bell inequalities have been violated in any experimental realisation.

The prototype of an experiment on Bell inequalities is described as follows [23]. The inequality here is a constraint on the correlation functions between the polarizations of two separated particles. A source sends a pair of entangled photons in the state $|\psi\rangle = \frac{1}{2}(|01\rangle_{AB} + |10\rangle_{AB})$ to two polarization analyzers characterized by the angles θ_A, θ_B, and then to a pair of detectors registering the polarizations $\pm$. It is possible to rotate the analyzers to different angles $\theta_{A'}, \theta_{B'}$, in such a way that the detection occurs in a different basis. Being $\langle I^{\pm}_{A,B}\rangle_{|\psi\rangle}$ the intensities measured by the detectors, which correspond to the probabilities of detecting the photons in a certain polarization, and given the second order correlation functions $\langle I^{\pm}_A I^{\pm}_B\rangle_{|\psi\rangle}$, the expectation value of the polarizations, when the analyzers are set to angles θ_A, θ_B, has been calculated to be

$$E(\theta_A, \theta_B) = \frac{\langle (I^+_B - I^+_A)(I^-_B - I^-_A)\rangle_{|\psi\rangle}}{\langle (I^+_B + I^+_A)(I^-_B + I^-_A)\rangle_{|\psi\rangle}}. \tag{1.1.29}$$

Then, the Bell inequality in the so called CHSH form derived in [24] reads:

$$B = |E(\theta_A, \theta_B) - E(\theta_A, \theta_{B'}) + E(\theta_{A'}, \theta_{B'}) + E(\theta_A, \theta_{B'})| \leq 2. \tag{1.1.30}$$

After straightforward calculations of intensities and correlation functions, one has

$$E(\theta_A, \theta_B) = \cos 2(\theta_A - \theta_B), \tag{1.1.31}$$

and the constraints given by the problem imply that

$$B = |3\cos 2(\theta_A - \theta_B) - \cos 6(\theta_A - \theta_B)|. \tag{1.1.32}$$

Calling $(\theta_A - \theta_B) = \alpha$, we have $B = |3\cos 2\alpha - \cos 6\alpha|$. The plot of B *vs* α is depicted in Fig. 1.1. The inequality is violated for

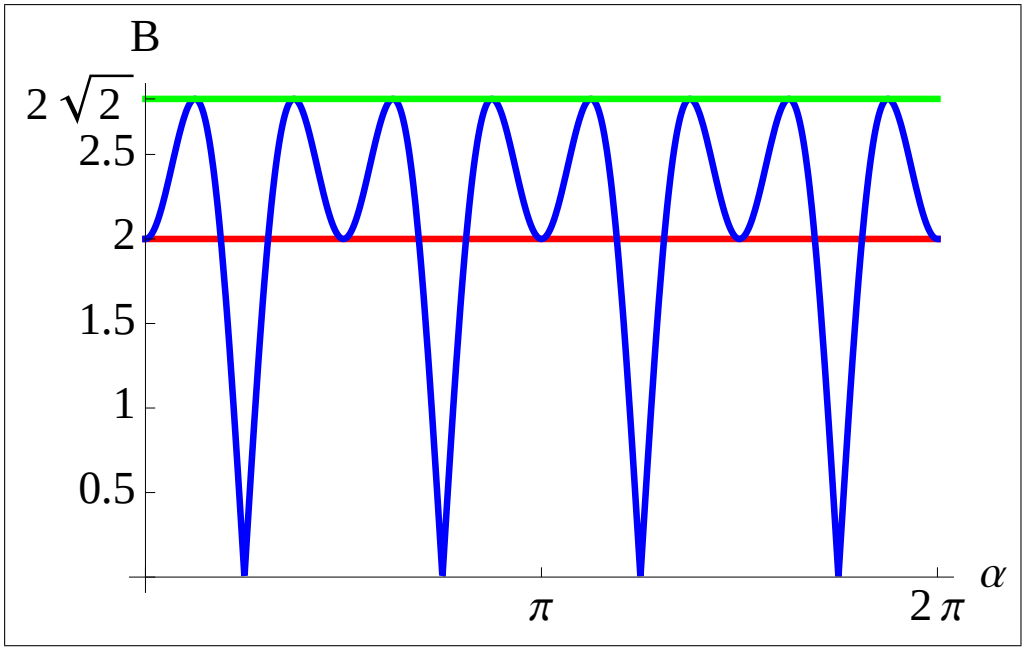

Figure 1.1: (Colours online) Violation of Bell inequality B in the CHSH form. Quantum Mechanics implies $0 \leq B \leq 2\sqrt{2}$ (blue and green line), thus beating the limit $B = 2$ (red line) reached by alternative hidden variable models.

$$\begin{aligned}
0 + k\pi \leq \quad & \alpha \quad \leq \arctan\left(\sqrt{-3+2\sqrt{3}}\right) + k\pi \\
\arctan\left(\sqrt{1+\frac{2}{3}\sqrt{3}}\right) + k\pi \leq \quad & \alpha \quad \leq \frac{\pi}{2} + k\pi \\
\frac{\pi}{2} + k\pi \leq \quad & \alpha \quad \leq \pi - \arctan\left(\sqrt{1+\frac{2}{3}\sqrt{3}}\right) + k\pi \\
\pi - \arctan\left(\sqrt{-3+2\sqrt{3}}\right) + k\pi \leq \quad & \alpha \quad \leq \pi + k\pi, \qquad k \in \mathbb{Z}.
\end{aligned} \tag{1.1.33}$$

The non-local correlations, which correspond to the entanglement between the photons, allow an experimenter to violate the Bell inequality. Indeed, the two particles are in a maximally entangled state. We note that for pure states entanglement and non-locality are synonyms: a violation of Bell inequalities occurs if and only if the state is entangled. Conversely, for mixed states, entanglement is necessary but not sufficient to ensure the violation of Eq. (1.1.30). For example, the Werner state $\rho = p|\psi\rangle\langle\psi| + (1-p)\mathbb{I}/4, p \in [0,1]$ [25] is entangled for $\frac{1}{3} < p \leq 1$, but violates Eq. (1.1.30) only when $\frac{1}{\sqrt{2}} < p \leq 1$ [20]. For a review on non-locality, refer to [26]. One could argue that these instantaneous non-local

correlations violate relativistic causality, which states that information (and any other thing) does not travel faster than light. But it is not the case. Calling Alice the observer performing measurement on the system A, and being Bob the one on the system B, after that Alice has performed a measurement, the only way she has to communicate to Bob the result is through a slower-than-light channel. Otherwise, Bob cannot know the polarization of the second photon before measuring it. We also remark that non-local correlations do not necessarily concern spatially separated objects, but just incompatible set of observables.
The arguments discussed in this section are a consequence of the postulates of Quantum Mechanics. There is no *a priori* reason to suppose that the Nature behaves in this way, but all the experiments carried out in the last century have confirmed with spectacular accuracy that is the case. For instance, the value of the muon magnetic moment obtained theoretically fits the experimental result by an error of 10^{-12} [27]. This is the magnitude order of the difference between the weight of a battleship with and without a one pound coin on board.

1.2 Quantum Information

1.2.1 Classical Information Theory

Information can be described mathematically, but is better to describe it physically. This statement could be appointed as the motto of Quantum Information, the research field studying how to exploit the law of Quantum Mechanics to manage information.
In his Master's Thesis [28], Shannon conceived and provided solid mathematical grounds for Information Theory. This is a theoretical programme where the concept of information is quantitatively described in a probabilistic framework. Indeed, probability is about what we know, the information we have or could obtain on some event. The nature of such information, e.g. the content of a message, does not play any role: whatever piece of information is always codified in random variables that assume a certain range of values. One could

ask how much information is gained if these variables take a particular value, and what is the most convenient way to convey or store information. In order to codify information, we want to minimise the errors during its manipulation and transmission. Less symbols we use, smaller is the probability of error. One cannot transmit any information content with an alphabet of only one symbol, thus at least two symbols are needed. Indeed, the fundamental unit of measurement in information theory is the *bit*, an object that either takes the value 0 or 1. A bit is physically represented, for example, by a light switch, and a sequence of bits allows us to transmit a message. Information is quantified in terms of *uncertainty*. Given a random variable X taking the values $\{x_i\}$ with probability $\{p_i\}$, the associated Shannon entropy is defined as $\mathcal{H}(X) = -\sum_i p_i \log_2 p_i$. It is a measure of the uncertainty we have on a stochastic event and, in the same way, it quantifies the information content of the variable X, which is the average information one obtains by knowing the value of X. The Shannon entropy is the simplest quantity which satisfies three basic axioms:

- It is a function only of the probability p: $\mathcal{H}(X) = \mathcal{H}(p_i)$;
- It is a smooth function of the probability p (true by construction);
- The information obtained by knowing the values of two *independent* variables X, Y is the sum of the information gained by each of them separately: $\mathcal{H}(X, Y) = \mathcal{H}(X) + \mathcal{H}(Y)$.

1.2.2 Quantum interpretation of Information

The fact that information is measured by an entropy suggested a potential link to Physics. Seminal works of Szilard, Landauer and Feynman remarked, naively speaking, that information is inherently physical (see [17] for an overview), and an information theory based on Physics laws is necessarily quantum mechanical. Indeed, the two main theories that describe the physical reality are Relativity and Quantum Mechanics. However, at "human" magnitude scales, say from $10^{-5}m$ to $10^{5}m$, classical physics is sufficient for our purposes: it approximates

very well both of them. But to study the galaxies and the Universe overall, Relativity is needed. On the other hand, to explore properties of atoms and in general the microscopic world, Quantum Physics is the most reliable tool we have. The quantum effects are negligible for macroscopic bodies (the probability that a car goes through a wall by tunnelling effect, appearing safely on the other side of it, is different from zero, but it is very low), but they become important for applications in telecommunications (lasers, fiber optics) and information technology (cryptography and computing), where dealing with an increasing miniaturisation of the devices and low energy regimes is a necessity. Remarkably, quantum features are useful to improve our capability to perform information-related tasks [17].

In the quantum scenario, the information is stored in the quantum states of a physical system. The random variables are replaced by the observables and their possible values by the eigenvalues of the observables. The corresponding unit of information is the quantum bit or *qubit*. The qubit is a quantum system described by the state $|\psi\rangle$. Then, a qubit can be in the states $|0\rangle, |1\rangle$ or, and this is the crucial difference with the bit, a quantum coherent superposition of the orthogonal states $|0\rangle$ and $|1\rangle$, for example $|\psi\rangle = \frac{1}{\sqrt{2}}(|0\rangle + |1\rangle)$. In general, for pure states one has

$$|\psi\rangle = a|0\rangle + b|1\rangle, \qquad |a|^2 + |b|^2 = 1, \tag{1.2.1}$$

where a, b are complex numbers. A quantum projective measurement in the $\{|0\rangle, |1\rangle\}$ basis sends the qubit to $|0\rangle$ with probability $|a|^2$ or onto $|1\rangle$ with probability $|b|^2$. A qubit is physically implemented, for instance, by a spin of an electron or a nucleus, or the polarization of a photon.

The seminal argument which led to the development of a Quantum Information theory is the following. Even if only one bit of information can be accessed in a qubit (e.g. by making a measurement), we can nevertheless store and process an arbitrary amount of information in the relative phase between $|0\rangle$ and $|1\rangle$. The Shannon entropy is replaced by the von Neumann entropy $\mathcal{S}$ in the

quantum domain[4] (for the main properties, see [29]). The entropy of a state ρ (in finite dimension) is defined as

$$\mathcal{S}(\rho) = -\mathrm{Tr}[\rho \log_2 \rho] = -\sum_k \lambda_k \log_2 \lambda_k, \tag{1.2.2}$$

where $\{\lambda_k\}$ are the eigenvalues of ρ. The von Neumann entropy $\mathcal{S}$ is a parameter that quantifies the *mixedness* of a state. If the state is pure, its entropy is zero, while a maximally mixed state has the largest possible amount of entropy, which is $\log d$, where d is the dimension of the system.

A fundamental difference with respect to the Shannon entropy emerges as a consequence of entanglement: given a bipartite state ρ_{AB}, its global entropy $\mathcal{S}(\rho_{AB}) \equiv \mathcal{S}(A,B)$ can be lower than one of the marginal entropies $\mathcal{S}(A), \mathcal{S}(B)$ (this never happens for the Shannon entropy). A bipartite state $|\psi\rangle_{AB}$ with entropy $\mathcal{S}(A,B) = 0$ could have mixed subsystems with non-vanishing entropy. For example, let us consider again the two-qubit entangled state $\frac{1}{\sqrt{2}}(|00\rangle + |11\rangle)$. One has $\mathcal{S}(A,B) = 0, \mathcal{S}(A) = \mathcal{S}(\mathrm{Tr}_B[\rho_{AB}]) = 1$. This result implies that the quantum conditional entropy $\mathcal{S}(B|A) = \mathcal{S}(A,B) - \mathcal{S}(A)$ is negative.

Entanglement, which is a consequence of superposition principle, turns out to be an important resource for Quantum Information. Its most relevant application is the *quantum teleportation* [30]: Alice can transmit a qubit to Bob if and only if they share entanglement and a classical communication channel (or a quantum channel). Entanglement is a necessary ingredient for quantum teleportation [20]. In the simplest realisation, the protocol runs in this way. Alice has two registers A and C, while Bob controls the system B. The subsystems A and B are entangled, and Alice wants to send the qubit C to Bob. The global state is

$$\begin{aligned} |\psi\rangle_{ABC} &= |\phi\rangle_{AB} \otimes |\alpha\rangle_C \\ &= \frac{1}{\sqrt{2}}(|00\rangle_{AB} + |11\rangle_{AB}) \otimes \frac{1}{\sqrt{2}}(a|0\rangle_C + b|1\rangle_C). \end{aligned} \tag{1.2.3}$$

[4] One can still consider the Shannon entropy associated to the outcomes distributions of a measurement: given an observable K being measured in a state $|\psi\rangle$, one has $\mathcal{H}(K)_{|\psi\rangle} = -\sum_i p_\psi(k_i) \log_2 p_\psi(k_i)$.

Alice changes the basis on AC by a local rotation. The state now reads

$$\begin{aligned} |\psi\rangle_{ABC} &= \frac{1}{2}\Big(|\phi^+\rangle_{AC}\otimes(a|0\rangle_B+b|1\rangle_B)+|\phi^-\rangle_{AC}\otimes(a|0\rangle_B-b|1\rangle_B) \\ &+ |\psi^+\rangle_{AC}\otimes(b|0\rangle_B+a|1\rangle_B)+|\psi^-\rangle_{AC}\otimes(b|0\rangle_B-a|1\rangle_B)\Big), \end{aligned} \tag{1.2.4}$$

where $|\psi^\pm\rangle=\frac{1}{\sqrt{2}}(|01\rangle\pm|10\rangle), |\phi^\pm\rangle=\frac{1}{\sqrt{2}}(|00\rangle\pm|11\rangle)$. The set $\{|\psi^\pm\rangle,|\phi^\pm\rangle\}$ is known as the Bell basis [20]. A local projective measurement made by Alice on the Bell basis sends the global state in one of the four states

$$\begin{aligned} \frac{1}{2}|\phi^\pm\rangle_{AC} &\otimes (a|0\rangle_B\pm b|1\rangle_B) \\ \frac{1}{2}|\psi^\pm\rangle_{AC} &\otimes (b|0\rangle_B\pm a|1\rangle_B). \end{aligned} \tag{1.2.5}$$

Finally, Alice communicates (by two classical bits) the result of the measurement to Bob. The latter, if the post-measurement state of Alice is $|\phi^+\rangle$, has already received the qubit initially stored in C. Otherwise, he makes a local unitary and obtains it. Remarkably, the classical, slower-than-light communication channel is a necessary ingredient to carry out the protocol.

In Quantum Information, one needs to quantify the amount of available resources for a given task. Thus, it is necessary to introduce the paradigm of *measure* of entanglement, say $\mathcal{E}$. For pure states, the entanglement is equal to the von Neumann entropy of one of the two subsystems, $\mathcal{E}(\rho_{\text{pure}})=\mathcal{S}(A)=\mathcal{S}(B)$, while several functions have been adopted to measure quantitatively entanglement in mixed states [20]. There are some properties that a measure of entanglement $\mathcal{E}(\rho_{AB})$ must satisfy :

- Vanishing if and only if the state is separable:
  $\mathcal{E}(\sum_i p_i\rho_{i,A}\otimes\rho_{i,B})=0, \qquad \mathcal{E}(\rho_{AB}^{\text{ent}})>0;$
- Being invariant under local unitary operations:
  $\mathcal{E}\Big((U_A\otimes U_B)\rho_{AB}(U_A\otimes U_B)^\dagger\Big)=\mathcal{E}(\rho_{AB});$
- Being monotonically decreasing under a specific class of quantum op-

erations, called Local Operations and Classical Communication (LOCC): $\mathcal{E}\left(\Phi_{\mathrm{LOCC}}(\rho_{AB})\right) \leq \mathcal{E}(\rho_{AB})$.

The first property is a requirement of *faithfulness* of the measure[5]. The invariance under local unitary transformations ensures the basis independence of the concept of entanglement. The third requirement means that two scientists, working in distant labs on two systems that are only classically correlated, cannot increase their entanglement by making local operations on their own systems and communicate their results by a classical communication line. Any local operation takes the form $\Phi_{\mathrm{local}}(\rho_{AB}) = \sum_{ij} \frac{1}{\mathrm{Tr}[\rho_{AB}(A_i \otimes B_j)^\dagger (A_i \otimes B_j)]} (A_i \otimes B_j)\rho_{AB}(A_i \otimes B_j)^\dagger$, where $\{A_i\}, \{B_i\}$ are local Kraus operators. The LOCC are difficult to characterize [20]. Here we mention a strictly larger class of operations which contains the LOCC one, the class of separable operations, whose general form is $\Phi_{\mathrm{sepLOCC}}(\rho_{AB}) = \sum_i \frac{1}{\mathrm{Tr}[\rho_{AB}(A_i \otimes B_i)^\dagger (A_i \otimes B_i)]} (A_i \otimes B_i)\rho_{AB}(A_i \otimes B_i)^\dagger$ [31, 32].

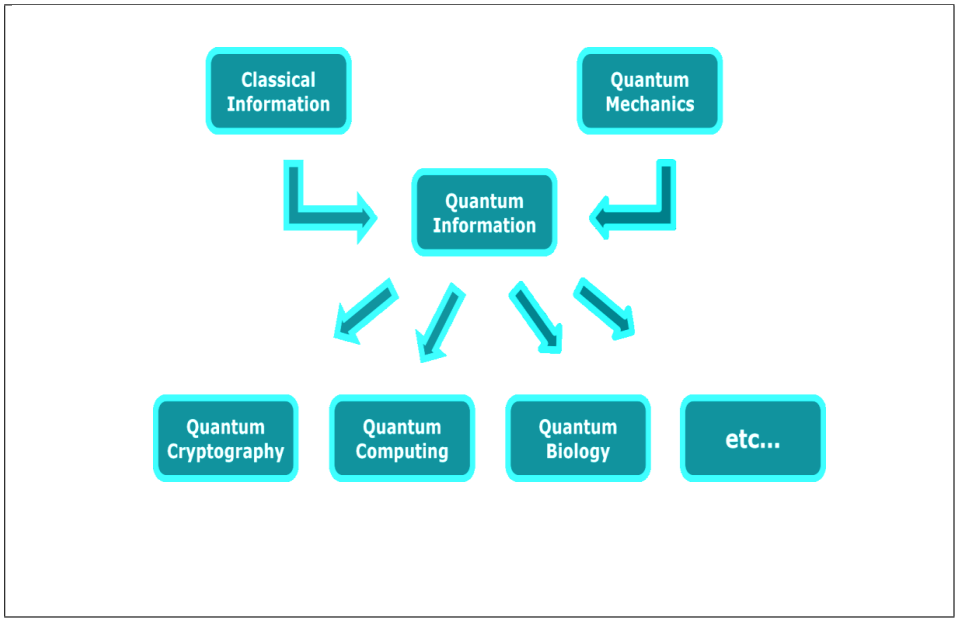

Figure 1.2: Quantum Information genealogy.

Finally, we remark that, while Quantum Information is the result of the application of Quantum Mechanics principles to Information Theory, this is not a

[5]Note that some widely exploited entanglement measures as the *negativity* and the *distillable entanglement* can be zero even on certain entangled states [20].

one-way relationship. Quantum Information techniques have been exploited to investigate foundational aspects of Quantum Mechanics as well as favoured the development of quantum-enhanced technology with immediate commercial impact (e.g. quantum cryptographic protocols). Moreover, a wide range of brand new research fields have been started up and propelled by taking advantage of Quantum Information concepts and methods (Fig. 1.2).

1.3 A hierarchy of quantum states: classical and quantum correlations

1.3.1 Quantum Discord

We have claimed that a pivotal role in the success of Quantum Information is played by the exploitation of entanglement, i.e. correlations between parts of composite systems which cannot be described within a classical picture. Traditionally, entanglement is considered a synonym of quantum correlations [21]. The statement is true for pure states: entanglement is equal to non-locality and encompasses every possible notion of "quantumness", as remarked in Sec. 1.1.4. Conversely, for mixed states the situation is more complex. We saw that entanglement is necessary but not sufficient to violate Bell inequalities, thus the sets of non-local states is smaller and lies inside the set of entangled states.
The message of this section is that even mixed separable states show quantum correlations. We will follow the historical path which led to define a class of quantum correlations (QC) which is more general than entanglement. The QC will be indirectly defined as the difference between total and classical correlations.

One of the lessons we apprehend from Quantum Mechanics is that the measurement process disturbs the state of a physical system. This differs from what happens in the classical scenario. Hence, it is possible to conclude that

the disturbance induced by a measurement on a state is a good evidence of its quantumness. We are here interested to study a bipartite system in which a local measurement on one of the subsystem is made. The disturbance induced by the measurement on the system changes the properties of the global state, in particular the amount of correlations between the two subsystems.
Let us consider the statistical correlations described by the classical Information Theory. The correlations between two random variables X and Y, taking values $\{x_i\}, \{y_j\}$ with probabilities $\{p_i\}, \{q_j\}$, represent the information shared by the two variables, and are measured by the *mutual information* $\mathcal{I}$, defined as

$$\mathcal{I}(X:Y) = \mathcal{H}(X) + \mathcal{H}(Y) - \mathcal{H}(X,Y), \tag{1.3.1}$$

where $\mathcal{H}(X,Y) = -\sum_{ij} r_{ij} \log_2 r_{ij}, \sum_j r_{ij} = p_i, \sum_i r_{ij} = q_j$ is the joint entropy of X and Y. For independent variables, the third axiom satisfied by the Shannon entropy implies $\mathcal{I}(X:Y) = 0$. Reminding the Bayesian rules, the mutual information enjoys other equivalent expressions: $\mathcal{I}(X:Y) = \mathcal{I}(Y:X) = \mathcal{J}(X:Y) = \mathcal{J}(Y:X)$, where

$$\begin{aligned} \mathcal{J}(X:Y) &= \mathcal{H}(X) - \mathcal{H}(X|Y) \\ \mathcal{J}(Y:X) &= \mathcal{H}(Y) - \mathcal{H}(Y|X). \end{aligned} \tag{1.3.2}$$

The conditional entropy $\mathcal{J}(X:Y)$(or $\mathcal{J}(Y:X)$) represents the average uncertainty (ignorance) we have on $X(Y)$ given the value of $Y(X)$:

$$\begin{aligned} \mathcal{H}(X|Y) &= \mathcal{H}(X,Y) - \mathcal{H}(Y) = -\sum_{ij} r_{ij} \log_2 \frac{r_{ij}}{q_j} \\ &= -\sum_{ij} q_j \frac{r_{ij}}{q_j} \log_2 \frac{r_{ij}}{q_j} = \sum_j q_j \mathcal{H}(X|y_j) \\ \mathcal{H}(Y|X) &= \mathcal{H}(X,Y) - \mathcal{H}(X) = -\sum_{ij} r_{ij} \log_2 \frac{r_{ij}}{p_i} \\ &= -\sum_{ij} p_i \frac{r_{ij}}{p_i} \log_2 \frac{r_{ij}}{p_i} = \sum_i p_i \mathcal{H}(Y|x_i). \end{aligned} \tag{1.3.3}$$

The mutual information has also an equivalent formulation in terms of the sta-

tistical distance (yet not symmetric) between the joint distribution r_{ij} and the product of the marginal ones:

$$\mathcal{I}(X:Y) = \mathcal{R}(X||Y) = -\sum_{ij} r_{ij} \log_2 \left(\frac{r_{ij}}{p_i q_j}\right), \tag{1.3.4}$$

where $\mathcal{R}$ is the relative entropy, or Kullback-Leibler divergence [33].

In the quantum scenario, the random variables are replaced by a bipartite system AB with a density matrix $\rho \equiv \rho_{AB}$, consisting of subsystems A, B with marginal density matrices ρ_A, ρ_B. The quantum analogue of Eq. (1.3.1) reads

$$\mathcal{I}(\rho) \equiv \mathcal{I}(A:B) = \mathcal{S}(A) + \mathcal{S}(B) - \mathcal{S}(A,B). \tag{1.3.5}$$

The quantum mutual information quantifies the amount of total (classical and quantum) correlations between the two subsystems. For example, for the (maximally) entangled pure state $\rho_{\text{Bell}} = |\psi^+\rangle\langle\psi^+|$, we have $\mathcal{I}(\rho_{\text{Bell}}) = 2$ bits, where one bit is the amount of classical correlations and there is one bit of entanglement ($\mathcal{S}(\rho_A) = \mathcal{S}(\rho_B) = 1$). Correlations between subsystems cannot be increased if the subsystems A, B evolve independently: the mutual information is non-increasing under local operations Φ_A, Ξ_B: $\mathcal{I}((\Phi_A \otimes \Xi_B)\rho) \leq \mathcal{I}(\rho)$, and is invariant under local unitary transformations. The equivalence to the (quantum) relative entropy still holds [34]:

$$\mathcal{I}(\rho) = \mathcal{R}(\rho||\rho_A \otimes \rho_B) = \text{Tr}[\rho \log_2 \rho] - \text{Tr}[\rho \log_2(\rho_A \otimes \rho_B)]. \tag{1.3.6}$$

One is tempted to write a quantum version of $\mathcal{J}$ as well:

$$\begin{aligned} \mathcal{J}(A:B) &= \mathcal{S}(A) - \mathcal{S}(A|B), \\ \mathcal{J}(B:A) &= \mathcal{S}(B) - \mathcal{S}(B|A). \end{aligned} \tag{1.3.7}$$

From now on, we focus on $\mathcal{J}(B:A)$. We said that $\mathcal{S}(B|A) = S(A,B) - S(A)$ is the quantum conditional entropy. However, in general $\mathcal{J}$ does *not* represent

the mutual information of the post-measurement state, which depends on the observable one has measured on the subsystem A. Intuitively, if we measure an observable $K^A = K_A \otimes \mathbb{I}_B$, the state is projected on one of the eigenstates of K^A, while a measurement of an observable $K^{A'} = K'_A \otimes \mathbb{I}_B$ not commuting with K^A projects the state in an eigenstate of $K^{A'}$ that is different from the K^A's one. We recall that a local measurement $\{M^A = M_A \otimes \mathbb{I}_B\}$ on A maps the system into a statistical ensemble $\{p_k, \rho_k \equiv \rho_{B|\Pi_k^A}\}$, such that $\rho_k = \frac{(M_{A,k}\otimes\mathbb{I}_B)\rho(M_{A,k}^\dagger\otimes\mathbb{I}_B)}{p_k}$, where $p_k = \mathrm{Tr}[\rho M_k^{A\dagger} M_k^A]$. Thus, the quantum version of Eq. (1.3.3) is $S(B|\{M^A\}) = \sum_k p_k S(\rho_k)$[6], and the quantity

$$\mathcal{J}(B:A)_{\{M^A\}} = S(B) - S(B|\{M^A\}), \tag{1.3.8}$$

evaluates the average information gained on the subsystem B after that the local measurement $\{M^A\}$ has been performed. The key point is that, conversely to the classical case, this quantity is always smaller than the quantum mutual information in the initial state:

$$\mathcal{I}(\rho) = \mathcal{J}(B:A) \geq \mathcal{J}(B:A)_{\{M^A\}}, \forall \{M^A\}. \tag{1.3.9}$$

Indeed, it is easy to verify that $S(B|\{M^A\}) \geq S(B|A)$ (for the proof, see [35]). Therefore, the mutual information , which measures the total (classical and quantum) correlations, decreases after the measurement. Since classical correlations are certainly kept invariant[7], the correlations which have been lost appear to be genuinely quantum. Also, they seem to evaluate how much the state is disturbed by the quantum measurement. The state is *only* classically correlated if and only if there exists at least one measurement $\{M^A\}$ on A that does not affect the mutual information and achieves the equality in Eq. (1.3.9): $\mathcal{I} = \mathcal{J}_{\{M^A\}}$. We are able to quantify the QC of a state by finding the minimum of the conditional entropy $S(B|\{M^A\})$ over all the possible measurements on A, i.e. determining the maximum of $\mathcal{J}_{\{M^A\}}$, which is the largest possible amount

[6] From now on, we refer to this quantity as the quantum conditional entropy.

[7] It is legit to assume this point of view, as in the classical case $\mathcal{I} = \mathcal{J}$ for any random variable.

of correlations preserved after a measurement on A, and then subtracting it to the total correlations the system had before the measurement, which are measured by the mutual information $\mathcal{I}$. The amount of classical correlations is expressed by the mutual information obtained by considering the least disturbing measurement [35–37]:

$$\mathcal{C}(B:A) = \max_{\{M^A\}} \mathcal{J}(B:A)_{M^A} = \mathcal{S}(B) - \min_{\{M^A\}} \sum_k p_k \mathcal{S}(B|\{M_k^A\}). \quad (1.3.10)$$

Indeed, it satisfies all the requirements of a good measure of classical correlations [37]:

- It is zero if and only if the state is uncorrelated:
  $\mathcal{C}(B:A)(\rho_A \otimes \rho_B) = 0$, otherwise $\mathcal{C}(B:A)(\rho) > 0$;
- For pure states: $\mathcal{C}(B:A)(\rho_{\text{pure}}) = \mathcal{C}(A:B)(\rho_{\text{pure}}) = \mathcal{S}(A) = \mathcal{S}(B)$;
- It is invariant under local unitary operations:
  $\mathcal{C}(B:A)\Big((U_A \otimes U_B)\rho(U_A \otimes U_B)^\dagger\Big) = \mathcal{C}(B:A)(\rho)$;
- It is not-increasing under local operations:
  $\mathcal{C}(B:A)\Big((\Phi_A \otimes \Xi_B)\rho\Big) \leq \mathcal{C}(B:A)(\rho)$.

Consequently, the amount of QC is measured by the *quantum discord* [35, 36]:

$$\begin{aligned} \mathcal{D}^A(\rho) &= \mathcal{I}(\rho) - \mathcal{C}(B:A) \\ &= \mathcal{S}(A) - \mathcal{S}(A,B) + \min_{\{M^A\}} \sum_k p_k \mathcal{S}(B|\{M_k^A\}). \end{aligned} \quad (1.3.11)$$

We note that quantum discord is not symmetric. By performing the measurement on Bob's subsystem rather than on Alice's one returns in general a different value of discord: $\mathcal{D}^A \neq \mathcal{D}^B$. Thus, we state that the discord $\mathcal{D}^{A(B)}$ quantifies the amount of QC between Alice and Bob *as perceived* by Alice (Bob). From now on, we will always consider local measurements on A. In the case of pure bipartite states, discord equals the marginal entropy of one of the two subsystems, which is a *bona fide* measure of entanglement: $\mathcal{D}^A = \mathcal{D}^B = \mathcal{S}(A) = \mathcal{S}(B)$.

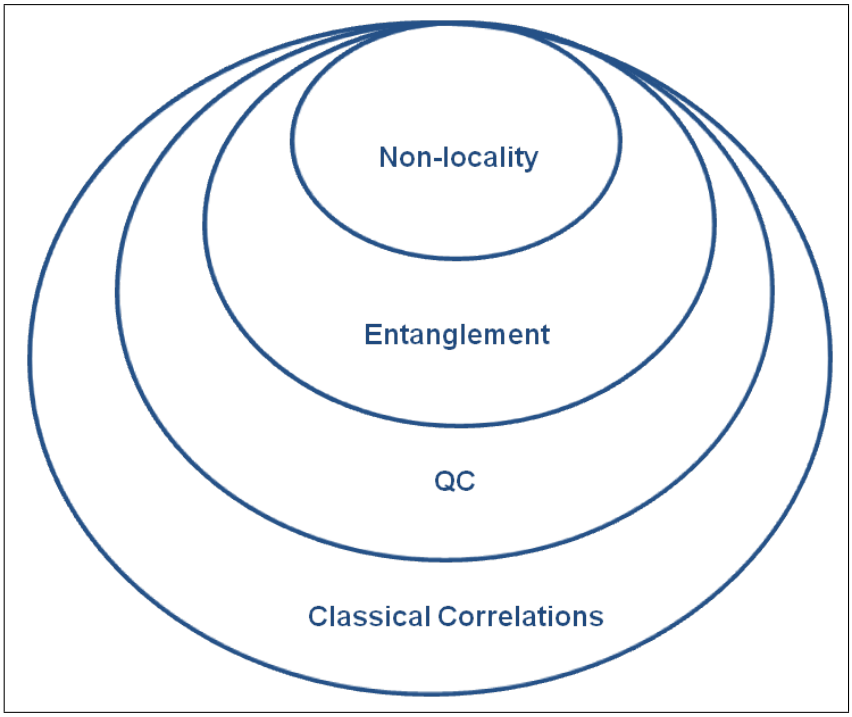

Figure 1.3: Classification of correlations in quantum states of compound systems.

The analysis of the correlations properties in bipartite systems involves a refinement of the classification of the states of the systems themselves (Fig. 1.3). It is immediate to verify that not only entangled states, but almost all separable states have a non-vanishing quantum discord [38], i.e. are affected by the measurement process, thus they exhibit some quantum properties. In the set of separable states, it is identified the subclass of *classical-quantum states* [39], defined as

$$\begin{aligned} \rho_{CQ} &= \sum_i p_i |i\rangle\langle i| \otimes \rho_{B,i} \\ \rho_{QC} &= \sum_j p_j \rho_{A,j} \otimes |j\rangle\langle j|, \end{aligned} \tag{1.3.12}$$

such that $\mathcal{D}^A(\rho_{CQ}) = \mathcal{D}^B(\rho_{QC}) = 0$, where $\{|i\rangle\}, \{|j\rangle\}$ are orthonormal vector sets. Indeed, by making a projective measurement $\{\Pi_i^A\}$ on the basis $\{|i\rangle\}$ returns $\rho_{CQ}^{\Pi^A} = \sum_i \Pi_i^A \rho_{CQ} \Pi_i^A = \rho_{CQ}$, and leaves the state unperturbed. Then, the set of the genuinely classically correlated states, called *classical-classical* states,

Qualitative description	Implicit form	Example
Non-local	$\{\rho : \rho$ violates Bell ineq.$\}$	$\rho = p\|\psi^+\rangle\langle\psi^+\| + (1-p)\mathbb{I}/4, \quad \frac{1}{\sqrt{2}} < p \leq 1$
Entangled	$\{\rho : \rho \neq \sum_i p_i \rho_{A,i} \otimes \rho_{B,i}\}$	$\rho = p\|\psi^+\rangle\langle\psi^+\| + (1-p)\mathbb{I}/4, \quad \frac{1}{3} < p \leq 1$
Separable quantum correlated	$\rho = \sum_i p_i \rho_{A,i} \otimes \rho_{B,i}, \rho_{A,i} \neq \|i\rangle\langle i\|$	$\rho = p\|\psi^+\rangle\langle\psi^+\| + (1-p)\mathbb{I}/4, \quad 0 < p \leq \frac{1}{3}$
Classical-quantum correlated	$\rho = \sum_i p_i \|i\rangle\langle i\| \otimes \rho_{B,i}$	$\rho = \frac{1}{2}\left[\|0+\rangle\langle 0+\| + \|1\rangle\langle 1\| \left(\frac{1}{2}(\|+\rangle\langle +\| + \|-\rangle\langle -\|)\right)\right]$
Classically correlated	$\rho = \sum_{ij} p_{ij} \|ij\rangle\langle ij\|$	$\rho = \frac{1}{2}(\|0+\rangle\langle 0+\| + \|1-\rangle\langle 1-\|)$

Table 1.1: Hierarchy of bipartite quantum states.

consists of states of the form

$$\rho_{CC} = \sum_{ij} p_{ij} |i\rangle\langle i| \otimes |j\rangle\langle j|. \tag{1.3.13}$$

Clearly, we have $\mathcal{D}^A(\rho_{CC}) = \mathcal{D}^B(\rho_{CC}) = 0$. We notice that not only the classical states are just a subset of the separable states, but it is possible to show that the states with zero discord are a null measure subset of the set of separable states [38], that is the set of classical-quantum and classical-classical states. We summarise the hierarchy of bipartite states based on correlations in Table 1.1.

1.3.2 Properties of QC measures, motivation for studying them, and open issues

The quantitative and qualitative evaluation of QC captured the interest of the quantum information community. Quantum discord is not the only way to measure QC. Several alternative quantifiers have been introduced in literature [35, 37, 40–44, DG1, DG7]. For a comprehensive review, about both bipartite and multipartite QC, the reader should refer to [45].

The proposed QC measures are grouped in two main classes: entropic quantities, such as the original quantum discord itself, and geometric ones. An entropic measure is usually introduced to provide an information theoretic or a thermodynamical interpretation of QC [46], but it is generally difficult to be computed explicitly [45, DG14]. The geometric measures of QC are instead constructed by fixing a metric in the Hilbert space of the quantum states, and then using it to evaluate the distance between the state under examination and the set of classical (zero discord) states. For example, the *relative entropy of discord*

introduced in [44] and defined as $\mathcal{Q}^{A(B)}(\rho) = \min_{\rho_{CQ(QC)}} \mathcal{R}(\rho||\rho_{CQ(QC)})$, represents the distance in terms of relative entropy between the state under scrutiny and the closest classical state. Other geometric measures have been appreciated for their computability, as the geometric discord introduced in [43] (we will discuss this measure in Ch. 2).

The theory of entanglement has been amply developed [20], leading to a set of well motivated requirements that any *bona fide* entanglement measure should satisfy, as we have seen in the previous Section. A similar formal backbone has been built for QC indicators as well. To render the paradigm of QC widely accessible and appealing experimentally, and be able to reveal truly quantum rather than classical features in laboratory systems, one should first identify those quantifiers of QC that are faithful, namely vanishing on all classical states, and satisfy a set of criteria on the same line of what is expected for an entanglement measure. The peculiar properties of a reliable QC measure, say $\mathcal{Q}$, are:

- It is zero if and only if the state is classically correlated:
  $\mathcal{Q}^{A}(\rho_{CQ}) = 0$, $\mathcal{Q}^{B}(\rho_{QC}) = 0$, otherwise $\mathcal{Q}^{A(B)}(\rho) > 0$;
- It is an entanglement measure for pure states:
  $\mathcal{Q}^{A(B)}(\rho_{\text{pure}}) = \mathcal{E}(\rho_{\text{pure}})$;
- It is invariant under local unitary operations:
  $\mathcal{Q}^{A(B)}\Big((U_A \otimes U_B)\rho(U_A \otimes U_B)^{\dagger}\Big) = \mathcal{Q}^{A(B)}(\rho)$;
- It is not-increasing under local operations on the unmeasured party:
  $\mathcal{Q}^{A}\Big((\mathbb{I}_A \otimes \Phi_B)\rho\Big) \leq \mathcal{Q}^{A}(\rho), \qquad \mathcal{Q}^{B}\Big((\Phi_A \otimes \mathbb{I}_B)\rho\Big) \leq \mathcal{Q}^{B}(\rho).$

The first condition is just the requirement of faithfulness, while the second one reflects the fact the for pure states QC, entanglement (and non-locality) coincide. The third property is still intuitive, as a local change of basis should not affect correlations. Finally, the last property states that $\mathcal{Q}^{A(B)}$ is non-increasing by local operations on Bob (Alice). On the other hand, an interesting peculiar feature of QC, related to their asymmetry, is that they can be increased by local operations on the measured subsystem: $\mathcal{Q}^{A}\Big((\Phi_A \otimes \mathbb{I}_A)\rho\Big) > \mathcal{Q}^{A}(\rho)$ [47, 48]

(from now on, we focus on $\mathcal{Q}^A$, the same results apply to $\mathcal{Q}^B$ straightforwardly). In general, given a classically correlated state, QC can be created by local operations whenever the commutativity of density operators is not preserved: every local channel Φ^A which does not satisfy $[\Phi^A(\rho), \Phi^A(\sigma)] = 0$, for any two density matrices ρ, σ such that $[\rho, \sigma] = 0$, creates QC in a classically correlated state: $\mathcal{Q}^A(\Phi^A(\rho_{CQ})) > 0$.

There are two main motivations for studying QC. The first one is foundational. QC represent an unexplored conceptual paradigm in the quantum theory. A recent study confirmed that QC cannot be described by a classical probabilistic framework [49]. In particular, QC are a natural benchmark of *decoherence* [50], that is the loss of quantum coherence in a quantum system due to the interaction with the environment. Technically, if the state of a single system S is described by a density matrix having off-diagonal elements in a given basis of interest, then coherence is present. An important question is to extend the concept of coherence to multipartite systems. It has been shown that QC are the most general signature of coherence, in this sense: If and only if QC are shared among parts of a compound system, then quantum coherence is guaranteed in *any* local basis [51]. Therefore, QC are the minimal requirement for nontrivial quantumness in multipartite systems. Some interesting questions arise: we would like to know the amount of QC a state has, and when correlations of what states under what conditions present some potentially exploitable peculiarities (e.g. resilience under dissipation, computational speed-up, etc). On this hand, a great deal of interest has been recently addressed to the study of the QC dynamics in open quantum systems [52–54], i.e. how the QC between the system and the environment, or between parts of the system under investigation, behave under dissipative dynamics (see Fig. 1.4). In general, QC have been proven to be much more robust than entanglement and easier to be created under interaction of common and independent reservoirs. This is a straightforward result: QC can be created by local operations from a classically correlated

state, and vanish only on a null-measure set of states [38].

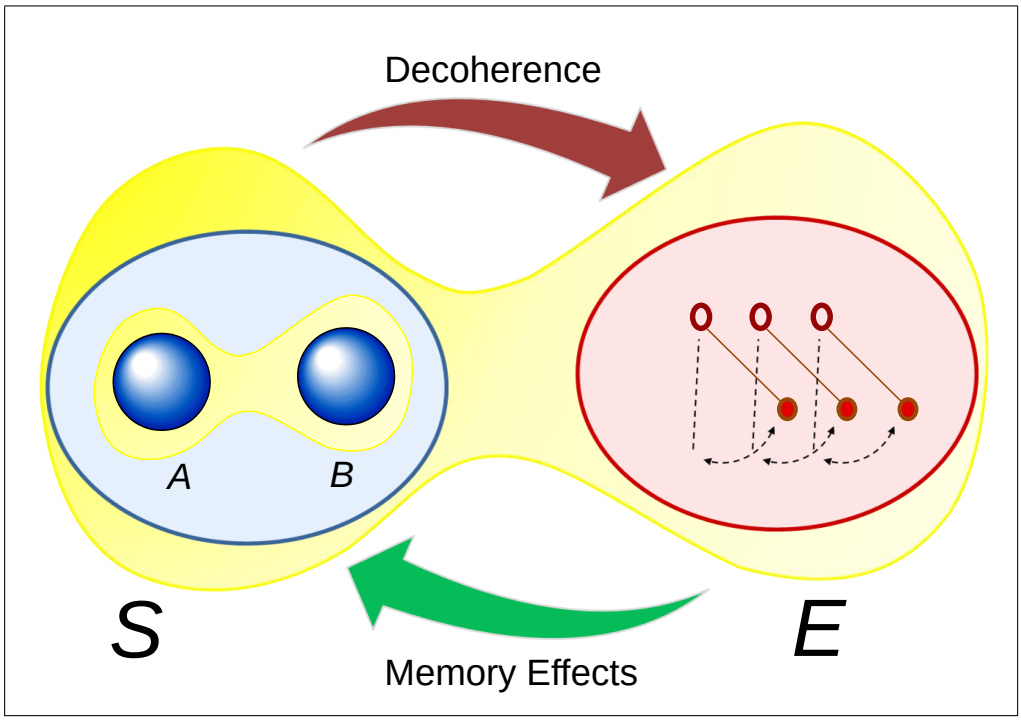

Figure 1.4: (Colours online) In an open quantum system, the system under scrutiny, say S, interacts with a second system or a bunch of systems, collectively called environment E. The interaction entails a two-way exchange of information: $S \rightarrow E$ (decoherence) and $S \leftarrow E$ (memory effects). The coupling $S - E$ determines the QC between S and E (big yellow shade) as well as the QC between the parties A, B (the small yellow shade).

The second reason that makes QC interesting is their potential exploitability for building quantum computers. Non-locality is intensively exploited in quantum cryptography [26], while entanglement is proven to be a necessary condition for quantum speed-up in computational algorithms with pure states (with some warnings, see [55]). On the other hand, there is no general prescription for mixed states. It is therefore legit to wonder if separable but quantum-correlated (i.e. $\mathcal{Q} > 0$) states might be a useful for entanglement-free algorithms. An ultimate answer is missing. The current state of knowledge in the field is summarized in Table 1.2. Nevertheless, quantum discord admits an operational interpretation in some communication protocols with mixed states, such as the local broadcasting [39], the quantum state merging [46, 56], the entanglement

activation [51, 57] and the access to information due to coherent interaction[8] [58]. The geometric discord has been linked quantitatively to the performance of the remote state preparation protocol for (a class of) two-qubit states [59], while the relative entropy of discord [44] has been shown to be a resource for entanglement distribution [42, 60]. Yet, the most relevant application is in the Deterministic Quantum Computation Model with One Qubit (DQC1), introduced in [61].

The DQC1 algorithm is a non-universal quantum computing protocol estimating the normalized trace of a unitary matrix U. It provides an exponential speed up compared to the best known classical algorithm for this specific task [62–64]. The surprising feature of the DQC1 is that this enhancement in the performance is obtained despite a vanishing amount of entanglement required by the computation. Thus, it sounds an appropriate ground to study the potential of QC. In particular, the protocol works as follows. An ancillary qubit (Alice's subsystem) is initially in a state with arbitrary polarization μ: $\rho_A^{in} = \frac{1}{2}(\mathbb{I}_2 + \mu\sigma_3)$, while the state of Bob is an n-qubit maximally mixed state: $\rho_B^{in} = \frac{1}{2^n}\mathbb{I}_{2^n}$. Given an initial uncorrelated state $\rho^{in} = \rho_A^{in} \otimes \rho_B^{in}$, referring to the scheme of Fig. 1.5, the protocol returns the final state

$$\begin{aligned} \rho^{\text{out}} &= C_U(H_A \otimes \mathbb{I}_B)\rho^{in}(H_A \otimes \mathbb{I}_B)^\dagger C_U^\dagger \\ &= \frac{1}{2^{n+1}} \left(\begin{array}{c|c} \mathbb{I}_{2^n} & \mu U^\dagger \\ \hline \mu U & \mathbb{I}_{2^n} \end{array}\right). \end{aligned} \tag{1.3.14}$$

where we denote by $H = \frac{1}{\sqrt{2}} \begin{pmatrix} 1 & 1 \\ 1 & -1 \end{pmatrix}$ a Hadamard gate to be performed on Alice side, being $C_U = \left(\begin{array}{c|c} \mathbb{I}_{2^n} & 0_{2^n} \\ \hline 0_{2^n} & U \end{array}\right)$ the controlled-U operation [17], where U is the unitary matrix whose trace has to be estimated. It is easy to see that the

[8] In that case, the quantum discord for Gaussian states of continuous variables systems has been considered [65].

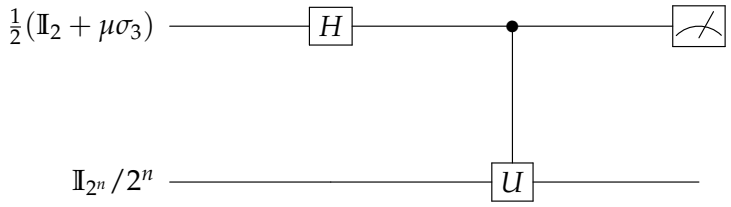

Figure 1.5: DQC1 model with a n-qubit state in a maximally mixed state and an attached ancilla of polarization μ. Measuring σ_1, σ_2 on the ancilla returns the real and imaginary part of $\mathrm{Tr}[U]$.

output state for Alice is

$$\rho_A^{\text{out}} = \frac{1}{2}\begin{pmatrix} 1 & \frac{\mu}{2^n}\mathrm{Tr}[U^\dagger] \\ \frac{\mu}{2^n}\mathrm{Tr}[U] & 1 \end{pmatrix}. \tag{1.3.15}$$

The measurement of the ancilla polarization yields an estimation of the trace of the unitary matrix: $\langle\sigma_1\rangle_{\rho_A^{\text{out}}} = \mathrm{Re}\left[\mathrm{Tr}[U]/2^n\right], \langle\sigma_2\rangle_{\rho_A^{\text{out}}} = \mathrm{Im}\left[\mathrm{Tr}[U]/2^n\right]$. For estimating the trace with error ϵ are necessary $\frac{1}{\mu^2\epsilon^2}$ runs of the protocol, independently of the number of qubits n, while the best classical algorithm requires an exponential number of measurements to obtain the same accuracy [61, 66]. Let us turn our attention to the correlations in the final state of the computation. The entanglement between the ancilla and the n-qubit register is manifestly zero and does not increase with the number of qubits involved (yet, there is entanglement in other bipartitions [62]). On the other hand, the quantum discord across the splitting $A - B$ is monotonically increasing with the polarization of the ancilla, which is the resource of the protocol: $\mathcal{D} \propto \mu$. To evaluate the amount of QC for $n \gg 1$ is not trivial. We will pick the DQC1 model as privileged case study to calculate QC in Secs. 3.2.2, 4.1.4. To date, there is still neither a classical algorithm for estimating the trace of a unitary matrix reaching the same performance of the DQC1, nor a definitive theorem stating that it is impossible to find it. We remark that one could pick a unitary U which does not create QC in the final state [43]. However, in order to reach a quantum speed-up, QC must be created in the intermediate states during the computation, obtained by splitting the unitary and Hadamard gates in a set of operations (for technical details, see

[67]).

Also, QC have been studied as a potential resource for quantum metrology. In particular, by employing mixed separable states with QC rather than classical ones appears to guarantee a better accuracy in the (more general than DQC1) phase estimation protocol [68]. Yet, there is still no solid theoretical proof that the quantum-enhancement in such task is due to QC.

Feature/Resource (state)	Non-local	Entangled	Sep. quantum correlated	Class. correlated
Non-locality	> 0	≥ 0	$= 0$	0
Entanglement	> 0	> 0	$= 0$	0
QC	> 0	> 0	> 0	0
Potential for Quant. Tech.	Yes	Yes	?	No

Table 1.2: Characterisation of states of composite systems based on the degree of correlations between their subsystems and their potential exploitability for quantum technology.

Finally, we anticipate that in the next chapters three main issues will be tackled:

- Problem I: quantum discord, and any other entropic QC measure, are hard to be computed;
- Problem II: the experimental detection of the QC of an unknown state is challenging;
- Problem III: the killer application of QC is missing: there is no full-fledged foundational and operational interpretation for them, and the rationale behind their asymmetry is not well understood.

1.4 Summary of Chapter 1

- It is theoretically proven as well as experimentally tested that the exploitation of entangled states improves our ability to manage information in several ways. Indeed, the usefulness of a particular state of a quantum system for a number of tasks could be traced back to the presence of internal correlations among parts of the system, which correspond to the knowledge that an observer Alice, probing a subsystem A, gains about the state of another

subsystem B, controlled by another observer Bob, and vice versa. An important contribution to the development of Quantum Information and affine disciplines is definitely due to this fundamental result [17, 20].

- Quantum entanglement has been considered for a long time as *the* necessary ingredient for *any* theoretical landmark and experimental quest to beat the limits imposed within the classical scenario [35–37]. However, it has been recently shown that even separable states might play a relevant role in performing better-than-classical communication and information protocols. It is interesting to note that almost all separable states of compound systems are inherently quantum, as their subsystems may share QC, i.e. a statistical dependence which is not described by the classical probabilistic theory. It is interesting to study the foundational and practical merits of QC.

- For pure states, QC equal entanglement, while for mixed states this is not the case. Conversely to entanglement, QC can increase even under local operations on the measured subsystem. The recent literature on the field contains a vast zoology of QC measures, which share some *bona fide* properties [45]. The most popular QC measure is the quantum discord, which has a clear-cut interpretation in information theory: discord equals the difference of the total correlations between two subsystems A and B before and after a local measurement is performed on one of them.

- The current research in QC spans a wide range of questions. Three main problems will be addressed: how to calculate QC in bipartite states of finite dimensional systems, how to evaluate QC in an experiment without knowing the full density matrix of the state; what is a possible physical interpretation of the asymmetry of QC.

CHAPTER 2

Playing with quantum discord and other QC measures

This is a technical chapter, collecting the results reported in [DG1, DG2, DG3]. To evaluate QC is in general computationally demanding. I tackle the problem of quantifying QC in bipartite states of finite dimensional system. First, I provide a general prescription to calculate the quantum discord of two-qubit states (contribution from G. Adesso in the comparison with geometric discord). Then, I investigate the interplay between measures of entanglement and QC, finding an unexpected relation between geometric discord and negativity (the problem was suggested by G. Adesso). I remark that this was one of the first attempts to link QC and entanglement measures. To date, it has been essentially overcome by more solid and ambitious studies on the topic [51, 57, 69]. Finally, I deal with the peculiar asymmetry of QC: I introduce a measure which evaluates the state disturbance of local measurements made on both the subsystems (the initial idea is of M. Paternostro, I acknowledge contributions from him and G. Adesso in deriving the technical results).

2.1 Quantum discord for two-qubit states

2.1.1 Overview

The evaluation of quantum discord is a hard task from a computational point of view, implying an optimization of the conditional entropy $\mathcal{S}(B|\{M^A\})$, and consequently of the post-measurement mutual information defined in Eq. (1.3.10), over all local (generalized) measurements on one party, which is often obtainable by numerical methods only. A closed analytical solution is known in the case of arbitrary two-mode Gaussian states [65], under the restriction of Gaussian local measurements. Narrowing our overview to two-qubit states, an analytical expression of discord has been derived in particular for the subclass of rank-two states [70] and the so-called X-states [71–74]. A successful attempt to generalize this procedure has not been advanced yet [45], apart from an upper bound quantity for the discord defined in [74]. The difficulty in calculating quantum discord motivated the introduction of alternative measures of QC correlations. In particular, the *geometric discord* [43] is one such a measure, which quantifies the amount of QC of a state in terms of its minimal distance from the set of genuinely classical states. The geometric discord involves a simpler optimization and is easily computable for arbitrary two-qubit states. However, its relationship with the original quantum discord is not entirely clear. We are going to present an algorithm to calculate quantum discord for general two-qubit states. First, we obtain an explicit and simplified expression for the conditional entropy, exploiting the Bloch representation of the density matrix; then, we introduce new variables that allow to set the optimization conditions in a closed form. Finally, we associate them to constraints over the eigenvalues of the statistical ensemble obtained after the measurement process. This approach qualifies as the most efficient and reliable way to evaluate quantum discord for arbitrary states of two qubits. Exploiting this algorithm, we perform a numerical exploration of the Hilbert space of two-qubit states to compare quantum discord and the geometric discord as quantifiers of QC. We shed light on the relationship

between these two quantities by identifying the states that extremize geometric discord at fixed quantum discord (and vice versa). We are motivated by the aim of establishing a reliable hierarchy of quantum states based on physically and mathematically consistent criteria. We find that, interestingly, the quantum discord of a two-qubit state never exceeds its (normalized) geometric discord. In analogy with the study of maximal entanglement [75], the notion of maximal QC is measure-dependent. The feasibility in a specific experimental realization will determine which, among the various classes of maximally quantum correlated states, are the most suitable ones to be employed for applications.

2.1.2 Setting

In this section, we restrict our attention to two-qubit states. An analytical algorithm has been proposed for the subclass of states with maximally mixed marginals (described by five real parameters) in [71]. Also, an extension to states spanned by seven real parameters, called X-states because of the peculiar form of their density matrix (with vanishing elements outside the leading diagonal and the anti-diagonal), has been introduced in [72], and amended by [73]. Here, we attempt to generalize the procedure to the entire class of two-qubit states. We focus on projective measurements, for the sake of simplicity[1], even if the least disturbing measurement has been proven to be a rank-one POVM [66].

First, one needs to express the 4×4 density matrix of a two-qubit state in the so-called Bloch form [76, 77]:

$$\begin{aligned} \rho &= \frac{1}{4}\sum_{i,j=0}^{3} R_{ij}\sigma_i \otimes \sigma_j \\ &= \frac{1}{4}\Bigg(\mathbb{I}_4 + \sum_{i=1}^{3} x_i\sigma_i \otimes \mathbb{I}_2 \\ &\quad + \sum_{j=1}^{3} y_j \mathbb{I}_2 \otimes \sigma_j + \sum_{i,j=1}^{3} t_{ij}\sigma_i \otimes \sigma_j\Bigg), \end{aligned} \tag{2.1.1}$$

[1] Note that the difference between the quantum discord calculated by optimising over projective measurements only and the one obtained including POVM is about 10^{-4} [45].

where $R_{ij} = \mathrm{Tr}[\rho(\sigma_i \otimes \sigma_j)]$, $\sigma_0 = \mathbb{I}_2$, σ_i $(i = 1,2,3)$ are the Pauli matrices, $\vec{x} = \{x_i\}, \vec{y} = \{y_i\}$ are the three-dimensional Bloch vectors associated to the subsystems A, B, and t_{ij} denote the elements of the correlation matrix T. We consider that, by performing local unitary transformations, we can recast the density matrix for an arbitrary two-qubit state in the Bloch normal form [71, 78]

$$\begin{aligned} \rho' &= \frac{1}{4}(\mathbb{I}_4 + \sum_i a_i \sigma_i \otimes \mathbb{I}_2 + \sum_i b_i \mathbb{I}_2 \otimes \sigma_i \\ &+ \sum_i c_i \sigma_i \otimes \sigma_i), \end{aligned} \tag{2.1.2}$$

that is a density matrix completely defined by nine real parameters arranged in three 3-dimensional column vectors $\vec{a} = \{a_i\}$, $\vec{b} = \{b_i\}$ and $\vec{c} = \{c_i\}$. This is a consequence of the fact that local unitary operations $\rho' = (U_A \otimes U_B)\rho(U_A \otimes U_B)^\dagger$ correspond to left and right multiplication of the Bloch matrix R with orthogonal matrices [78],

$$R' = \begin{pmatrix} 1 & 0 \\ 0 & O_A^t \end{pmatrix} R \begin{pmatrix} 1 & 0 \\ 0 & O_B \end{pmatrix}, \tag{2.1.3}$$

with $O_{A,B} \in SO(3)$. It is then straightforward to obtain the normal form of Eq. (2.1.2): one needs to calculate the singular value decomposition of the lower diagonal $3 \otimes 3$ block T of R, $T = O_A C O_B^t$, divide O_A and O_B by their respective determinant (to make sure they both have determinant $+1$), and then apply Eq. (2.1.3). The density matrix is correspondingly transformed into the normal form of Eq. (2.1.2), where the c_i are identified with the elements of the diagonal matrix C, which equal the singular values of T. Every two-qubit state can be then transformed in its simplified normal form by means of local unitary transformations (which preserve quantum correlations, both entanglement and QC, by definition), so we restrict our analysis to density matrices of this type without incurring in any loss of generality.

Now, we move to calculate the quantum discord $\mathcal{D}^A$ for generic states in normal

form (from now on, we drop the index A):

$$\begin{aligned}\mathcal{D}(\rho) &= \mathcal{I}(A:B) - \mathcal{C}(B:A) \\ &= \mathcal{S}(A) - \mathcal{S}(A,B) + \min_{\{M^A\}} \sum_k p_k \mathcal{S}(B|\{M_k^A\}).\end{aligned} \tag{2.1.4}$$

The marginal entropy $\mathcal{S}(A)$ and the global entropy $\mathcal{S}(A,B)$ are trivial to obtain. Let us tackle the minimization of the conditional entropy.

2.1.3 General expression of the conditional entropy

Firstly, we have to write the conditional entropy in an explicit form, adopting for convenience the notation in [72]. We remind that a von Neumann measurement (from now on, just measurement) $\{P_k^A\} \equiv \{P_{A,k} \otimes \mathbb{I}_B\}$ sends the state of a two-qubit system in a statistical ensemble $\{p_k, \rho_k \equiv \rho_{B|P_k^A}\}$, such that

$$\rho \to \rho_k = \frac{(P_{A,k} \otimes \mathbb{I}_B)\rho(P_{A,k} \otimes \mathbb{I}_B)}{p_k}, \tag{2.1.5}$$

where

$$\begin{aligned} p_k &= \mathrm{Tr}[\rho(P_{A,k} \otimes \mathbb{I}_B)] \\ P_{A,k} &= V \Pi_{A,k} V^\dagger \\ \Pi_{A,k} &= |k\rangle\langle k|_A, \;\; k = 0,1 \\ V &\in \mathrm{SU}(2). \end{aligned} \tag{2.1.6}$$

The average entropy over the ensemble is written as

$$\begin{aligned} \tilde{\mathcal{S}} &= \sum_k p_k \mathcal{S}(B|\{P_k^A\}) = \sum_k p_k \mathcal{S}(\rho_k) \\ &= p_0 S_0 + p_1 S_1, \end{aligned} \tag{2.1.7}$$

where S_0, S_1 are the entropies associated to ρ_0, ρ_1.

The measurement is defined by the projectors $\{P_k^A\}$ and is consequently parametrized by the elements of the special unitary matrix V, which we write in the basis of

the Pauli matrices:

$$\begin{aligned} V &= v_0 \mathbb{I}_2 + i\vec{v}\cdot\vec{\sigma} \\ &= \begin{pmatrix} v_0 + iv_3 & iv_1 + v_2 \\ iv_1 - v_2 & v_0 - iv_3 \end{pmatrix}. \end{aligned} \tag{2.1.8}$$

We notice that the real vector $\{v_0, \vec{v}\} = \{v_i\}$ has norm one: $\sum_i v_i^2 = 1$, and it is possible to rearrange the four parameters in three variables only, for example in this way:

$$\begin{aligned} h &= v_0 v_1 + v_2 v_3 \\ j &= v_1 v_3 - v_0 v_2 \\ k &= v_0^2 + v_3^2. \end{aligned} \tag{2.1.9}$$

Setting the vectors $\vec{X} = \{2j, 2h, 2k-1\}$ and $\vec{m}_\pm = \{m_{i\pm}\} = \{b_i \pm c_i X_i\}$, we have that, after a straightforward calculation, the conditional entropy takes the expression:

$$\begin{aligned} \tilde{\mathcal{S}} &= -\frac{1}{4}\Bigg\{(1-\vec{a}\cdot\vec{X})\Bigg[\left(1-\frac{|\vec{m}_-|}{1-\vec{a}\cdot\vec{X}}\right)\log_2\left(1-\frac{|\vec{m}_-|}{1-\vec{a}\cdot\vec{X}}\right) \\ &+ \left(1+\frac{|\vec{m}_-|}{1-\vec{a}\cdot\vec{X}}\right)\log_2\left(1+\frac{|\vec{m}_-|}{1-\vec{a}\cdot\vec{X}}\right)\Bigg] \\ &+ (1+\vec{a}\cdot\vec{X})\Bigg[\left(1-\frac{|\vec{m}_+|}{1+\vec{a}\cdot\vec{X}}\right)\log_2\left(1-\frac{|\vec{m}_+|}{1+\vec{a}\cdot\vec{X}}\right) \\ &+ \left(1+\frac{|\vec{m}_+|}{1+\vec{a}\cdot\vec{X}}\right)\log_2\left(1+\frac{|\vec{m}_+|}{1+\vec{a}\cdot\vec{X}}\right)\Bigg]\Bigg\}. \end{aligned} \tag{2.1.10}$$

This result is consistent with the formula provided in the Appendix of [74], but we have reached a simpler expression by exploiting the normal form of the density matrix, Eq. (2.1.2). However, we have to remark that in this picture there is still an amount of redundancy [74]. A projective measurement on a two-qubit state is characterized by two independent variables only, identifiable as the angles θ and ϕ, which parametrize a generic one-qubit pure state as $|\psi\rangle =$

$\cos\theta|0\rangle + e^{i\varphi}\sin\theta|1\rangle$, and the Bloch sphere of coordinates $\{x, y, z\}$ in this way,

$$\begin{cases} x &= 2j = 2\cos\theta\sin\theta\cos\phi \\ y &= 2h = 2\cos\theta\sin\theta\sin\phi \\ z &= 2k - 1 = 2\cos^2\theta - 1. \end{cases} \tag{2.1.11}$$

It is immediate to verify that the following constraint holds

$$k^2 + h^2 + j^2 = k. \tag{2.1.12}$$

The algorithm originally designed for X-states in [72] is flawed, as it does not consider the mutual dependence of h, j, k, thus is reliable only for a more restricted class of states identified in [73].

The above mapping enables us to parameterize the conditional entropy defined in Eq. (2.1.10) as a function of the azimuthal and polar angles θ, ϕ; we then write $\tilde{\mathcal{S}}(h, j, k) = \tilde{\mathcal{S}}(\theta, \phi)$ and perform the optimization of $\tilde{\mathcal{S}}$ over these two independent variables.

2.1.4 Optimization

In accordance with [72], we investigate symmetries in the expression of the conditional entropy. We immediately notice the invariance under the transformation $\theta \to \theta \pm \pi/2$, which is translated in:

$$\begin{cases} k \to 1 - k \\ h \to -h \\ j \to -j. \end{cases} \tag{2.1.13}$$

We appreciate this with an explicit example. Let us pick an arbitrary state, such

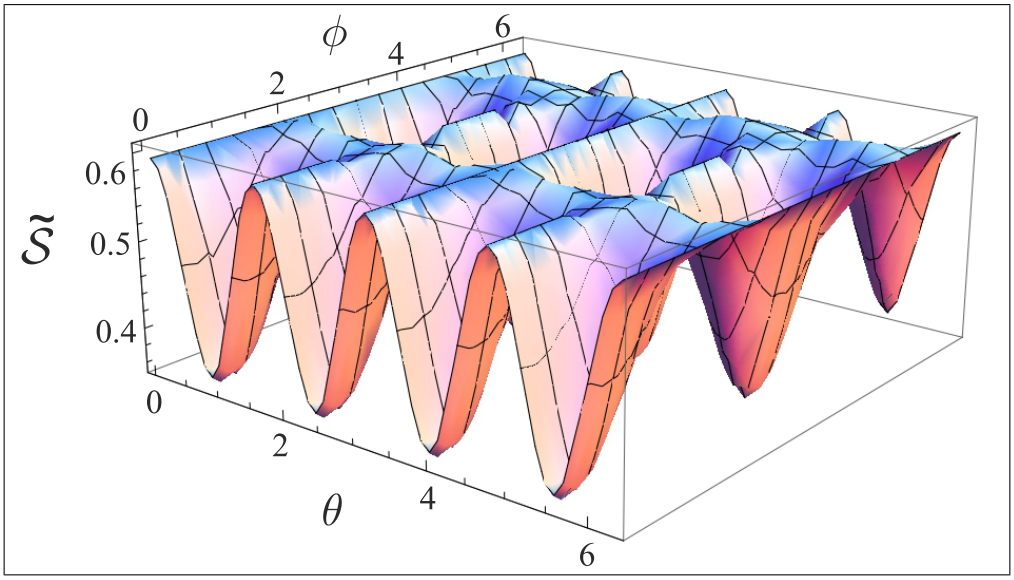

Figure 2.1: (Colours online) Example of conditional entropy $\tilde{\mathcal{S}}$ for the random two-qubit state in Eq. (2.1.14). The angles θ and ϕ parametrize the measurement: we appreciate the symmetry properties of $\tilde{\mathcal{S}}$ with respect to such variables, expressed by the invariance $\tilde{\mathcal{S}}(\theta, \phi) = \tilde{\mathcal{S}}(\theta \pm \pi/2, \phi)$. All the plotted quantities are dimensionless.

as

$$\begin{pmatrix} 0.437 & 0.126+0.197i & 0.0271-0.0258i & -0.274+0.0997i \\ 0.126-0.197i & 0.154 & -0.0115-0.0187i & -0.0315+0.170i \\ 0.0271+0.0258i & -0.0115+0.0187i & 0.0370 & 0.00219-0.0367i \\ -0.274-0.0997i & -0.0315-0.170i & 0.00219+0.0367i & 0.372 \end{pmatrix}; \tag{2.1.14}$$

we operate with local unitary transformations on it, obtaining a new state ρ (albeit with the same entropies and discord) described by the simplified normal form presented in Eq. (2.1.2); we then perform a projective measurement on subsystem A, obtaining an ensemble whose conditional entropy is plotted in Fig. 2.1. One sees that there are no further apparent symmetries for the conditional entropy. The analysis so far, while not being conclusive, allows us just to refine the problem by safely letting the optimization of the conditional entropy to be restricted to the interval $\theta \in [0, \pi/2)$. To determine the minimum of $\tilde{\mathcal{S}}$, we need to calculate its derivatives with respect to θ and ϕ. The dependence on these variables involves logarithms of non-linear quantities, so we do not expect to solve analytically the problem in any case, whatever ingenious

variables we might choose. However, we seek to write the two constraints in a compact and elegant form. Let us impose

$$\begin{cases} p &= \vec{a}\cdot\vec{X} \\ r_+ &= |\vec{m}_+| \\ r_- &= |\vec{m}_-|. \end{cases} \tag{2.1.15}$$

After a bit of algebra, we obtain

$$\begin{aligned} \tilde{\mathcal{S}} &= -\frac{1}{4}\Big\{(1-p-r_-)\log_2(1-p-r_-) \\ &+ (1-p+r_-)\log_2(1-p+r_-) \\ &+ (1+p+r_+)\log_2(1+p+r_+) \\ &+ (1+p-r_+)\log_2(1+p-r_+) \\ &- 4+2\Big(-(1-p)\log_2(1-p) \\ &- (1+p)\log_2(1+p)\Big)\Big\}. \end{aligned} \tag{2.1.16}$$

Now, we set the partial derivatives to zero,

$$\begin{cases} \frac{\partial\tilde{\mathcal{S}}}{\partial\theta} = \frac{\partial\tilde{\mathcal{S}}}{\partial p}\frac{\partial p}{\partial\theta} + \frac{\partial\tilde{\mathcal{S}}}{\partial r_+}\frac{\partial r_+}{\partial\theta} + \frac{\partial\tilde{\mathcal{S}}}{\partial r_-}\frac{\partial r_-}{\partial\theta} = 0 \\ \\ \frac{\partial\tilde{\mathcal{S}}}{\partial\phi} = \frac{\partial\tilde{\mathcal{S}}}{\partial p}\frac{\partial p}{\partial\phi} + \frac{\partial\tilde{\mathcal{S}}}{\partial r_+}\frac{\partial r_+}{\partial\phi} + \frac{\partial\tilde{\mathcal{S}}}{\partial r_-}\frac{\partial r_-}{\partial\phi} = 0\,. \end{cases}$$

Defining the quantities

$$\begin{aligned} \alpha &= \mathrm{Det}\left[\begin{pmatrix} \frac{\partial p}{\partial\theta} & \frac{\partial p}{\partial\phi} \\ \frac{\partial r_+}{\partial\theta} & \frac{\partial r_+}{\partial\phi} \end{pmatrix}\right] \\ \beta &= \mathrm{Det}\left[\begin{pmatrix} \frac{\partial p}{\partial\theta} & \frac{\partial p}{\partial\phi} \\ \frac{\partial r_-}{\partial\theta} & \frac{\partial r_-}{\partial\phi} \end{pmatrix}\right] \\ \gamma &= \mathrm{Det}\left[\begin{pmatrix} \frac{\partial r_+}{\partial\theta} & \frac{\partial r_+}{\partial\phi} \\ \frac{\partial r_-}{\partial\theta} & \frac{\partial r_-}{\partial\phi} \end{pmatrix}\right], \end{aligned} \tag{2.1.17}$$

after some manipulations, the stationarity conditions take the form

$$\begin{cases} \frac{1}{4}\log_2\left(\frac{1+p-r_+}{1+p+r_+}\right)+\frac{1}{2}\log_2\left(\frac{(1+p)(1-p-r_-)}{(1-p)(1+p-r_+)}\right)\frac{\beta}{\alpha+\beta+\gamma}=0 \\ \\ \frac{1}{4}\log_2\left(\frac{1-p-r_-}{1-p+r_-}\right)-\frac{1}{2}\log_2\left(\frac{(1+p)(1-p-r_-)}{(1-p)(1+p-r_+)}\right)\frac{\alpha}{\alpha+\beta+\gamma}=0. \end{cases} \tag{2.1.18}$$

We see immediately that this system is further simplified to

$$\begin{cases} \frac{\log_2\left(\frac{1+p-r_+}{1+p+r_+}\right)}{\beta}+\frac{\log_2\left(\frac{1-p-r_-}{1-p+r_-}\right)}{\alpha}=0 \\ \\ \frac{1}{4}\log_2\left(\frac{1-p-r_-}{1-p+r_-}\right)-\frac{1}{2}\log_2\left(\frac{(1+p)(1-p-r_-)}{(1-p)(1+p-r_+)}\right)\frac{\alpha}{\alpha+\beta+\gamma}=0. \end{cases} \tag{2.1.19}$$

We can still express these equations as relations among the eigenvalues of the ensemble $\{p_k,\rho_k\}$. Calling λ_0^+,λ_0^- the eigenvalues of ρ_0 and λ_1^+,λ_1^- the eigenvalues of ρ_1, we have

$$\begin{aligned} \lambda_0^\pm &= \frac{1}{2}\left(1\pm\frac{r_-}{1-p}\right) \\ \lambda_1^\pm &= \frac{1}{2}\left(1\pm\frac{r_+}{1+p}\right), \end{aligned} \tag{2.1.20}$$

After some straightforward algebra, one shows that the vanishing of the derivatives of $\tilde{\mathcal{S}}$ occurs when the following constraints are satisfied

$$\begin{cases} \lambda_0^- = \dfrac{\left(\frac{\lambda_1^+}{\lambda_1^-}\right)^{\frac{\alpha}{\beta}}}{1+\left(\frac{\lambda_1^+}{\lambda_1^-}\right)^{\frac{\alpha}{\beta}}} \\ \\ \lambda_1^- = \lambda_0^-\left(\frac{\lambda_0^+}{\lambda_0^-}\right)^{\frac{\alpha+\beta+\gamma}{2\alpha}}. \end{cases} \tag{2.1.21}$$

These two transcendental equations can be solved numerically. They represent the most compact formulation to date for the problem of calculating the quantum discord of arbitrary two-qubit states. Let us call s_i the solutions obtained, corresponding to values $\{\theta_i,\phi_i\}$. In order to establish if they represent minima of $\tilde{\mathcal{S}}$, we adopt the conventional method and evaluate the signature of the Hes-

sian matrix H at the points $\{\theta_i, \phi_i\}$, and, in case of $\mathrm{Det}\,[H] = 0$, we study the sign of the functions $\delta_i = \tilde{\mathcal{S}}(\theta, \phi) - \tilde{\mathcal{S}}(\theta_i, \phi_i)$. Naming $\{\theta_{mj}, \phi_{mj}\}$ the angles such that H is positive definite or $\delta_i > 0$, the absolute minimum of the conditional entropy is defined as

$$\min_{\{P_{Bk}\}} \sum_k p_k \mathcal{S}(B|A_{\{P_{Ak}\}}) = \min_{\{\theta_{mj}, \phi_{mj}\}} \tilde{\mathcal{S}}(\theta_{mj}, \phi_{mj}). \tag{2.1.22}$$

The quantum discord for generic two-qubit states of the form of Eq. (2.1.2) finally reads

$$\mathcal{D}(\rho) = \mathcal{S}(A) - \mathcal{S}(A, B) + \min_{\{\theta_{mj}, \phi_{mj}\}} \tilde{\mathcal{S}}(\theta_{mj}, \phi_{mj}). \tag{2.1.23}$$

2.1.5 Geometric discord

It has been argued that the experienced difficulty of calculating quantum discord can be coped, for two-qubit states, with the introduction of its geometric version, called geometric discord [43].

As we have remarked in Sec. 1.3.2, almost all (entangled or separable) states are disturbed by a local measurement on A; however, there is a subclass of states which is invariant and presents zero discord, i.e. the classical-quantum states [39], whose elements have a density matrix of the form $\rho_{CQ} = \sum_i p_i |i\rangle\langle i| \otimes \rho_{B,i}$. A classical-quantum state is not perturbed by a projective measurement on the $\{|i\rangle\}$ basis: $\sum_i \Pi_i^A \rho_{CQ} \Pi_i^A = \rho_{CQ}$.

Letting Ω be the set of classical-quantum two-qubit states, and ρ_{CQ} be a generic element of this set, the geometric discord D_G is defined as the distance between the state ρ and the closest classical-quantum state. In the original definition [43], the (squared) Hilbert-Schmidt distance is adopted. Recalling that $||A||_2^2 = \mathrm{Tr}[AA^t] = \sum_i a_i^2$ is the square of the Hilbert-Schmidt norm of a matrix A with eigenvalues $\{a_i\}$, the geometric discord has been introduced as

$$D_G(\rho) = 2 \min_{\rho_{CQ} \in \Omega} ||\rho - \rho_{CQ}||_2^2. \tag{2.1.24}$$

The quantity D_G in Eq. (2.1.24) vanishes for classical-quantum states and is one

for maximally entangled states $\rho = |\psi\rangle\langle\psi|$, $|\psi\rangle = d^{-1/2}\sum_{j=0}^{d-1}|j\rangle\otimes|j\rangle$. The geometric discord enjoys two nice theoretical interpretations. First, it quantifies the disturbance induced by local von Neumann projective measurements $\Pi^A = \Pi_A \otimes \mathbb{I}_B$ on the subsystem A [79]

$$D_G(\rho) = 2\min_{\Pi^A}\|\rho - \Pi^A(\rho)\|_2^2 . \tag{2.1.25}$$

Moreover, it can be recast as the (Hilbert-Schmidt) distance of a state from itself after the action of a "root-of-unity" local unitary operation[2] on Alice $U^A = U_A \otimes \mathbb{I}_B$ [80]:

$$D_G(\rho) = 2\min_{U^A}\|\rho - U^A\rho U^{A\dagger}\|_2^2 . \tag{2.1.26}$$

We again remark that D_G is not symmetric under subsystems swapping: performing the measurement on Bob rather than on Alice would lead to define another class of QC signatures.

More important, it is possible to obtain an explicit closed expression of D_G for two-qubit states. Reminding Eq. (2.1.1), it is shown in [43] that the geometric discord is given by

$$D_G(\rho) = \frac{1}{2}(||\vec{x}\vec{x}^t||_2 + ||T||_2^2 - k), \tag{2.1.27}$$

with k being the largest eigenvalue of the matrix $\vec{x}\vec{x}^t + TT^t$ (in case of measurement on Bob, one needs to replace $\vec{x}$ with $\vec{y}$ and TT^t with T^tT). Such an expression in Eq. (2.1.27) can be also recast as the solution to a variational problem [79]: namely, for two qubits,

$$D_G = 2\left(\mathrm{Tr}[C^tC] - \max_A \mathrm{Tr}[AC^tCA^t]\right) , \tag{2.1.28}$$

where $C = R/2$ and the maximum is taken over all 2×4 isometries $A = \frac{1}{\sqrt{2}}\begin{pmatrix} 1 & \vec{a} \\ 1 & -\vec{a} \end{pmatrix}$, with $\vec{a}$ a three-dimensional unit vector.

[2] Unitaries whose eigenvalues are permutations of roots of unity.

We will show in Ch. 3 that we may do even better than this, by writing geometric discord in terms of observable quantities. It is easy to see that D_G in [43] was not normalized to one: its maximum value was $1/2$ for two-qubit states. So we found natural to add the factor 2, in order to make a comparison with the quantum discord $\mathcal{D}$.

Potential issues with the geometric discord

It is important to discuss the consistency of geometric discord D_G as a reliable estimator of QC. Recent works have shown that measures built on the Hilbert-Schmidt norm, as geometric discord is, can increase under local reversible operations on the unmeasured subsystem, being biased by the purity of the global state [81, DG10]. This is contrast with one of the *bona fide* criteria for QC measures (Sec. 1.3.2). In spite of that, geometric discord is still a useful signature of QC in a number of relevant cases. For example, it can be safely used to investigate correlations between system and environment in open quantum evolutions, which are globally unitary thus leaving the purity unchanged. Even for a bipartite state under local decoherent evolutions, as studied in Ch. 3, the geometric discord enjoys common dynamical behaviour with other full fledged measures of QC [35, 52, 82]. Specifically, for a system of two qubits (keeping the dimension fixed), as in our case, the problem highlighted in [81] does not occur. Also, it has been shown that D_G is a valid lower bound to measures of QC based on relative entropy [45].

2.1.6 Comparison between quantum discord and geometric discord

We use our results to compare the quantum discord $\mathcal{D}$ with the geometric discord D_G for general two-qubit states [3]. We have generated up to 10^6 random two-qubit states. After transforming each of them into the normal form of Eq. (2.1.2), we have calculated their quantum discord $\mathcal{D}$, as numerically ob-

[3] A similar study has been recently attempted in J. Batle, A. Plastino, A. R. Plastino, and M. Casas, arXiv:1103.0704, albeit without identification of the extremal states.

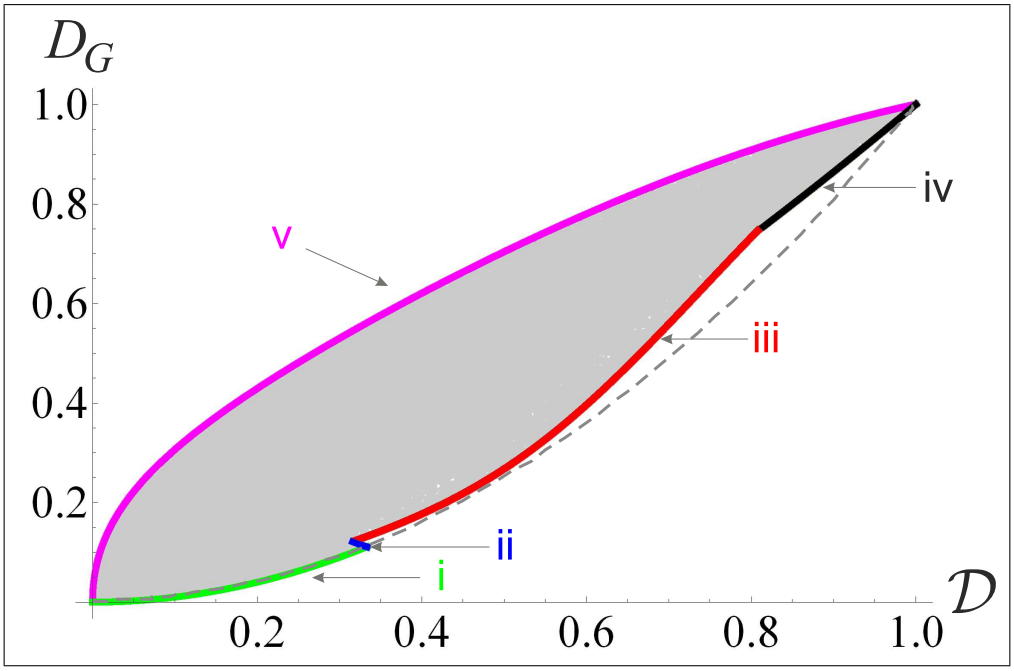

Figure 2.2: (Colours online) Comparison between normalized geometric discord D_G and quantum discord $\mathcal{D}$ for 10^6 randomly generated two-qubit states. The dashed line is obtained by taking the equality sign in Eq. (2.1.30). Refer to the main text for details of the other boundary curves. All the plotted quantities are dimensionless.

tained from the algorithm of Sec. 2.1.4, and their normalized geometric discord D_G. The latter admits an explicit analytic expression for states ρ in normal form, derived from Eq. (2.1.27):

$$D_G(\rho) = \frac{1}{2}(||\vec{a}\vec{a}^t||_2 + ||\vec{c}\vec{c}^t||_2 - \tilde{k}), \tag{2.1.29}$$

where $\tilde{k}$ is the largest eigenvalue of the matrix $\vec{a}\vec{a}^t + \vec{c}\vec{c}^t$.

The results are shown in Fig. 2.2. We notice that physical states of two qubits fill up a two-dimensional area in the space of the two QC measures, meaning that the two impose inequivalent orderings on the set of mixed two-qubit quantum states; this is reminiscent of the case of entanglement measures (see e.g. [75]). Nevertheless, at fixed quantum discord, the geometric discord admits exact lower and upper bounds (and vice versa). We have identified them numerically.

First of all, we have observed that an interesting relationship holds for arbitrary

two-qubit states,

$$D_G \geq \mathcal{D}^2 \,. \tag{2.1.30}$$

In other words, the quantum discord for any two-qubit state does never exceed the square root of its (normalized) distance from the set of classical-quantum states. The corresponding boundary curve is plotted as a dashed (gray) line in Fig. 2.2. However, we see that such a bound is tight only in the region $0 \leq \mathcal{D} \leq 1/3$, in which it coincides with what we refer to as branch (i) (see Fig. 2.2), while it is not attainable for higher degrees of non-classical correlations. The tight lower bound in the whole $\{\mathcal{D}, D_G\}$ plane accommodates states with minimal geometric discord at fixed quantum discord, or equivalently maximal quantum discord at fixed geometric discord. Such extremal states are constituted by the union of four different families, which sit on branches (i)-(iv) in Fig. 2.2:

(i) (Green online) This branch is filled by so-called α states [83]

$$\rho_\alpha = \begin{pmatrix} \frac{\alpha}{2} & 0 & 0 & \frac{\alpha}{2} \\ 0 & \frac{1-\alpha}{2} & 0 & 0 \\ 0 & 0 & \frac{1-\alpha}{2} & 0 \\ \frac{\alpha}{2} & 0 & 0 & \frac{\alpha}{2} \end{pmatrix}, \quad 0 \leq \alpha \leq 1/3\,, \tag{2.1.31}$$

for which $\mathcal{D}(\rho_\alpha) = \alpha$ and $D_G(\rho_\alpha) = \alpha^2$, thus saturating Eq. (2.1.30).

(ii) (Blue online) This small branch is filled by a subclass of the two-parameter family

$$\rho_r = \begin{pmatrix} (1-a)/2 & 0 & 0 & r/2 \\ 0 & a & 0 & 0 \\ 0 & 0 & 0 & 0 \\ r/2 & 0 & 0 & (1-a)/2 \end{pmatrix}, \tag{2.1.32}$$
$$\frac{1}{3} \leq a \leq \frac{5}{14}\,, \quad \sqrt{4a - 3a^2 - 1}\,,$$

with $r \in \left[\sqrt{4a - 3a^2 - 1},\, \frac{1-a}{3}\right]$ given by the solution to $\frac{2r \tanh^{-1}\left(\sqrt{a^2+r^2}\right)}{\sqrt{a^2+r^2}}$

$+\ln(-a-r+1)-\ln(-a+r+1)+2\tanh^{-1}(r)=0$. The geometric discord of these states is simply $D_G(\rho_r)=a^2$, while their quantum discord is calculated in [83]. We highlight the presence of the "pimple" at the joint between branches (i) and (ii), a recurring feature in the profile of extremal states involving quantum discord [83, 84].

(iii) (Red online) This branch accommodates asymmetric X-states of the form

$$\rho_g=\begin{pmatrix} a & 0 & 0 & \sqrt{a-a^2-ac} \\ 0 & c & 0 & 0 \\ 0 & 0 & 0 & 0 \\ \sqrt{a-a^2-ac} & 0 & 0 & 1-a-c \end{pmatrix}, \qquad a=\frac{1-2c+2c^2-g}{2c},\ 0\leq g\leq 1, \tag{2.1.33}$$

with

$$c\in\left[\frac{1-\sqrt{g}}{2},\frac{1}{2}-\begin{cases}\frac{1}{2}\sqrt{2g-1}, & g>\frac{1}{2};\\ 0, & \text{otherwise;}\end{cases}\right],$$

solution to $8(1-2c)c^2\tanh^{-1}\left(\sqrt{8(c-1)c-2g+3}\right)-4c^2$ $\times\sqrt{8(c-1)c-2g+3}\tanh^{-1}(1-2c)+2\sqrt{8(c-c^2)-2g+3}$ $\times\left(2c^2+g-1\right)\tanh^{-1}\left(\frac{3c-2c^2+g-1}{c}\right)=0$. For these states, $D_G(\rho_g)=g$ and $\mathcal{D}(\rho_g)=\frac{1}{\ln 4}\Big[-\ln(-4c(a+c-1))-2\sqrt{4c(a+c-1)+1}$ $\times\tanh^{-1}\left(\sqrt{4c(a+c-1)+1}\right)-2\ln(1-a)+4a\tanh^{-1}(1-2a)+2\ln(2-2c)-4c\tanh^{-1}(1-2c)\Big]$.

(iv) (Black online) Pure states $\rho_p=|\psi\rangle\langle\psi|_{AB}$ occupy the top-right-most branch, for which the discord equals the marginal von Neumann entropy, $\mathcal{D}(\rho_p)=\mathcal{S}(\rho_A)=-p\log_2 p-(1-p)\log_2(1-p)$, and the geometric discord equals the marginal linear entropy, $D_G(\rho_p)=2(1-\mathrm{Tr}[\rho_A^2])=4\mathrm{Det}\,[\rho_A]=4p(1-p)$, where we have denoted the eigenvalues of the reduced density matrix ρ_A by $\{p,1-p\}$.

On the other hand, the upper boundary (v) in Fig. 2.2, despite being single-

branched, is more involved and we are unable to provide a tractable parametrization of the states that saturate it. They can be sought among symmetric X-states of full rank, but with the two biggest eigenvalues dominating the other two. The extremal curve has been obtained as the result of extensive numerical optimization, in which the parameter space has been finely sliced in discrete intervals of nearly constant discord, and for each interval the datapoint corresponding to the random state with the maximum geometric discord has been selected. Joining all such extremal states we have obtained the smooth (Magenta online) line of Fig. 2.2. The two measures $\mathcal{D}$ and D_G correctly coincide on classical-quantum states Eq. (1.3.12), where both vanish, and on maximally entangled Bell states, where both reach unity.

2.2 Interplay between computable measures of entanglement and QC

2.2.1 Entanglement and QC measures

We stress again that on pure bipartite states of arbitrary quantum systems, entanglement and QC are just synonyms. Both of them collapse onto the notion of lack of information about the system under scrutiny, when only a subsystem is probed. Quantitatively, this implies that any meaningful measure of entanglement or QC should just reduce to some monotonic function of the marginal entropy of each reduced subsystem, when applied to pure bipartite states. The question becomes significantly more interesting for mixed bipartite states. One would expect to find an amount of QC that is no less than some valid entanglement monotone. In this section we prove such an intuition to hold true for a particular choice of quantifiers of entanglement and QC, on arbitrary two-qubit states and on a relevant subclass of two-qudit states.

We recall that a zoo of entanglement measures (say $\mathcal{E}$ the amount of entanglement they aim to quantify) have been introduced [20, 85], and in a more recent

drift several measures have been proposed as well to evaluate the degree of QC (say $\mathcal{Q}$) in composite systems [45]. It seems reasonable to expect that

$$\mathcal{Q} \geq \mathcal{E} \tag{2.2.1}$$

should hold for a *bona fide* chosen pair of quantifiers (see also [69]). However, this claim turns out to be not mathematically fulfilled in some canonical cases. Selecting for instance two well-established entropic quantifiers such as the "entanglement of formation" [86] as an entanglement monotone, and the quantum discord as a measure of QC, one finds that the latter may be greater as well as smaller than the former depending on the states, and no clear hierarchy is established, even in the simple cases of two-qubit systems or two-mode Gaussian states [65]. An interesting study has recently succeeded in describing entanglement, classical and QC under a unified geometric picture [44], by quantifying each type of correlations in terms of the smallest distance (according to the relative entropy) from the corresponding set of states without that type of correlations. For example, the amount of entanglement in a state ρ is given by the relative-entropic distance between ρ and its closest separable state, and it is called *relative entropy of entanglement* [87]. In this context, our expectation holds: the relative entropy of entanglement $\mathcal{E}_R$ is automatically smaller than the so-called relative entropy of quantumness $\mathcal{Q}_R$ [51], which in turn quantifies the minimum relative entropic-distance from the set of purely classically correlated states (a null-measure subset of the convex set of separable states [38]). The latter measure $\mathcal{Q}_R$ has been recently interpreted operationally within an "activation" framework that recognizes the value of QC as the necessary and sufficient resource to generate entanglement with an ancillary system [51] (see also [57]). Such a protocol is sufficiently general to let one define, in a natural way, quantumness measures $\mathcal{Q}_\mathcal{E}$ associated to any proper entanglement monotone $\mathcal{E}$. In this way the question of the validity of Eq. (2.2.1) becomes especially meaningful given the natural compatibility of the involved quantifiers [69]. However, there is a non-trivial optimization step required for the calculation of each $\mathcal{Q}_\mathcal{E}$

that hinders the explicit computability of the desired resources.

Here we choose *computable* measures for entanglement and QC. In the case of entanglement, we adopt the squared "negativity" $\mathcal{N}^2$ [88], which is a measure of abstract algebraic origin, quantifying how much a bipartite state fails to satisfy the positivity of partial transpose (PPT) criterion for separability introduced by Peres and the Horodeckis [89]. In the case of QC, we pick the geometric discord D_G. Both measures are taken to be normalized between 0 and 1. In particular, we introduce the normalised version of the geometric discord for arbitrary mixed states ρ of a $d \otimes d$ quantum system,

$$D_G(\rho) = \frac{d}{d-1} \min_{\rho_{CQ} \in \Omega} \|\rho - \rho_{CQ}\|_2^2 . \tag{2.2.2}$$

Despite the very different origin and nature of these two measures, we prove that Eq. (2.2.1) holds, namely $D_G \geq \mathcal{N}^2$, for arbitrary mixed states of two qubits. Furthermore, we prove that the inequality $D_G \geq \mathcal{N}^2$ extends to arbitrary pure states of two qudits for any higher dimension d. Our results demonstrate an interesting hierarchy between two apparently unrelated quantifiers of quantum correlations, for both of which closed formulas (and experimentally friendly detection schemes, as we will show in Ch. 3) are available on the classes of states considered.

2.2.2 Negativity

According to the PPT criterion [89], if a state ρ of a bipartite quantum system is separable, then the partially transposed matrix ρ^{t_A} is still a valid density operator, namely it is positive semidefinite. The matrix ρ^{t_A} is defined as the result of the transposition performed on only one (A, in this case) of the two subsystems in some given basis. Even though the resulting ρ^{t_A} does depend on the choice of the transposed subsystem and on the transposition basis, the statement $\rho^{t_A} \geq 0$ is invariant under such choices [89]. For $2 \otimes 2$ and $2 \otimes 3$ mixed states [89], for arbitrary $d \otimes d'$ pure states, and for all Gaussian states of $1 \otimes n$ mode continuous

variable systems [90], the PPT criterion is a necessary and sufficient condition for separability and, at the same time, its failure reliably marks the presence of entanglement. In all the other cases, there exist states which can be entangled yet with a positive partial transpose: they are so-called bound entangled states, whose entanglement cannot be distilled by means of local operations and classical communications (LOCC) [91].

On a quantitative level, the negativity of the partial transpose, or, simply, "negativity" $\mathcal{N}(\rho)$ [88, 92] can be adopted as a valid, computable measure of (distillable) entanglement for arbitrary bipartite systems. The negativity of a quantum state ρ of a bipartite $d \otimes d$ system is defined as

$$\mathcal{N}(\rho) = \frac{1}{d-1}(\|\rho^{t_A}\|_1 - 1)\,, \tag{2.2.3}$$

where

$$\|A\|_1 = \mathrm{Tr}[|A|] = \sum_i |a_i| \tag{2.2.4}$$

stands for the 1-norm, or trace norm, of the matrix A with eigenvalues $\{a_i\}$. The quantity $\mathcal{N}(\rho)$ is proportional to the modulus of the sum of the negative eigenvalues of ρ^{t_A}, quantifying the extent to which the partial transpose fails to be positive.

The negativity $\mathcal{N}$ is an easily computable entanglement measure, and it has been proven to be (along with its square $\mathcal{N}^2$) convex and monotone under LOCC [88]. The squared negativity $\mathcal{N}^2$ satisfies a monogamy inequality on the sharing of entanglement for multiqubit systems: for example, given a tripartite system ρ_{ABC}, one has $\mathcal{N}^2(AB|C) - \mathcal{N}^2(A|B) - \mathcal{N}^2(A|C) \geq 0$, where $\mathcal{N}^2(i|j)$ is the entanglement between subsystems i, j. [93]. We observe that picking the square of the negativity as entanglement measure is unconventional, yet necessary in this case: we want to make a mathematically consistent comparison of measures, both acting quadratically on the eigenvalues of the density matrix (compare the expressions in Eq. (2.2.2) and Eq. (2.2.3)).

2.2.3 Geometric discord *vs* Negativity in two-qubit systems

The main result of this Section is:

Theorem. *For every two-qubit state ρ, the geometric quantum discord is always greater or equal than the squared negativity,*

$$D_G(\rho) \geq \mathcal{N}^2(\rho)\,. \tag{2.2.5}$$

Let us review the formulas needed to evaluate the two chosen measures for generic two-qubit states. We remind that the normalized geometric discord D_G, Eq. (2.1.24), takes the form of Eq. (2.1.27). Concerning the negativity $\mathcal{N}$, Eq. (2.2.3), it is known that a two-qubit state ρ is separable if and only if $\rho^{t_A} \geq 0$ [89], and, for entangled two-qubit states ρ, at most one eigenvalue of the partial transpose ρ^{t_A} can be negative [78]. Denoting by $\{\lambda_i\}$ the eigenvalues of ρ^{t_A} in decreasing order, for two-qubit entangled states we have $\lambda_1 \geq \lambda_2 \geq \lambda_3 \geq 0 \geq \lambda_4$ and the negativity of ρ takes the form [88]

$$\mathcal{N} = \|\rho^{t_A}\|_1 - 1 = 2|\lambda_4|\,, \tag{2.2.6}$$

while for separable states ($\lambda_4 \geq 0$) one has $\mathcal{N} = 0$.

We first compare entanglement and QC in the simple instance of pure two-qubit states $\rho^p = |\psi\rangle\langle\psi|$. Up to local unitary operations (which leave correlations invariant), a two-qubit pure state can be written in its Schmidt decomposition, corresponding to a density matrix of the form

$$\rho^p = \begin{pmatrix} \frac{1}{2}\left(\sqrt{1-\mathcal{N}^2}+1\right) & 0 & 0 & \frac{\mathcal{N}}{2} \\ 0 & 0 & 0 & 0 \\ 0 & 0 & 0 & 0 \\ \frac{\mathcal{N}}{2} & 0 & 0 & \frac{1}{2}\left(1-\sqrt{1-\mathcal{N}^2}\right) \end{pmatrix}. \tag{2.2.7}$$

It is straightforward to show that in this case,

$$D_G(\rho^p) = \mathcal{N}^2(\rho^p) \equiv S_L(\rho^p_A)\,, \tag{2.2.8}$$

where $S_L(\rho^p_A) = 4\mathrm{Det}\,[\rho^p_A]$ denotes the marginal linear entropy of one subsystem in its reduced state. As expected, entanglement and QC correctly coincide for pure two-qubit states, and specifically the two chosen measures (geometric discord and squared negativity) collapse onto the very same quantifier of local lack of purity.

For two-qubit mixed states, our intuition dictates that the amount of QC should exceed entanglement. This is formalized in Theorem 2.2.3, which we are now ready to prove.

Proof. We focus on the case of entangled states, as Eq. (2.2.5) trivially holds when ρ is separable.
First, we have a look at the original formulation of geometric discord in [43]: the closest classical-quantum state $\bar{\chi} \in \Omega$ that achieves the minimum of the Hilbert-Schmidt norm $||\rho - \rho_{CQ}||_2^2$ is such that $\mathrm{Tr}[\rho\bar{\chi}] = \mathrm{Tr}[\bar{\chi}^2]$. Thus, we rewrite Eq. (2.1.24) as

$$\begin{aligned} D_G(\rho) &= 2 \min_{\rho_{CQ}\in\,\Omega} \|\rho - \rho_{CQ}\|_2^2 = 2\left(\mathrm{Tr}[\rho^2] - \mathrm{Tr}[\bar{\chi}^2]\right) \\ &= 2\left(\mathrm{Tr}[\rho^{t_A\,2}] - \mathrm{Tr}[\bar{\chi}^2]\right). \end{aligned} \tag{2.2.9}$$

Then, defining by $\vec{\lambda} = \{\lambda_i\}$ the vector of eigenvalues of ρ^{t_A} in decreasing order ($\lambda_1 \geq \lambda_2 \geq \lambda_3 \geq 0 \geq \lambda_4$), and similarly calling $\vec{\varsigma} = \{\varsigma_i\}$ the vector of eigenvalues of $\bar{\chi}$ ($\varsigma_1 \geq \varsigma_2 \geq \varsigma_3 \geq \varsigma_4 \geq 0$), recalling that the Hilbert-Schmidt norm is invariant under partial transposition [78], we obtain $\sum_{i=1}^4 \varsigma_i^2 = \mathrm{Tr}[\rho^{t_A}\bar{\chi}]$. We further exploit the Hoffman-Wielandt theorem [94], which implies that

$$\|\rho^{t_A} - \bar{\chi}\|_2^2 \geq \sum_{i=1}^4 |\lambda_i - \varsigma_i|^2 = \sum_{i=1}^3 |\lambda_i - \varsigma_i|^2 + (|\lambda_4| + \varsigma_4)^2. \tag{2.2.10}$$

Thus, we have

$$\sum_{i=1}^{4} \varsigma_i^2 = \sum_{i=1}^{4} \lambda_i \varsigma_i. \tag{2.2.11}$$

Now, let us consider the function

$$f(\vec{\lambda}, \vec{\varsigma}) = \sum_{i=1}^{3} \lambda_i |\lambda_i - \varsigma_i| - |\lambda_4|(|\lambda_4| - \varsigma_4); \tag{2.2.12}$$

it is easy to see that, performing an optimization by the Lagrange multipliers method, the minimum of f keeping fixed $|\lambda_4|$ and ς_4 (say f') is reached when $\lambda_1 = \lambda_2 = \lambda_3 = \frac{(1+|\lambda_4|)}{3}$ and $\varsigma_1 = \varsigma_2 = \varsigma_3 = \frac{1-\varsigma_4}{3}$. Hence, we have

$$f'(|\lambda_4|, \chi_4) = (1 + |\lambda_4|) \left(\frac{1 + |\lambda_4|}{3} - \frac{1 - \varsigma_4}{3} \right) - |\lambda_4|(|\lambda_4| - \varsigma_4).$$

Furthermore, by optimizing over ς_4 we obtain f'', which is the minimum of f at fixed $|\lambda_4|$ (which means that the negativity is kept fixed):

$$f''(|\lambda_4|) = \frac{1 + |\lambda_4|}{3} - |\lambda_4| \geq 0. \tag{2.2.13}$$

Finally, the last inequality implies $\sum_{i=1}^{3} \lambda_i |\lambda_i - \varsigma_i| \geq |\lambda_4|(|\lambda_4| - \varsigma_4)$, which implies

$$\sum_{i=1}^{3} \lambda_i |\lambda_i - \varsigma_i| + |\lambda_4|(|\lambda_4| + \varsigma_4) \geq 2|\lambda_4|^2,$$

and thanks to Eq. (2.2.11) this yields

$$\sum_{i=1}^{4} |\lambda_i - \varsigma_i|^2 \geq 2|\lambda_4|^2, \tag{2.2.14}$$

which is equivalent to Eq. (2.2.5), thus demonstrating the claim. This concludes the proof of Theorem 2.2.3 for all two-qubit mixed states. □

To illustrate the comparison between geometric discord and squared negativity, we plot in Fig. 2.3 the physical region filled by 10^5 randomly generated two-qubit states in the space D_G versus $\mathcal{N}^2$. Along with the (red online) lower

bound emerging from Theorem 2.2.3, saturated by pure states (Eq. (2.2.7)) for which $D_G = \mathcal{N}^2$, we notice the existence of an upper bound as well on D_G at fixed negativity. This shows that the QC (measured by geometric discord) in excess of entanglement (measured by squared negativity) are somehow constrained. Two-qubit states saturating the (green online) upper bound can be sought within the class of rank-two X-shaped density matrices of the form

$$\rho^X = \begin{pmatrix} a & 0 & 0 & \sqrt{ad} \\ 0 & b & \sqrt{bc} & 0 \\ 0 & \sqrt{bc} & c & 0 \\ \sqrt{ad} & 0 & 0 & d \end{pmatrix}, \tag{2.2.15}$$

where $d = 1 - a - b - c$ and $b = \left[2 - 2a - 2c + 2\left(-1 + 6a - 7a^2 + 6c - 18ac - 7c^2 + 4\sqrt{2}\sqrt{ac(-1+2a+2c)^2}\right)^{\frac{1}{2}}\right]/4$, with a and c varying in the parameter range $0 \leq a, c \leq 1/2$, $-1 + 6a - 7a^2 + 6c - 18ac - 7c^2 + 4\sqrt{2}\sqrt{ac}|2a + 2c - 1| \geq 0$. The remaining optimization of D_G at fixed $\mathcal{N}^2$ can be efficiently done numerically.

In the limiting case of separable two-qubit states, $\mathcal{N}(\rho^{sep}) = 0$, the maximum value of the (normalized) geometric discord has been analytically found to be[4]

$$D_G(\rho^{sep}_{opt}) = \frac{1}{4}. \tag{2.2.16}$$

This is achieved by imposing the edge of separability, $\lambda_4 = 0$, that corresponds to $ad = bc$ in Eq. (2.2.15). The maximum D_G is then reached e.g. for $a = c =$

[4]We remark that in the original analysis [43] an attempt has been made to find the two-qubit separable states with maximum geometric discord, within the family of Bell diagonal states (symmetric states with maximally mixed marginals). The edge states identified in that study have been reported to possess an unnormalized geometric discord of $1/6$, which would correspond, in our notation, to $D_G = 1/3$ (thus apparently higher than the tight bound $D_G = 1/4$ that we find here). However, such a reported value is unfortunately wrong, as following the very same analysis of [43] one finds instead for those edge separable Bell diagonal states an unnormalized value of the discord equal to $1/18$, corresponding to $D_G = 1/9$ in our notation. Our analysis plus extensive numerical investigation confirm that no separable two-qubit state can achieve a higher (normalized) geometric discord than $1/4$, and in particular no Bell diagonal separable state can come even close to saturate such a bound.

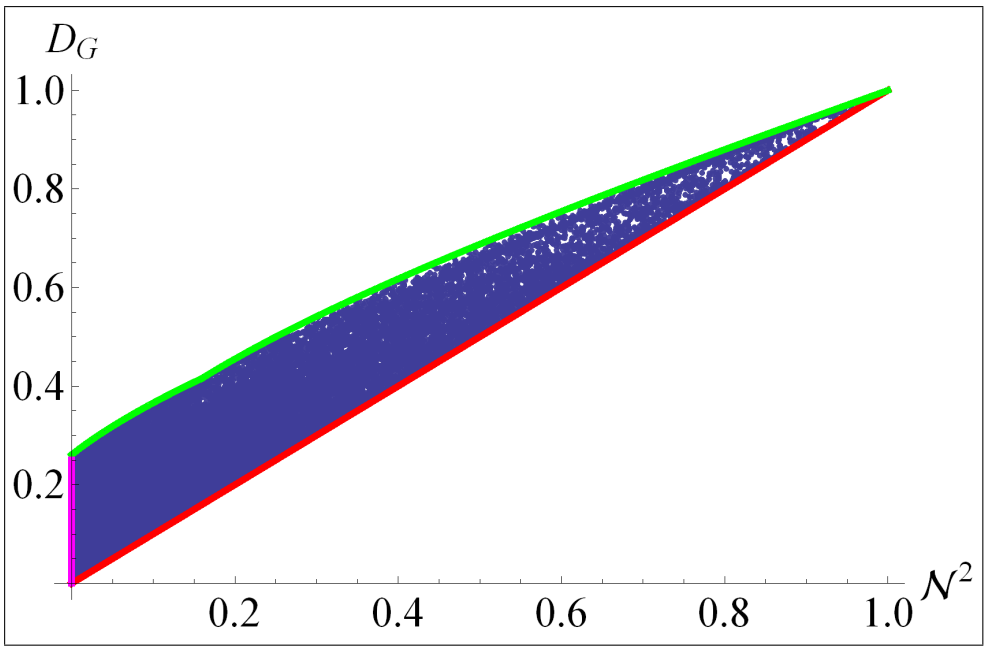

Figure 2.3: (Colours online) Geometric quantum discord D_G versus squared negativity $\mathcal{N}^2$ for 10^5 randomly generated states of two qubits. The lower boundary (red online) in both plots accommodates pure states. The upper boundary (green online) is saturated by a subclass of rank-two states of the form Eq. (2.2.15), while the (magenta online) vertical side line at $\mathcal{N}^2 = 0$ is filled by separable states yet with non-zero QC, which reach up to the value $D_G = 1/4$ on states of the form Eq. (2.2.17). All the plotted quantities are dimensionless.

$\frac{1}{8}\left(2+\sqrt{2}\right)$. Notice that the corresponding state ρ_{opt}^{sep},

$$\rho_{opt}^{sep} = \begin{pmatrix} \frac{1}{8}\left(2+\sqrt{2}\right) & 0 & 0 & \frac{1}{4\sqrt{2}} \\ 0 & \frac{1}{8}\left(2-\sqrt{2}\right) & \frac{1}{4\sqrt{2}} & 0 \\ 0 & \frac{1}{4\sqrt{2}} & \frac{1}{8}\left(2+\sqrt{2}\right) & 0 \\ \frac{1}{4\sqrt{2}} & 0 & 0 & \frac{1}{8}\left(2-\sqrt{2}\right) \end{pmatrix}, \quad (2.2.17)$$

upon swapping the subsystems A and B, becomes of the classical-quantum form of Eq. (1.3.12), which means to be a state with zero D_G, that is a classical-quantum state. This suggests that the maximum geometric discord for two-qubit separable states is obtained on an extremely asymmetric state (the marginal state ${\rho_{opt}^{sep}}_A$ is maximally mixed, while the marginal state of subsystem B is quasi-pure, $\mathrm{Tr}\left[{\rho_{opt}^{sep}}_B^{\,2}\right] = 3/4$), that displays no signature of QC at all if subsystem A rather than B is probed by local measurements. The example in Eq. (2.2.17) is

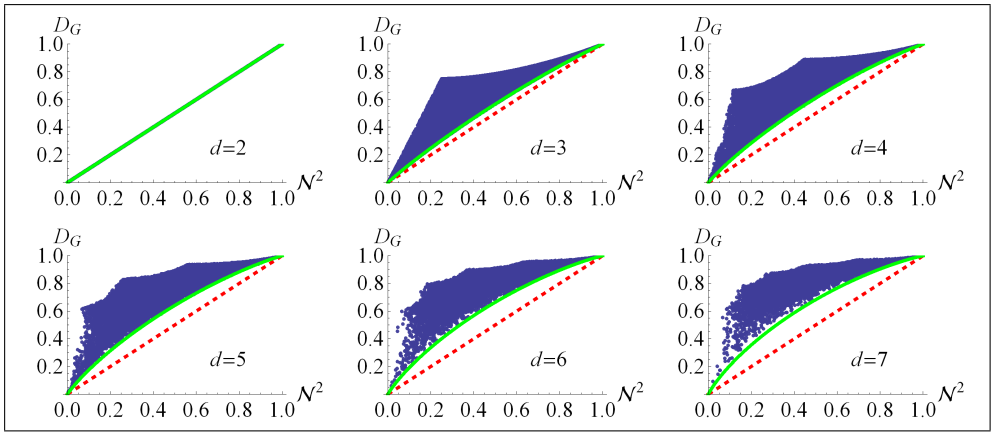

Figure 2.4: (Colours online) Geometric quantum discord versus squared negativity for 3×10^4 (per panel) randomly generated states pure states of two qudits with $d = 2, \ldots, 7$. The two measures coincide for $d = 2$ (pure two-qubit states). The dashed line (red online) $D_G = \mathcal{N}^2$ is not attainable for intermediate values of both measures, while a tighter lower bound (solid green online) on D_G exists at fixed negativity, given by Eq. (2.2.25). Such a bound is saturated by states with Schmidt decomposition as in Eq. (2.2.24). The upper bound on D_G at fixed negativity is more structured. Notice that the plots in this Figure can be also interpreted as the span of the pair of entanglement measures τ_2 [95] *vs* $\mathcal{N}^2$ [88] for two-qudit pure states. All the plotted quantities are dimensionless.

just one of an entire class of two-qubit states that enjoy the same property [51].

The full allowed range $0 \leq D_G \leq 1/4$ for the geometric discord of separable states (magenta line in Fig. 2.3) can be spanned for instance by mixtures of the form $\rho_p^{sep} = p\rho_{opt}^{sep} + (1-p)I/4$, with $0 \leq p \leq 1$, for which $D_G(\rho_p^{sep}) = p^2/4$.

2.2.4 Geometric discord *vs* Negativity in higher-dimensional systems

We provide extensions of the results of the previous Section to pure states of $d \otimes d$ and $d \otimes d'$ systems.

Pure $d \otimes d$ states

We first generalize Theorem 2.2.3 to arbitrary pure states of two qudits. Namely, we prove the following theorem.

Theorem. *For every pure two-qudit state* $|\psi\rangle \in \mathbb{C}^d \otimes \mathbb{C}^d$, *the geometric quantum*

discord is always greater or equal than the squared negativity,

$$D_G(\psi) \geq \mathcal{N}^2(\psi)\,. \tag{2.2.18}$$

Proof. Any pure state $|\psi\rangle \in \mathbb{C}^d \otimes \mathbb{C}^d$ is rewritten without loss of generality in the Schmidt decomposition [17]:

$$|\psi\rangle = \sum_{j=0}^{d-1} \sqrt{\alpha_j}|j\rangle \otimes |j\rangle\,, \tag{2.2.19}$$

where the Schmidt coefficients are probability amplitudes, $\sum_j \alpha_j = 1$.

The geometric discord Eq. (2.1.24) is computed in this case in accordance with Luo and Fu [79, 96] as well as our general formula Eq. (2.2.2). The closest classical state to $|\psi\rangle$, entering the definition Eq. (2.1.24), turns out to be the completely uncorrelated state $\rho^{\otimes} = \rho_A \otimes \rho_B$, obtained as the tensor product of the marginal states $\rho_A = \mathrm{Tr}_B(|\psi\rangle\langle\psi|)$ and $\rho_B = \mathrm{Tr}_A(|\psi\rangle\langle\psi|)$. This implies

$$D_G(\psi) = \frac{d}{d-1}\left(1 - \sum_i \alpha_i^2\right) = \frac{2d}{d-1}\sum_{j>i}\alpha_i\alpha_j\,. \tag{2.2.20}$$

Meanwhile, the negativity (Eq. (2.2.3)) is given by [88]

$$\begin{aligned}\mathcal{N}(\psi) &= \frac{1}{d-1}\left[\left(\sum_i \sqrt{\alpha_i}\right)^2 - \sum_i \alpha_i\right] \\ &= \frac{1}{d-1}\left[\left(\sum_i \sqrt{\alpha_i}\right)^2 - 1\right].\end{aligned} \tag{2.2.21}$$

We know from [97] that an inequality holds:

$$4\sum_{j>i}\alpha_i\alpha_j \geq \frac{2}{d(d-1)}\left[\left(\sum_i \sqrt{\alpha_i}\right)^2 - 1\right]^2, \tag{2.2.22}$$

and we obtain

$$2\frac{d}{d-1}\sum_{j>i}\alpha_i\alpha_j \geq \frac{1}{(d-1)^2}\left[\left(\sum_i \sqrt{\alpha_i}\right)^2 - 1\right]^2 . \tag{2.2.23}$$

The left side is the normalized geometric discord, while on the right we have the normalized squared negativity. □

We have already seen that for $d = 2$, the two measures D_G and $\mathcal{N}^2$ indeed coincide on pure states. However, for any $d > 2$, the geometric discord is strictly larger than the negativity. This seems to go against the expectation that QC should reduce to entanglement on pure states. In fact, D_G does reduce to an entanglement measure on two-qudit pure states, but such a measure is different from the squared negativity for $d \geq 3$. The pure-state entanglement monotone that takes the very same expression as in Eq. (2.2.20) is a particular coefficient τ_2 of the characteristic polynomial of the non-trivial block of the Gram matrix of pure two-qudit states (see [95] for details). Such a measure has not been studied for mixed states, and it is an interesting (yet technically challenging) open problem to see whether the hierarchy $D_G \geq \tau_2$ holds for two-qudit mixed states beyond $d = 2$.

Coming back to our measures of choice in this Chapter, geometric discord and squared negativity, we visualize their interplay on pure two-qudit states with increasing d. We have generated a large ensemble of two-qudit states up to $d = 7$ with random Schmidt coefficients. At fixed negativity, the geometric discord displays both upper and lower bounds. The upper bounds are multi-branched, with an increasing number of nodes appearing with increasing d. The lower bounds are regular curves lying strictly above the bisector for any $d > 2$, with $D_G = \mathcal{N}^2$ occurring only at the extremal points where both vanish (on factorized states) or both reach the maximum (on maximally entangled states). We find that, for any d, the pure two-qudit states that achieve the minimum geometric discord at fixed negativity (green curve in Fig. 2.4) have a pe-

culiar distribution of Schmidt coefficients:

$$\begin{aligned} \alpha_0 &= \sin^2\theta\,, \\ \alpha_i &= \frac{\cos^2\theta}{d-1} \;\; \forall\, i = 1,\ldots,d-1\,, \end{aligned} \tag{2.2.24}$$

with $\arccos\sqrt{(d-1)/d} \leq \theta \leq \pi/2$. Since this is true for every pure state in the special case $d = 2$, this is a further proof that on two-qubit pure states D_G equals $\mathcal{N}^2$ as observed in the previous Section. The lower bound on D_G at fixed $\mathcal{N}$ as saturated by the states of Eq. (2.2.24) is given by

$$\begin{aligned} D_G^{low}(\mathcal{N}) &= [2(d-R-1)+(d-2)(d-1)\mathcal{N}] \\ &\times \left[2\left((d-1)^2+R\right)-(d-2)(d-1)\mathcal{N}\right] \\ &\times \left[(d-1)^2 d^2\right]^{-1}\,, \end{aligned} \tag{2.2.25}$$

with $R = \sqrt{(d-1)^2(1-\mathcal{N})[1+(d-1)\mathcal{N}]}$.

Generic $d \otimes d'$ states

Encouraged by the previous results, one could conjecture that of the inequality $D_G \geq \mathcal{N}^2$ holds even for generic mixed states of arbitrary $d \otimes d'$ dimensional systems, i.e. for arbitrary bipartite states of any dimension. Indeed, it might be interesting to uncover an universal ordering relationship between the two measures. In this case, the geometric discord could be computed according to the prescription of [98], while the negativity still captures all entanglement potentially present in the states [89]. However, a disprove and a counterexample to such a conjecture recently appeared in [99].

2.3 Symmetric measure of QC

2.3.1 A *strongly* faithful QC measure

It is legit to wonder if the inherent asymmetry of quantum discord and geometric discord is a serious limitation to catch all the quantum properties of the given state of a compound system and, on a foundational perspective, if correlations should depend on which party of the system is probed. We will provide an argument for the latter issue in Ch. 4, while here we focus on the former one. One would be tempted to just pick $\min[\mathcal{D}^A, \mathcal{D}^B]$ as a reliable symmetric measure of QC, but such quantity still vanishes for classical-quantum states, even if they really show some quantumness. On the other hand, the quantity $\max[\mathcal{D}^A, \mathcal{D}^B]$ would overestimates QC. Thus, it is preferable to extend the paradigm of QC to the case in which the measurement is made on *both* Alice and Bob at the same time. We will then obtain a measure which is symmetric with respect to the swapping the subsystems as well as vanishing *only* on classical-classical states (we call this property strong faithfulness).

Motivated by these premises, we assess the characterization of QC focusing on the paradigmatic instance of two-qubit states. A QC measure that is symmetric has been introduced in [41] and called MID (Measurement-induced disturbance). Unfortunately, this quantity is flawed and overestimate QC, as we are going to show. We first deploy a quantitative benchmarking test of quantum discord and MID as tools to investigate the interplay between QC and global state mixedness. We find that the non-optimized nature of MID makes such indicator unfaithful, being non-zero and even maximal on some classical-classical states. On the other hand, due to its asymmetric definition [35], discord is not strongly faithful, as it does not reliably detect the fine discrimination between classical-classical and so-called *classical-quantum* states [39], which still possess some quantum correlations, but exhibit zero discord. We thus propose to employ an *ameliorated* version of MID as a measure of QC, which we refer to as "AMID", operatively associated to the minimal state disturbance upon joint

local measurements (in the spirit of [39, 40]). AMID is symmetric by construction, plays a clear role as quantum complement to the "classical mutual information", and vanishes on and only on all classical-classical states, yielding a strongly faithful quantification of QC.

Reaching beyond the recent efforts of [83], and inspired by an analogous earlier study of maximally entangled mixed states (MEMS) [75], we furthermore identify and characterize rigorously the maximally quantum-correlated mixed states of two qubits at given values of the global von Neumann entropy (vNE). In the entropic plane, discord and AMID admit exactly the same (rather structured) set of extremal states. The result provides hints of the maximal robustness of two-qubit QC against decoherence. Our investigation sheds unforeseen light onto a topic of vast theoretical and practical interest. The families of extremal states identified can be experimentally engineered by means of light-atom interfaces [100] or all-optical setups, and the QC are directly measured in laboratory via suitable local detections or computed from the reconstructed (by means of tomography) density matrices [53].

2.3.2 Maximally quantum-correlated mixed states of two qubits: Discord *vs* MID

We saw that discord is, in general, asymmetric as $\mathcal{D}^A \neq \mathcal{D}^B$ with $\mathcal{D}^B$ obtained by swapping the roles of A and B. As we seen in the previous section, no closed formulas are known for $\mathcal{D}^A$ on two-qubit states, other than special cases [71, 72].

Luo introduced MID starting from the observation that a bipartite state containing no QC commutes with the operators describing any complete projective measurement [41]. On the other hand, although a state ρ_{AB} may be intrinsically quantum, any complete bi-local projective measurement makes it classical as a result of a decoherence-by-measurement process [41]. The least disturbing measurement is conjectured to be a bi-local projection which leaves invariant the marginal states of Alice and Bob. If $\rho_A = \sum_k p_k \Pi_{A,k}$ and $\rho_B = \sum_l p_l \Pi_{B,l}$, MID is then defined by restricting the attention to the complete projective mea-

surement $\{\Pi \equiv \Pi_{AB,kl} \equiv \Pi_{A,k} \otimes \Pi_{B,l}\}$ determined by the eigenprojectors $\Pi_{j,k}$ of ρ_j (k=1, 2), and reads

$$\begin{aligned} \mathcal{M}(\rho) &= \mathcal{I}(\rho) - \mathcal{I}(\rho^{\Pi}) \\ &= \Big(\mathcal{S}(\rho_A) + \mathcal{S}(\rho_B) - \mathcal{S}(\rho)\Big) - \Big(\mathcal{S}(\rho_A^{\Pi}) + \mathcal{S}(\rho_B^{\Pi}) - \mathcal{S}(\rho^{\Pi})\Big) \\ &= \mathcal{S}(\rho^{\Pi}) - \mathcal{S}(\rho)\,, \end{aligned} \tag{2.3.1}$$

where $\rho^{\Pi} \equiv \rho_{AB}^{\Pi}$ is the state resulting from the application of Π_{AB}. Note that the second step is due to the invariance of the marginal states: $\mathcal{S}(\rho_{A,B}^{\Pi}) = \mathcal{S}(\rho_{A,B})$.

We begin our analysis by investigating QC versus global state mixedness (vNE) for two qubits, looking in particular for the families of extremal states [5]. We have generated up to 2×10^6 random two-qubit density matrices, uniformly in the space of Hermitian, positive semidefinite matrices, and for each of them we have evaluated $\mathcal{S}$, $\mathcal{M}$ (analytically) and $\mathcal{D}^A$ (numerically). Most notably, although our study has been performed using unconstrained density matrices, we have found that the so-called X states of the form

$$\rho^X = \begin{pmatrix} \rho_{11} & 0 & 0 & \rho_{14} \\ 0 & \rho_{22} & \rho_{23} & 0 \\ 0 & \rho_{23}^* & \rho_{33} & 0 \\ \rho_{14}^* & 0 & 0 & \rho_{44} \end{pmatrix}, \quad \text{with} \quad \sum_{j=1}^{4} \rho_{jj} = 1\,, \tag{2.3.2}$$

allow us to span the whole physically-allowed regions of the planes studied in this work, boundaries included. We will thus use the states in Eq. (2.3.2) as our starting ansatz to seek analytical candidates to be the extremal states. A posteriori, this appears as a natural choice, as all known MEMS [75] and states that maximize discord at fixed entanglement [83] fall into this class.

In Fig. 2.5 (a) we plot the distribution of discord versus vNE for a sample of 2×10^5 random two-qubit states. Although a profile similar to the one for $\mathcal{D}^A$ *vs* linear entropy is retrieved [83], including the peculiar region around $\mathcal{S} = \log_2 3$

[5] A similar study has been recently pursued for discord vs linear entropy [83]. Here we use vNE as a more "compatible" measure of mixedness, given the entropic nature of $\mathcal{D}$ and MID.

where discord increases at the expense of entanglement [75], we reveal interesting differences regarding the classes of extremal states drawing the boundary of the physically allowed area. These have been determined, in our investigation, by looking for the conditions to impose on ρ^X so as to achieve the absolute maximum of $\mathcal{D}^A$ at fixed $\mathcal{S}$. Recalling that analytic expressions for the discord of X states are available [72], the problem is efficiently solved using the Lagrange-multiplier method, in a way similar to [75], and searching for the stationary points of the function $\mathcal{D}^A(\rho^X)+\lambda(\mathcal{S}(\rho^X)-\tilde{\mathcal{S}})$ with $\tilde{\mathcal{S}} \in [0,2]$ being an assigned value of vNE. The solution is analytical and the resulting boundary states are presented in the following.

2.3.3 Derivation of MQCMS

We detail the analytical derivation of the maximally quantum correlated mixed states (MQCMS) collected in Table 2.1. Within the family of X states of two qubits Eq. (2.3.2), we focus on the class of generalized Bell states ρ^B [75], defined by

$$\begin{aligned} \rho^B_{11} &= \rho^B_{44} = (\lambda_1+\lambda_3)/2, \quad \rho^B_{22} = \lambda_2, \quad \rho^B_{33} = \lambda_4, \\ \rho^B_{14} &= (\lambda_1-\lambda_3)/2, \quad \rho^B_{23} = 0\,, \end{aligned} \tag{2.3.3}$$

up to permutations of the eigenvalues λ_i. This class encompasses all known types of MEMS for various measures of mixedness and entanglement [75], as well as the maximally discordant states at given entanglement of formation [83]; furthermore, our numerical simulation reveals that states of the form Eq. (2.3.3)

ρ	$\mathcal{S}(\rho \equiv \rho_{AB})$	colour
ρ^R with $0 \le a \le \frac{1}{3}$, $r = r^\star(a)$	$[0, 0.9231)$	black
ρ^W with $0 \le f \le 1$	$[0.9231, 1.410)$	red
ρ^P with $b = 0$	$[1.410, 1.497)$	blue
ρ^P with $0 \le b \le 1$, $a = a^\star(b)$	$[1.497, 1.585)$	green
ρ^W with $-\frac{1}{3} \le f \le 0$	$[1.585, 2]$	red

Table 2.1: Maximally quantum-correlated mixed states of two qubits, corresponding range of the von Neumann entropy, and colour code for the curves in Fig. 2.5(a),(c); the values of the parameters $a^\star$ and $r^\star$[6].

alone are able to fill the whole upper region in the physically allowed $\mathcal{D}^A vs\ \mathcal{S}$ diagram, thus a posteriori confirming the validity of the ansatz.

We proceed by applying the method of Lagrange multipliers to find stationary points of the discord of such states at fixed global vNE. Since they are X states, one determines their discord $\mathcal{D}^A$ by using the algorithm presented in [72]. We have $\mathcal{D}^A(\rho^B) = \min\{d_1, d_2\}$, where d_1, d_2 are functions of the eigenvalues $\vec{\lambda} \equiv \{\lambda_i\}$. The first term is given by:

$$
\begin{aligned}
d_1(\vec{\lambda}) &= -\left[4(\lambda_1+2\lambda_2+\lambda_3)\left(\lambda_1+\lambda_3+2\lambda_4\right)\right]^{-1}\left(\left(\lambda_2-\lambda_4\right)^2-1\right) \\
&\times \left[\left|3\lambda_2+\lambda_4-1\right|\log_2\left(\frac{2\left(\lambda_2-\lambda_4+1\right)}{\left|3\lambda_2+\lambda_4-1\right|+\lambda_2-\lambda_4+1}-1\right)-2\left|\lambda_1-\lambda_3\right|\right. \\
&\times \log_2\left(-\frac{\left|\lambda_1-\lambda_3\right|+\lambda_2+\lambda_4-1}{\left|\lambda_1-\lambda_3\right|+\lambda_1+\lambda_3}\right)+\left|\lambda_2+3\lambda_4-1\right| \\
&\times \log_2\left(-\frac{2\left(\lambda_2-\lambda_4-1\right)}{\left|\lambda_2+3\lambda_4-1\right|-\lambda_2+\lambda_4+1}-1\right)-2\left|\lambda_2-\lambda_4\right| \\
&\times \log_2\left(\frac{2\left(\lambda_2+\lambda_4\right)}{\left|\lambda_2-\lambda_4\right|+\lambda_2+\lambda_4}-1\right)+\log_2\left(\left(\left(\lambda_2-\lambda_4\right)^2-1\right)^2\right) \\
&- \log_2\left(\lambda_2\lambda_4\right)+\log_2\left(\frac{1}{\left(\lambda_2+\lambda_4-1\right)^2}\right)+2\log_2\left(-2\lambda_3\left(\lambda_2+\lambda_3+\lambda_4-1\right)\right) \\
&- 2\log_2\left(\left(\lambda_1+2\lambda_2+\lambda_3\right)\left(\lambda_1+\lambda_3+2\lambda_4\right)\right) \\
&+ \lambda_2\left(\log_2\left(\lambda_2\right)-2\log_2\left(\lambda_3\right)+3\log_2\left(\lambda_4\right)+2\log_2\left(-\frac{1}{\lambda_2+\lambda_3+\lambda_4-1}\right)\right) \\
&+ \lambda_4\left(3\log_2\left(\lambda_2\right)+2\log_2\left(\left(\lambda_2-\lambda_4+1\right)\lambda_4\right)\right) \\
&+ \left.\lambda_4\left(-2\log_2\left(\lambda_3\left(\lambda_2-\lambda_4-1\right)\left(\lambda_2+\lambda_3+\lambda_4-1\right)\right)+\log_2\left(\frac{\left(\lambda_1+\lambda_3+2\lambda_4\right)^2}{\left(\lambda_2-\lambda_4+1\right)^2\lambda_4}\right)\right)\right],
\end{aligned}
\tag{2.3.4}
$$

while the second one is

$$
\begin{aligned}
d_2(\vec{\lambda}) &= \frac{1}{2}\left[\sqrt{\left(\lambda_1-\lambda_3\right)^2+\left(\lambda_2-\lambda_4\right)^2}\log_2\left(\frac{1-\sqrt{\left(\lambda_1-\lambda_3\right)^2+\left(\lambda_2-\lambda_4\right)^2}}{\sqrt{\left(\lambda_1-\lambda_3\right)^2+\left(\lambda_2-\lambda_4\right)^2}+1}\right)\right. \\
&+ \log_2\left(\frac{8\left(\lambda_2+\lambda_3+\lambda_4-1\right)^2}{\left(\left(\lambda_2-\lambda_4\right)^2-1\right)\left(\lambda_2^2+\left(2\lambda_3-1\right)\lambda_2+2\lambda_3^2+2\lambda_3\left(\lambda_4-1\right)+\left(\lambda_4-1\right)\lambda_4\right)}\right) \\
&+ \lambda_2\log_2\left(\frac{\lambda_2^2\left(-\lambda_2+\lambda_4+1\right)}{\left(\lambda_2-\lambda_4+1\right)\left(\lambda_2+\lambda_3+\lambda_4-1\right)^2}\right)+2\lambda_3\log_2\left(-\frac{\lambda_3}{\lambda_2+\lambda_3+\lambda_4-1}\right) \\
&+ \left.\lambda_4\log_2\left(\frac{\lambda_4^2\left(-\lambda_2+\lambda_4-1\right)}{\left(\lambda_2-\lambda_4-1\right)\left(\lambda_2+\lambda_3+\lambda_4-1\right)^2}\right)\right].
\end{aligned}
\tag{2.3.5}
$$

Now, we have to set two constraints: the vNE $\mathcal{S}(\rho^B) = -\sum_i \lambda_i \log_2 \lambda_i$ must be equal to a constant $\tilde{\mathcal{S}}$ and the trace of the density matrix must be obviously

equal to one. Therefore, we have to find maxima of the unconstrained functions:

$$\begin{aligned} f_1(\vec{\lambda}) &= d_1(\vec{\lambda}) + \nu(-\tilde{\mathcal{S}} - \sum_i \lambda_i \log_2 \lambda_i) + \mu(1 - \sum_i \lambda_i) \\ f_2(\vec{\lambda}) &= d_2(\vec{\lambda}) + \nu(-\tilde{\mathcal{S}} - \sum_i \lambda_i \log_2 \lambda_i) + \mu(1 - \sum_i \lambda_i). \end{aligned} \tag{2.3.6}$$

After some lengthy but straightforward algebra, we find that the stationary conditions for f_1 are solved by rank-3 states. Local maxima for the constrained discord d_1 are thus obtained in two independent cases:
(i) $\lambda_4 = 0$, corresponding to a two-parameter family of states encompassing the MEMS for the relative entropy of entanglement [75], whose density matrix ρ^R is given by the first line of Eq. (2.3.7); or
(ii) $\lambda_3 = 0$, corresponding to the two-parameter class described in [83], whose density matrix ρ^P is given by the third line of Eq. (2.3.7).

We repeat the same procedure looking for a maximum of f_2. In this case it is not difficult to see that Werner states ρ^W, which satisfy the relation $\lambda_2 = \lambda_3 = \lambda_4 = (1 - \lambda_1)/3$, solve the stationarity conditions, and one verifies that they provide a local maximum for the constrained discord d_2.

Other possible candidates (not equivalent up to local unitary transformations to the above considered classes of states) for MQCMS are excluded as they correspond to local minima, rather than maxima, of either d_1 or d_2 at fixed vNE. We are thus left with a competition between the three main families of Eq. (2.3.7), which we report for completeness: the rank-3 class ρ^R encompassing the MEMS for the relative entropy of entanglement [75], the Werner states ρ^W, and a two-parameter family ρ^P studied in [83]. Their density matrices are as in Eq. (2.3.2) with, respectively,

$$\begin{aligned} \rho^R_{11} &= \frac{1-a}{2}, \quad \rho^R_{22} = a, \quad \rho^R_{14} = \frac{r}{2}, \quad \rho^R_{33} = 0 \\ \rho^W_{11} &= \frac{1+f}{4}, \quad \rho^W_{22} = \rho^W_{33} = \frac{1-f}{4}, \quad \rho^W_{14} = \frac{f}{2} \\ \rho^P_{11} &= \rho^P_{14} = \frac{a}{2}, \quad \rho^P_{22} = \frac{1-a-b}{2}, \quad \rho^P_{33} = \frac{1-a+b}{2}, \end{aligned} \tag{2.3.7}$$

and $\rho_{23}^{R,W,P}$=0. The maximally quantum-correlated mixed states (MQCMS) according to quantum discord are then reported in Table 2.1. We observe an intricate profile of extremely "discordant" two-qubit states at fixed vNE, far more structured than any instance of MEMS, thus showing the non-trivial relation between QC and global state mixedness.

2.3.4 Comparison between quantum discord and MID

Let us now address a similar study when MID is used as a QC indicator. We aim at finding whether MID could be effective in providing a simpler yet meaningful picture of the behaviour of QC in two-qubit mixed states. As shown in Fig. 2.5 (b), we find indeed that the physically allowed region in the $\mathcal{M}$ *vs* $\mathcal{S}$ plane simplifies to a trapezium, whose upper extremity is spanned by two different extremal families only. The states attaining the horizontal (blue online) boundary in Fig. 2.5 (b) belong to the so-called β family [83] $\rho^{\beta} = \beta|\phi_+\rangle\langle\phi_+| + (1-\beta)|\psi_+\rangle\langle\psi_+|$ with $|\phi_+\rangle$=$(|00\rangle+|11\rangle)/\sqrt{2}$, $|\psi_+\rangle$=$(|01\rangle+|10\rangle)/\sqrt{2}$, $\beta\in[0,1]$. They have maximal MID, $\mathcal{M}$=1, regardless of β and thus of $\mathcal{S}$. On the other hand, by simple geometrical considerations, we see that
ρ^{δ}=$\delta\rho^{\beta=1/2}$+$(1-\delta)\mathbb{1}/4$ ($\delta \in [0,1]$), having

$$\mathcal{M}(\rho^{\delta}) = [(1-\delta)\log_2(1-\delta) + (1+\delta)\log_2(1+\delta)]/2 = 2-\mathcal{S}(\rho^{\delta}), \qquad (2.3.8)$$

fill up the diagonal (purple online) side of the trapezium. Quite strikingly, however, the boundary state $\rho^{\beta=1/2}$ and all the ρ^{δ}'s on the oblique edge of the trapezium have strictly $\mathcal{D}^A$=$\mathcal{D}^B$=0 and are thus classical-classical: MID manifestly overestimates QC, failing to meet the essential faithfulness requirement.

2.3.5 Ameliorated MID as a measure of QC

The evident overestimation given by MID, which is a consequence of the "rigidity" of the projective bases used in its definition, urges us to look for a more faithful figure of merit. The natural next step is to consider an *ameliorated* ver-

sion of the measurement-induced disturbance (or AMID) where arbitrary complete projective measurements are performed, locally, on parties A and B, and a subsequent optimization over any possible set of local projectors is achieved. We thus define AMID, for bipartite systems of any dimension, as

$$\begin{aligned} \mathcal{A}(\rho) &= \inf_{\Omega_{AB}} [\mathcal{I}(\rho) - \mathcal{I}(\rho^{\Omega})] = \mathcal{I}(\rho) - \mathcal{I}_c(\rho) \\ \mathcal{I}_c(\rho) &\equiv \sup_{\Omega_{AB}} \mathcal{I}(\rho^{\Omega}), \end{aligned} \tag{2.3.9}$$

where $\Omega_{AB,kl} = \Omega_{A,k} \otimes \Omega_{B,l}$ is an arbitrary complete (bi-local) projective measurement over the composite system. In particular, $\Omega_{A,k}$ and $\Omega_{B,l}$ are not necessarily made out of eigenprojectors and the search for the infimum over the set of Ω_{AB}'s entails the non-trivial optimization missing in MID [41]. Our definition is further motivated by the earlier analyses discussed in [40], where $\mathcal{I}_c$ in Eq. (2.3.9) is recognized as the classical mutual information (optimized over projective measurements), a proper symmetric measure of classical correlations in bipartite states. AMID is thus recast as the difference between total and classical mutual information, which has all the good prerequisites to be a *bona fide* measure of QC. From an operational point of view, the AMID can be interpreted as a measure of inefficiency of local broadcasting, a primitive task that can only be accomplished perfectly with classical-classical states [39].

The evaluation of Eq. (2.3.9) involves solving a double-optimization problem. However, for two qubits the techniques of [71, 72] enable us to streamline the formal apparatus needed for the quantification of AMID, as we made for the one-way discord. Any two-qubit state can be transformed by local unitary transformations (leaving AMID invariant by definition) into the form of Eq. (2.1.2). Also, any projector $\Omega_{j,k}$ for subsystem $j{=}A, B$ is written as $\Omega_{j,k}{=}V_j \Pi_{j,k} V_j^{\dagger}$ with $V_j{=}y_{j,0}\mathbb{1}_j{+}i\vec{y}_j{\cdot}\vec{\sigma}_j$ a special unitary matrix such that $\sum_{p=0}^{3} y_{j,p}^2{=}1$, $y_{j,p}{\in}[-1,1]$. After some operator algebra, one has $\rho'^{\Omega} = (\Omega_{A,k} \otimes \Omega_{B,l})\rho'(\Omega_{A,k} \otimes \Omega_{B,l}) = \Delta_{kl}(\Omega_{A,k} \otimes \Omega_{B,l})/4$, where the vectors γ_j (depending solely on $\vec{y}_j$) are defined

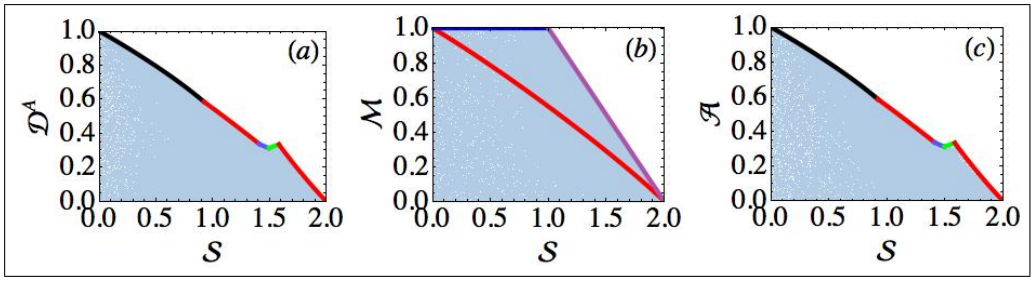

Figure 2.5: (Colours online) (a) Discord, (b) MID, and (c) AMID versus vNE for 2×10^5 random two-qubit states. The boundaries in (a),(c) correspond to the MQCMS of Table 2.1. In (b), the extremal states are ρ^β (horizontal, blue segment) and ρ^δ (oblique, purple segment), while Werner states ρ^W lie on the dashed (red) curve.

by the relation $V_j^\dagger \vec{\sigma}_{j,p} V_j = \alpha_{j,p}\vec{\sigma}_{j,1} + \beta_{j,p}\vec{\sigma}_{j,2} + \gamma_{j,p}\vec{\sigma}_{j,3}$, and

$$\Delta_{kl} = 1 + (-1)^k \vec{a}\cdot\vec{\gamma}_A + (-1)^l \vec{b}\cdot\vec{\gamma}_B + (-1)^{k+l} \sum_{p=1}^{3} \chi_p \gamma_{A,p}\gamma_{B,p}. \tag{2.3.10}$$

It is then convenient to introduce the new set of variables $\kappa_j = y_{j,0}^2 + y_{j,3}^2$, $h_j = y_{j,0}y_{j,1} + y_{j,2}y_{j,3}$, $w_j = y_{j,1}y_{j,3} - y_{j,0}y_{j,2}$ and $l_j = 1 - \kappa_j$, and then define

$$\mu(\kappa_A, h_A, w_A, \kappa_B, h_B, w_B) \equiv \mathcal{I}(\rho') - \mathcal{I}(\rho'^{\Omega}). \tag{2.3.11}$$

By formulating and solving the conditions for stationarity of $\mathcal{A}$, one evaluates AMID numerically. Remarkably, for the relevant class of X states (Eq. (2.3.2)), one finds (numerically) a closed expression of their AMID (as well as of their classical mutual information $\mathcal{I}_c$, see Eq. (2.3.9)):

$$\mathcal{A}(\rho^X) = \min[\mu(1/2, 0, 1/2, 1/2, 0, 1/2), \mu(1, 0, 0, 1, 0, 0)]\,, \tag{2.3.12}$$

thus complementing the results of us and [71, 72] on discord. By construction, one obtains $\mathcal{A} \leq \mathcal{M}$. More important, it is immediately evident that AMID, being intrinsically symmetric, is a strongly faithful measure of genuinely QC, which vanishes if and only if a state is classical-classical as defined in[39], and can be then adopted as a rightfully valid and well motivated alternative to quantum discord. We conclude by studying AMID *vs* vNE for arbitrary two-

qubit random states. Most notably (see Fig. 2.5 (c)), the physically allowed region in the $(\mathcal{S}, \mathcal{A})$ plane is found precisely congruent to the one in the $(\mathcal{S}, \mathcal{D}^A)$ one (Fig. 2.5 (a)) and admits *the same* boundaries (Table 2.1, for those states, $\mathcal{A}=\mathcal{D}^A=\mathcal{D}^B$). We thus promote the interpretation of the set of states in Table 2.1 as two-qubit MQCMS, being simultaneously extremal for discord and AMID, at fixed vNE. This highlights a fascinating connection between such entropic QC indicators, that impose inequivalent orderings on partially quantum states, but yield identical prescriptions for the extremal values at fixed mixedness. Our methods can be extended to reliably investigate QC in higher dimensional systems. On this hand, our contribution to a comparative study of discord, MID, and AMID for two-mode Gaussian states of continuous variable systems has been published in [DG8]. In this respect, we remark that the engineering of MQCMS is feasible via both atom-light interfaces and all-optical setups [100], which adds an appealing feature of experimental demonstrability to our work.

2.4 Summary of Chapter 2

- We have presented a reliable and effective algorithm for the evaluation of the quantum discord $\mathcal{D}$ of two-qubit states. We have simplified the optimization involved in calculating the conditional entropy, by removing the redundant degrees of freedom that are set to zero by means of local unitary transformations in the first place, and by properly taking into account the symmetries of the problem. The optimization problem for the conditional entropy, and equivalently for the discord, is recast into a compact form that implies an elegant relationship among the eigenvalues of the ensemble obtained after the local measurement process on one qubit. The derived transcendental constraints are amenable to direct numerical solution. We have then compared quantum discord with an alternative but affine quantity, the geometric discord D_G, identifying the classes of states with extremal values of geometric discord at fixed quantum discord. For a fixed geometric discord, maximal quantum discord is attained by different families of states depending

on the degree of QC, encompassing pure as well as mixed, symmetric and non-symmetric states. The the hierarchical bound $\mathcal{D} \leq \sqrt{D_G}$ holds for all two-qubit states.

- We have presented a qualitative and quantitative study of entanglement and QC for two-qubit states and for relevant instances of higher-dimensional states. First, we identified a computable measure of entanglement, the squared negativity $\mathcal{N}^2$ [88], and proved that it is always majorized by a compatible measure of QC, the geometric discord D_G [43], in the case of generic two-qubit states. The inequality is saturated for pure states. Then, we explored the pattern of the plane D_G vs $\mathcal{N}^2$, identifying the classes of two-qubit states with maximal geometric discord at fixed negativity. In particular, the bound is reached by a family of X states given in Eq. (2.2.15). Remarkably, for separable states the upper bound accommodates a fully asymmetric state, which is a state becoming a zero-discord classical-quantum state upon swapping of the subsystems. Finally, we extended our analysis to pure states of $d \otimes d'$ systems. For two-qudit pure states, we found that the hierarchy between geometric discord and squared negativity still holds rigorously. We characterized the states with minimal D_G at fixed $\mathcal{N}^2$: they present an elegant parametrization of the distribution of their Schmidt coefficients, allowing to express analytically the lower bound in the D_G vs $\mathcal{N}^2$ plane for any d as in Eq. (2.2.25).

- Going beyond a mere hierarchical state classification, our analysis naturally led to the proposal of adopting AMID, a strongly faithful quantum correlation quantifier linked to minimal state-disturbance after optimized bi-local measurements, and amounting to the quantum counterpart of the classical mutual information [40]. We explicitly computed AMID on X states and provided a recipe to calculate it for arbitrary two-qubit states by numerical simulations. The MQCMS can be rightfully regarded as the two-qubit states whose QC are maximally robust against state mixedness, and could thus to play a key role in realistic (noisy) implementations of quantum information

schemes based on QC as a resource [39, 53, 62].

Acknowledgments

I acknowledge fruitful discussions with V. P. Belavkin, S. Campbell, A. Datta, S. Luo, T. Paterek, F. Plastina, M. Piani, F. L. Semiao, A. Winter and K. Życzkowski.

CHAPTER 3

Experimental detection of Quantum Correlations

After having calculated QC on the paper, it is time to measure them in real world. The chapter comprises the results published in [DG4, DG5, DG6] and is organized in three parts. First, I present a theoretical study of the bipartite QC between a qubit and a d dimensional system, providing a state-independent formula for the geometric discord. I exploit the result to give a general prescription to measure the QC of a state experimentally without full information on its density matrix. Specifically, by introducing properly designed measures, the presented scheme allows us to quantify QC for arbitrary states of $2 \otimes d$ *systems without the need to reconstruct them by tomographic techniques. Then, I take in exam the specifics of the required experimental architecture in the optical and Nuclear Magnetic Resonance settings, discussing possible advantages and limitations in such contexts. Finally, I describe the experimental implementation of my proposal, which has been carried out at the Brazilian Center for Research in Physics (CBPF) of Rio de Janeiro. In particular: I.A. Silva and R. Auccaise performed the experiment, I made the theoretical analysis and all the authors of [DG6] contributed to the general discussion.*

3.1 Experimental measurement of quantum correlations: state of the art

3.1.1 The problem

It is known that entanglement is not directly measurable in laboratory. Indeed, there is not a self-adjoint operator quantifying the amount of entanglement of a state. Hence, an *a priori* knowledge of the density matrix appears necessary to evaluate entanglement. This is a serious drawback, since dealing with high dimensional systems makes the state reconstruction extremely demanding if not unfeasible in terms of required resources. The problem has been overcome by introducing non-trivial lower bounds to entanglement measures, expressed as non-linear functions of the density matrix coefficients, whose values is detected by means of a limited number of measurements [101, 102].

The situation is similar for QC. Qualitatively, we saw that QC are related to the disturbance induced by the measurement process on a physical system [41, 79], while concepts and tools from information theory allow their quantitative evaluation, given the state of the system. At this stage, the natural next step should be to establish a link between theoretical and experimental quantification of QC: One could try to recast a QC measure as a function of observable quantities. Unfortunately, they are all defined by means of a state-dependent optimization and seem not directly associable with Hermitian operators, whilst it is desirable to find ways to evaluate them by means of a smaller number of measurements than the ones required by tomographic techniques. In this direction, appreciable attempts to detect non-vanishing QC by observable witnesses have been realized [53, 63, 103]. In these works, an experimental measurement of a quantity W such that $\langle W \rangle_\rho > 0 \iff \mathcal{Q}(\rho) > 0$ is implemented. However, reminding that almost all states possess QC [38], it still seems worthy to pursue the more informative (but still experimentally manageable) quantitative characterization, given by measuring the amount of QC in the state.

3.1.2 Our solution

An entropic function as the quantum discord is not easily associable to observables, while taking into account distance-based measures offers a solution to such conundrum.

First, we show in Sec. 3.2 that the geometric discord defined in Eq. (2.1.27) admits a neat expression as a function of density matrix elements whose form is state-independent, being the minimisation in Eq (2.1.27) solved explicitly. We also introduce a tight lower bound Q of geometric discord whose formula appears even more manageable.

Then, in Sec. 3.3, we study the feasibility of the direct implementation of the non-tomographic measurement scheme required to detect the value of geometric discord and Q in an unknown state. In particular, we express it as a function of observable quantities $\langle O_i \rangle$, i.e. the expectation values of proper Hermitian operators O_i. The nature and the number of such operators is obviously dependent on the particular setting considered. Two possibilities are taken in exam: first, we focus on the quantum optical setup, which implies to recast Q in terms of expectation values of projectors and swap operators. The number of measurements required is independent of Bob's dimension d, but to carry out a quantum optics experiment appears to be hard. Moreover, we consider the Nuclear Magnetic Resonance (NMR) setting [104], in which we obtain information on the system by means of spin measurements. Here, the protocol allows us a gain (over full state tomography) which is linearly dependent on Bob's dimension. In spite of a minor advantage in terms of number of measurements, the NMR implementation is by far easier to realize than the optical one.

Finally, we experimentally verify the theoretical results by preparing an unknown two-qubit Bell diagonal state [17] (the choice of the state is due to experimental convenience exclusively) in a room temperature NMR system and retrieving the value of geometric discord by means of local measurements over one of the subsystems (Sec. 3.4). In this setting, the information is stored in

magnetic nuclear spins, while transformations and state preparation are implemented by applying highly controllable radio frequency (rf) pulses and magnetic field gradients. On the other hand, the environment affects the spin system by inducing relaxation that drives the system back to the thermal equilibrium distribution. We investigate the robustness of QC in the open quantum system framework, studying their dynamics under phase damping and amplitude damping channels acting separately on each qubit [18], which are the theoretical description of the noise in NMR. It is predicted that in such dynamical model, by appropriately engineering the initial state, QC measures should undergo a *sudden transition* during their evolution [52, 82], exhibiting different regimes of resilience to decoherence under noisy conditions. We carry out a comprehensive analysis of QC, by monitoring the evolution of geometric discord [43], a tight lower bound of it and the *negativity of quantumness*. The latter measure, introduced in [51] and discussed in detail in [105], is here investigated for the first time in open systems. Whenever the measured subsystem is a qubit, the negativity of quantumness equals the minimum trace distance from the set of zero-discord states. It is unfortunately harder to compute and less accessible experimentally then geometric discord and its lower bound: to measure it from direct data without tomography, we need a partial knowledge of the form of the state, specifically the fact that it is a Bell diagonal state. Both geometric discord and negativity of quantumness detect the same dynamical features as quantum discord (see also [106, 107]): being provided an appropriate choice of the initial state, the QC measures are kept frozen in time, then experience a sudden transition and start to decay exponentially. Conversely, the lower bound Q of geometric discord is less accurate and does not reveal any of the mentioned dynamical phenomena, as its expression is smooth at any time.

3.2 Observable measure of bipartite QC

3.2.1 Closed formula for geometric discord in terms of observables

We recall that, for a two-qubit state in the Bloch form Eq. (2.1.1), the geometric discord is given by

$$\begin{aligned} D_G(\rho) &= \frac{1}{2}(\|\vec{x}\|^2 + \|T\|_2^2 - 4k_{\max}) \\ &= 2(\mathrm{Tr}[S] - k_{\max}), \end{aligned} \tag{3.2.1}$$

where $k_{\max}$ is the largest eigenvalue of the matrix $S = \frac{1}{4}(X + \mathcal{T})$, with $X = \vec{x}\vec{x}^t, \mathcal{T} = TT^t$. The maximization of the eigenvalue of S can be solved explicitly. Since the characteristic equation of the matrix S is a cubic with real coefficients and roots, is easily worked out by standard techniques [108]. Indeed, the eigenvalues of S are found by solving a polynomial equation:

$$k^3 + a_0 k^2 + a_1 k + a_2 = 0, \tag{3.2.2}$$

where

$$\begin{aligned} a_0 &= -\mathrm{Tr}[S] \\ a_1 &= \frac{1}{2}(\mathrm{Tr}[S]^2 - \mathrm{Tr}[S^2]) \\ a_2 &= -\frac{1}{3}(a_1 \mathrm{Tr}[S] + a_0 \mathrm{Tr}[S^2] + \mathrm{Tr}[S^3]). \end{aligned} \tag{3.2.3}$$

Introducing the variables

$$\begin{aligned} q &= \frac{1}{9}(3a_1 - a_0^2) \\ r &= \frac{1}{54}(9a_0 a_1 - 27a_2 - 2a_0^3) \\ \theta &= \arccos\left(\frac{r}{\sqrt{-q^3}}\right), \end{aligned} \tag{3.2.4}$$

after a bit of algebra, one obtains

$$\begin{aligned} k_i &= \frac{1}{3}\left(\mathrm{Tr}[S] + 2\sqrt{-q^3}\cos\left(\frac{\theta+\alpha_i}{3}\right)\right) \\ q &= -\sqrt[3]{\frac{1}{4}(6\mathrm{Tr}[S^2] - 2\mathrm{Tr}[S]^2)} \\ \theta &= \arccos\left((2\mathrm{Tr}[S]^3 - 9\mathrm{Tr}[S]\mathrm{Tr}[S^2] + 9\mathrm{Tr}[S^3])\sqrt{2/(3\mathrm{Tr}[S^2] - \mathrm{Tr}[S]^2)^3}\right) \\ \{\alpha_i\} &= \{0, 2\pi, 4\pi\}. \end{aligned} \tag{3.2.5}$$

We now have state independent expressions for the eigenvalues of S. Also, we observe that θ is an arccosine function, thus its domain is $0 \leq \theta/3 \leq \pi/3$. The maximum of $\cos\left(\frac{\theta+\alpha_i}{3}\right)$ is then always reached for $\alpha_i \equiv \alpha_1 = 0$. Hence, $k_{\max} \equiv \max\{k_i\} = k_1$, and the geometric discord for an arbitrary two-qubit state ρ can be recast as an explicit function of the coefficients (ρ_{ij})

$$\begin{aligned} D_G(\rho) &= 2(\mathrm{Tr}[S] - k_1) \\ &= \frac{2}{3}\left(2\mathrm{Tr}[S] - \sqrt{6\mathrm{Tr}[S^2] - 2\mathrm{Tr}[S]^2}\cos\left(\frac{\theta}{3}\right)\right). \end{aligned} \tag{3.2.6}$$

At this point, we remind that the aim is to find an observable QC measure by quantifying them in terms of observable quantities. The geometric discord in Eq. (3.2.6) is just a function of polynomials of the density matrix entries. Protocols for writing linear and even non-linear functionals of (ρ_{ij}) in terms of expectation values of Hermitian unitary operators have been developed extensively. Furthermore quantum circuits estimating such quantities have been already designed [109]. For an overview of the state of the art of the field see [110–113]. Thus, in principle nothing prevents us from measuring geometric discord in real experimental setups. Unfortunately, in practice, the implementation of the required architecture seems rather challenging, hence it is valuable to make a further effort and trying to define a QC measure endowed with an even simpler and more accessible experimental evaluation.

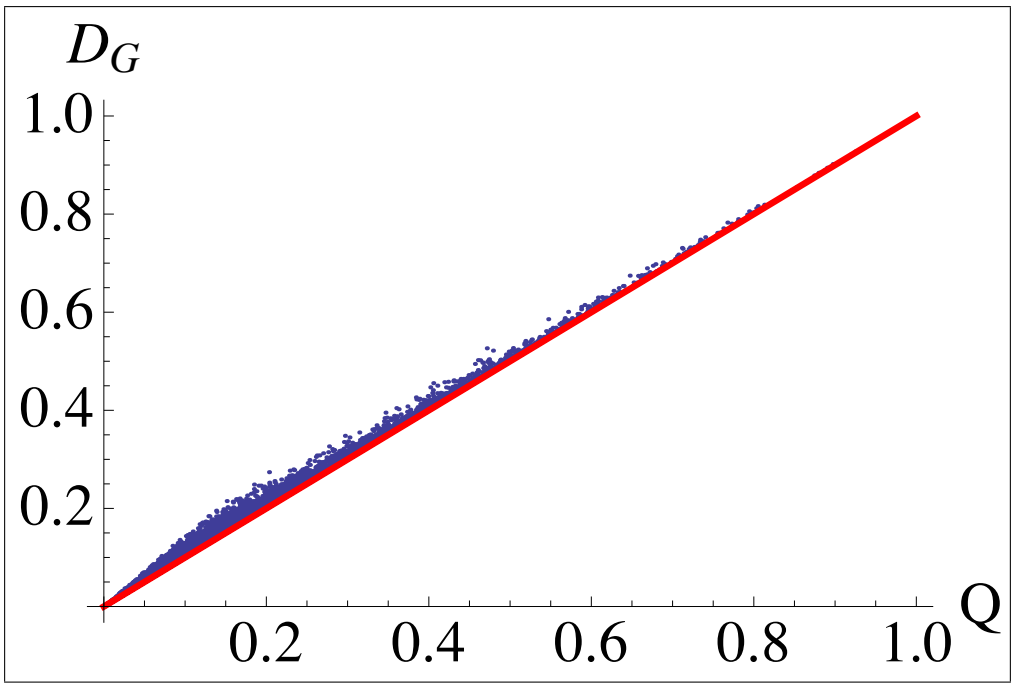

Figure 3.1: Geometric discord D_G versus Q. Sample of 10^4 randomly generated two-qubit states. The plotted quantities are dimensionless.

3.2.2 A tight lower bound of geometric discord

Moved by the previous considerations, we observe that in Eq. (3.2.6) one fixes $\theta = 0$ and define [DG4]

$$Q(\rho) = \frac{2}{3}\left(2\mathrm{Tr}[S] - \sqrt{6\mathrm{Tr}[S^2] - 2\mathrm{Tr}[S]^2}\right). \tag{3.2.7}$$

It is immediate to see, by the properties of the cosine function, that $D_G \geq Q$. In Fig. 3.1 we compare the two quantities in a numerical simulation, showing that Q is a very tight lower bound of geometric discord. More important, Q is still a *bona fide* QC measure[1]. Indeed, the following properties hold.

- $Q \geq 0$, being zero only for classical-quantum states ρ_{CQ}: $Q = 0 \iff D_G = 0$. To prove this, notice that the condition for vanishing Q is $\mathrm{Tr}[S]^2 = \mathrm{Tr}[S^2]$. By the Cayley-Hamilton theorem, reminding the characteristic equation Eq. (3.2.2), this implies $\mathrm{Tr}[S]^3 = \mathrm{Tr}[S^3]$ and consequently $D_G = 0$.

- For pure states, Q is equal to geometric discord, as it is easily proven. The

[1] Reminding that Q suffers the same pathologies of geometric discord highlighted in Sec. 2.1.5.

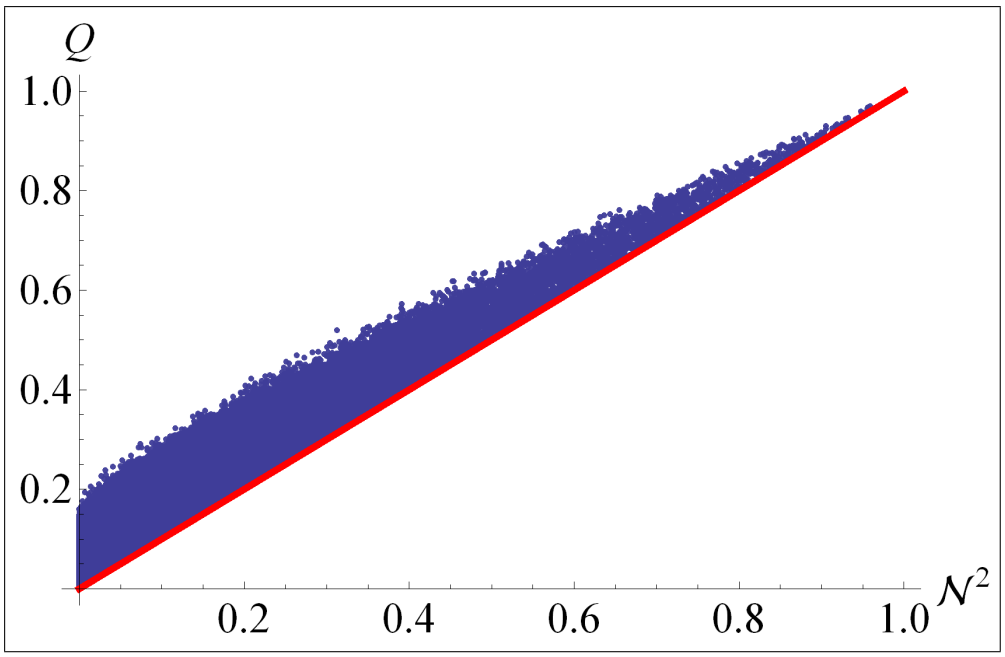

Figure 3.2: The lower bound Q of geometric discord versus squared negativity for a sample of 10^5 randomly generated two-qubit states. The chain of inequalities $D_G \geq Q \geq \mathcal{N}^2$ holds. The plotted quantities are dimensionless.

Schmidt decomposition of a pure state ρ_p of a two qubits reads

$$\rho_p = \sum_{ij=0,1} \sqrt{\alpha_i}\sqrt{\alpha_j}|ii\rangle\langle jj|, \tag{3.2.8}$$

where $\{\alpha_i\}$ are the Schmidt coefficients and $\sum_i \alpha_i = 1$ [17]. Simple algebraic steps return $\theta_p = 0$, thus $D_G(\rho_p) = Q(\rho_p)$.

For two-qubit states, numerical evidences show that a chain of inequalities holds: $D_G \geq Q \geq \mathcal{N}^2$, where $\mathcal{N}$ is the negativity. Indeed, reminding the results of Ch. 2, the three quantities coincide for pure states, and one observes that $Q \geq \mathcal{N}^2$ (Fig. 3.2). For a more advanced study of the interplay between QC and entanglement, see [51, 57, 69].

Extension to $2 \otimes d$ systems

We address the problem of measuring bipartite QC for states of $2 \otimes d$ systems, where subsystem A is the qubit. A generalization of geometric discord to catch bipartite QC in such a case has been derived (for finite d) in [98]. Its expression

is the very same as Eq. (3.2.1). The Bloch form for the state is

$$\rho = \frac{1}{2d}\left(\mathbb{I}_{2d} + \sum_{i=1}^{3} x_i \sigma_i \otimes \mathbb{I}_d + \sum_{j=1}^{d^2-1} y_j \mathbb{I}_2 \otimes \tau_j + \sum_{i=1}^{3}\sum_{j=1}^{d^2-1} t_{ij}\sigma_i \otimes \tau_j\right), \tag{3.2.9}$$

where we pick the generalized and normalized Gell-Mann matrices as the basis $\{\tau_j\}$ of the d-dimensional subsystem B. Obviously, $\{y_j\}$ is now a d-dimensional vector and T is a $3 \times (d^2-1)$ correlation matrix. One notices that the matrix $S = \frac{1}{2d}(X + \mathcal{T})$ has still 3×3 dimensions, thus its characteristic equation remains a cubic and we can repeat all the previous steps to write closed expressions for D_G and Q formally equivalent to Eqs. (3.2.6, 3.2.7). The procedure is extendible to $d = \infty$ according to the prescription of [DG10].

Case study: DQC1 model

We include a simple but meaningful case study to showcase a comparison of QC measures. Let us consider a four-qubit implementation of the DQC1 model introduced in Sec. 1.3.2. The case of an ancilla A *vs* $n = 3$ qubits has been recently investigated experimentally in [63, 64, 114]. Specifically, the designed unitary gate is $U = (a, a, b, 1, a, b, 1, 1)$, with $a = -(e^{-i3\pi/5})^4, b = (e^{-i3\pi/5})^8$. Referring to Fig. 3.3, the final state of the protocol is

$$\rho^{out} = \frac{1}{16}\left(\begin{array}{c|c} \mathbb{I}_8 & \mu U^\dagger \\ \hline \mu U & \mathbb{I}_8 \end{array}\right), \tag{3.2.10}$$

while the final state of the ancilla is

$$\rho_A^{\text{out}} = \frac{1}{2}\begin{pmatrix} 1 & \frac{\mu}{8}\text{Tr}[U^\dagger] \\ \frac{\mu}{8}\text{Tr}[U] & 1 \end{pmatrix}. \tag{3.2.11}$$

By measuring the ancilla polarization, one estimates the normalized trace of the unitary U: $\langle\sigma_1\rangle_{\rho_A^{\text{out}}} = \text{Re}\left[\text{Tr}[U]/8\right], \langle\sigma_2\rangle_{\rho_A^{\text{out}}} = \text{Im}\left[\text{Tr}[U]/8\right]$.

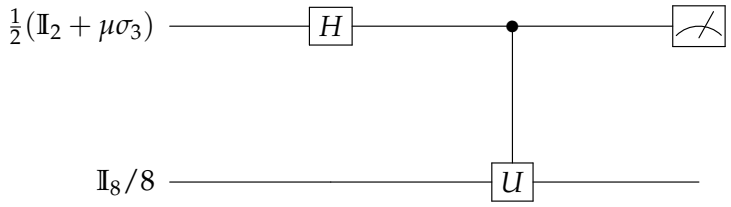

Figure 3.3: DQC1 model: a maximally mixed state of three qubits shares QC with an ancilla of polarization μ. The quantity $\mathrm{Tr}[U]$ is estimated by measuring the spins σ_1, σ_2 on the ancilla.

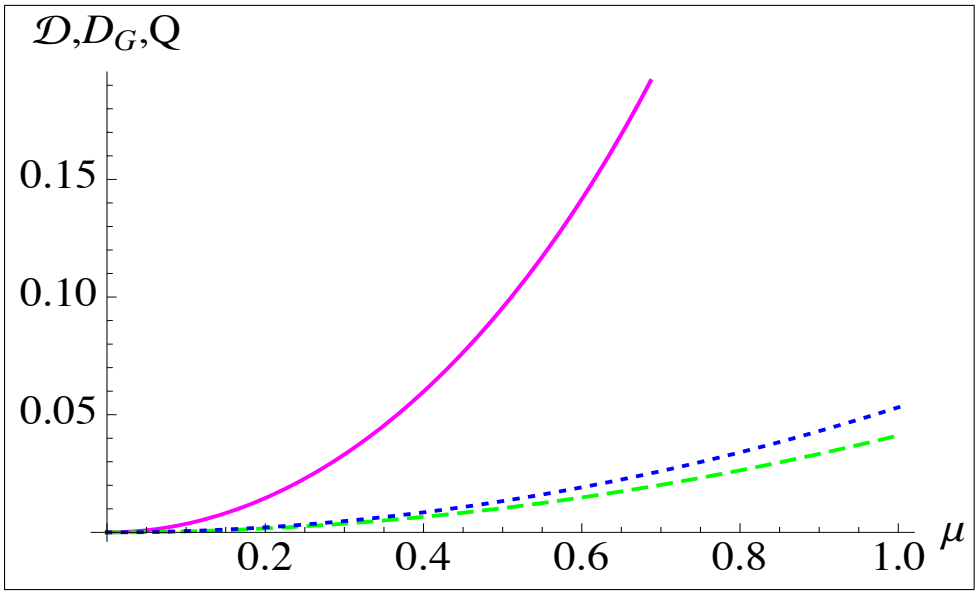

Figure 3.4: (Colours online) Bipartite QC for the final state in the four-qubit DQC1 model discussed in the text, as measured by $\mathcal{D}$ (magenta continuous line), D_G (blue dotted line) and Q (black dashed line) as functions of the initial ancilla polarization μ. All the plotted quantities are dimensionless.

We study the QC between the ancilla and the three qubits (measurement on the ancilla). In particular, we compare the behaviour of geometric QC measures as the geometric discord D_G and the lower bound Q with the entropic discord $\mathcal{D}$ defined in [35, 37]. The former measures are easily calculated from Eqs. (3.2.6, 3.2.7), while for the latter one we retrieve the approximated expression for the output states of the DQC1 model calculated in [40]:

$$\begin{aligned} D_G(\rho^{\text{out}}) &= 0.0531325\,\mu^2 \\ Q(\rho^{\text{out}}) &= 0.0402856\,\mu^2 \\ \mathcal{D}(\rho^{\text{out}}) &= 2 - h_2\left(\frac{1-\mu}{2}\right) - \log_2(1+\sqrt{1-\mu^2}) \\ &- (1-\sqrt{1-\mu^2})\log_2 e, \end{aligned} \tag{3.2.12}$$

where h_2 is the binary Shannon entropy: $h_2(p) = -(1+p)\log_2(1+p) - (1-p)\log_2(1-p)$. Surprisingly, it has been shown in [64] that the geometric discord of the DQC1 output state is directly linked to the trace of the square of the unitary matrix: $D_G(\rho^{\text{out}}) = \frac{\mu^2}{4}\frac{1}{2^n}(1 - \frac{\text{Tr}[U^2]}{2^n})$. In Fig. 3.4 we study the behaviour of QC measured by $\mathcal{D}, D_G, Q$ by varying the polarization of the ancilla in the initial state. As expected, the amount of bipartite QC between the ancilla and the three-qubit register is monotonically increasing with the polarization (and the purity) of the ancillary qubit.

3.3 Experimentally appealing form of QC measures

3.3.1 Proposal for quantum optics (to date, theory only)

In this section, we exploit the following powerful result (see [110] for the proof). It has been proven that any polynomial function of the density matrix entries $f(\rho_{ij})$ can be expressed in terms of expectation values of observables represented by Hermitian unitary operators $\{O_l\}$: $f(\rho_{ij}) = \tilde{f}(\langle O_l \rangle_\rho)$, which can be estimated by implementing the appropriate experimental architecture in the laboratory [110]. Our findings (Eqs. (3.2.6, 3.2.7)) allow to recast D_G and Q as functions of the density matrix elements, and of observable quantities:

$$\begin{aligned} D_G(\rho) &= f_{D_G}(\rho_{ij}) = \tilde{f}_{D_G}(O_l), \\ Q(\rho) &= f_Q(\rho_{ij}) = \tilde{f}_Q(O_l). \end{aligned} \tag{3.3.1}$$

The choice of the specific operators depends on the experimental setting. The estimation of functionals of density matrix elements (ρ_{ij}) has been vastly inves-

tigated in quantum optical settings. Some devices for the evaluation of meaningful quantities, for example the purity of the state $\mathrm{Tr}[\rho^2]$, have been built having as toolbox just the very basic principles of quantum computation. For a broad perspective on theoretical and experimental progresses in the field, the reader should refer to [110–113, 115]. It is important to stress that limits set by the cutting edge technology could prevent from implementing what has been successfully designed. So, from the very beginning, we look for a QC measure which is *really* accessible to experimentalists (see also [109]).

Let us consider the specific case study of the implementation of the measure of Q (which appears simpler than measuring the geometric discord) for a two-qubit state. The task, as evident from Eq. (3.2.7), is to recast the quantities $\mathrm{Tr}[S]$ and $\mathrm{Tr}[S^2]$ in terms of observables. We see that

$$\mathrm{Tr}[S] = \frac{1}{4}(\mathrm{Tr}[X] + \mathrm{Tr}[\mathcal{T}]), \mathrm{Tr}[S^2] = \frac{1}{16}(\mathrm{Tr}[X^2] + \mathrm{Tr}[\mathcal{T}^2] + 2\mathrm{Tr}[X\mathcal{T}])\,. \quad (3.3.2)$$

After some algebra, one obtains

$$\begin{aligned}
\mathrm{Tr}[X] &= 2\mathrm{Tr}[\rho_A^2] - 1 \\
\mathrm{Tr}[\mathcal{T}] &= 4(\mathrm{Tr}[\rho^2] - \mathrm{Tr}[\rho_A^2]/2 - \mathrm{Tr}[\rho_B^2]/2) + 1 \\
\mathrm{Tr}[X^2] &= (2\mathrm{Tr}[\rho_A^2] - 1)^2 \\
\mathrm{Tr}[X\mathcal{T}] &= -1 + 4\mathrm{Tr}[\rho^2](-1 + \mathrm{Tr}[\rho_A^2]) + 4\mathrm{Tr}[\rho_A^2] - 4\mathrm{Tr}[\rho_A^2]^2 + 2\mathrm{Tr}[\rho_B^2] \\
&+ 8\mathrm{Tr}[\rho(\rho_A \otimes \mathbb{I}_2)\rho(\rho_A \otimes \mathbb{I}_2)] - 8\mathrm{Tr}[\rho(\rho_A^2 \otimes \rho_B)] \\
\mathrm{Tr}[\mathcal{T}^2] &= -32(\mathrm{Tr}[\varsigma^4] + \mathrm{Tr}[\varsigma^3]) + 3(\mathrm{Tr}[\mathcal{T}]^2/2 - \mathrm{Tr}[\mathcal{T}] - 1/2), \qquad (3.3.3)
\end{aligned}$$

where $\varsigma = \rho - (\rho_A \otimes \mathbb{I}_2)/2 - (\mathbb{I}_2 \otimes \rho_B)/2$. Consequently, we write Q in terms of traces of (tensor product of) copies of the global and marginal density matrices

and their overlaps. In particular:

$$\begin{aligned}
\mathrm{Tr}[S] &= \mathrm{Tr}[\rho^2] - \mathrm{Tr}[\rho_B^2]/2 \\
\mathrm{Tr}[S^2] &= \frac{1}{4}(-2 - 8\mathrm{Tr}[\rho^4] + 8\mathrm{Tr}[\rho^3] + 6\mathrm{Tr}[\rho^2]^2 \\
&- 2\mathrm{Tr}[\rho^2](5 + \mathrm{Tr}[\rho_B^2]) - 2\mathrm{Tr}[\rho_A^2]^2 + 10\mathrm{Tr}[\rho_A^2] \\
&- \mathrm{Tr}[\rho_B^2]^2 + 12\mathrm{Tr}[\rho_B^2] - 6\mathrm{Tr}[\rho_A^2]\mathrm{Tr}[\rho_B^2] \\
&+ 4\mathrm{Tr}[\rho(\mathbb{I}_2 \otimes \rho_B)\rho(\mathbb{I}_2 \otimes \rho_B)] - 24\mathrm{Tr}[\rho(\rho_A \otimes \rho_B)] \\
&+ 8\mathrm{Tr}[\rho(\rho_A \otimes \mathbb{I}_2)\rho(\rho_A \otimes \mathbb{I}_2)] + 8\mathrm{Tr}[\rho^2(\rho_A \otimes \rho_B)]). \qquad (3.3.4)
\end{aligned}$$

The measure Q has been recast as a functional of (up to the fourth order) polynomials of the density matrix elements (ρ_{ij})[2], specifically traces of matrix powers and overlaps. We identify nine independent terms in the expressions of Eq. (3.3.4). Inspired by the historical lesson of non-tomographic entanglement detection [101, 102], we associate to them the expectation values of the operators for optical set up $\{O_l^{\mathrm{OPT}}\}_{l=1}^9$, and write $f_Q(\rho_{ij}) = \tilde{f}_Q(\langle O_l^{\mathrm{OPT}}\rangle_\rho)$. Explicitly, we pick as observables $\{O_l^{\mathrm{OPT}}\}$ the swap (V^2) and shift (V^k) operators:

$$\begin{aligned}
V^2 &= \sum_{i_A i_B j_A j_B} |ij\rangle\langle ji|_{AB} \\
V^k &= \sum_{i_1 \ldots i_k} |i_1, i_2 \ldots i_{k-1}, i_k\rangle\langle i_k, i_1 \ldots i_{k-2}, i_{k-1}|_{A_1 A_2 \ldots A_k}, \qquad (3.3.5)
\end{aligned}$$

acting on the matrix product ρ^k of k ($k \leq 4$) copies of the global and marginal density matrices and related overlaps. A swap operator exchanges the states of two systems: $V^2|ij\rangle_{AB} = |ji\rangle_{AB}$, while a shift operator makes a permutation around k parties: $V^k|i_1, i_2 \ldots i_{k-1}, i_k\rangle_{A_1 A_2 \ldots A_k} = |i_k i_1 i_2 \ldots i_{k-2} i_{k-1}\rangle_{A_1 A_2 \ldots A_k}$. The reason of our choice is that the expectation values of swap and shift operators equal the trace of many-copies overlaps of density matrices, and they are evaluable in quantum optics experiments [110–113, 115]. One has $\mathrm{Tr}[\rho^k] = \mathrm{Tr}[V^k \rho^{\otimes k}]$. Also, for two unknown states ρ_1, ρ_2, it has been proven that $\mathrm{Tr}[V^2 \rho_1 \otimes \rho_2] = \mathrm{Tr}[\rho_1 \rho_2]$ [111, 112]. More generally, we have $\mathrm{Tr}[\rho_1 \rho_2 \ldots \rho_k] = \mathrm{Tr}[V^k \rho_1 \otimes \rho_2 \otimes$

[2]For example, $\mathrm{Tr}[\rho^2] = \sum_{ij} \rho_{ij}^2$.

$\ldots \otimes \rho_k]$. We briefly present a proof of the last statement, see also [116] for a more elegant derivation. One sees that $\mathrm{Tr}[\rho_1\rho_2\ldots\rho_k] = \mathrm{Tr}[V^k\rho_1\otimes\rho_2\otimes\ldots\otimes\rho_k]$ by expanding the left-hand term in the equation:

$$\begin{aligned}\mathrm{Tr}[\rho_1\rho_2\ldots\rho_k] &= \sum_{i_1 j_1\ldots i_k j_k} \rho_1{}^{i_1}_{\ j_1}\rho_2{}^{i_2}_{\ j_2}\ldots\rho_{k-1}{}^{i_{k-1}}_{\ j_{k-1}}\rho_k{}^{i_k}_{\ j_k}\delta^{j_1}_{i_2}\delta^{j_2}_{i_3}\ldots\delta^{j_{k-1}}_{i_k}\delta^{j_k}_{i_1} \\ &= \sum_{i_1\ldots i_k} \rho_1{}^{i_1}_{\ i_2}\rho_2{}^{i_2}_{\ i_3}\ldots\rho_k{}^{i_{k-1}}_{\ i_k}\rho_k{}^{i_k}_{\ i_1}. \end{aligned} \tag{3.3.6}$$

Denoting by $\{|i\rangle\}$ a Hilbert space basis, given $\rho_{1\ldots k} = \otimes_i\rho_i$ and building the shift operator as chain of swaps, one has

$$\begin{aligned} V^k\rho_1\otimes\rho_2\otimes\ldots\otimes\rho_k &= \sum_{i_1 j_1\ldots i_k j_k} \rho^{i_1\ldots i_k}_{1\ldots k j_1\ldots j_k}|i_1 j_k\ldots i_{k-1}\rangle\langle j_1 i_k\ldots j_{k-1}|\ldots \\ \ldots &\quad |i_1\ldots i_{k-1}j_k\rangle\langle j_1\ldots j_{k-1}i_k|i_1\ldots i_{k-1}i_k\rangle\langle j_1\ldots j_{k-1}j_k|, \\ \mathrm{Tr}\left[V^k\rho_1\otimes\rho_2\otimes\ldots\otimes\rho_k\right] &= \sum_{i_1\ldots i_k}\rho^{i_1\ldots i_k}_{1\ldots k\ i_2\ldots i_1}\delta^{i_1}_{i_k} \\ &= \sum_{i_1\ldots i_k}\rho_1{}^{i_1}_{\ i_2}\rho_2{}^{i_2}_{\ i_3}\ldots\rho_k{}^{i_{k-1}}_{\ i_k}\rho_k{}^{i_k}_{\ i_1} \\ &= \mathrm{Tr}[\rho_1\rho_2\ldots\rho_k], \end{aligned} \tag{3.3.7}$$

thus the assertion is proven. For example, $\langle O_1^{\mathrm{OPT}}\rangle = \mathrm{Tr}[\rho^4] = \mathrm{Tr}[V^4\rho^{\otimes 4}]$, and so forth for the other terms. All the quantum circuits to be implemented for estimating $\langle O_l^{\mathrm{OPT}}\rangle_\rho$ have the same architecture, which is depicted in Fig. 3.5 (note the similarity to the DQC1 model). There is a Mach-Zender interferometer, which is modified by a controlled-O_l gate:

$$C_{O_l} = \left(\begin{array}{c|c} \mathbb{I}_{2^k} & 0_{2^k} \\ \hline 0_{2^k} & O_l \end{array}\right). \tag{3.3.8}$$

The final state at the end of the routine is

$$\begin{aligned}\rho^{\mathrm{fin}} &= M(|0\rangle\langle 0|_A\otimes\bigotimes_{i=1,k}\rho_i)M^\dagger, \\ M &= (H_A\otimes\mathbb{I}_{1,\ldots,k})\,C_{O_l}\,(H_A\otimes\mathbb{I}_{1,\ldots,k}).\end{aligned} \tag{3.3.9}$$

The visibility v related to the interference fringes yields the expectation value

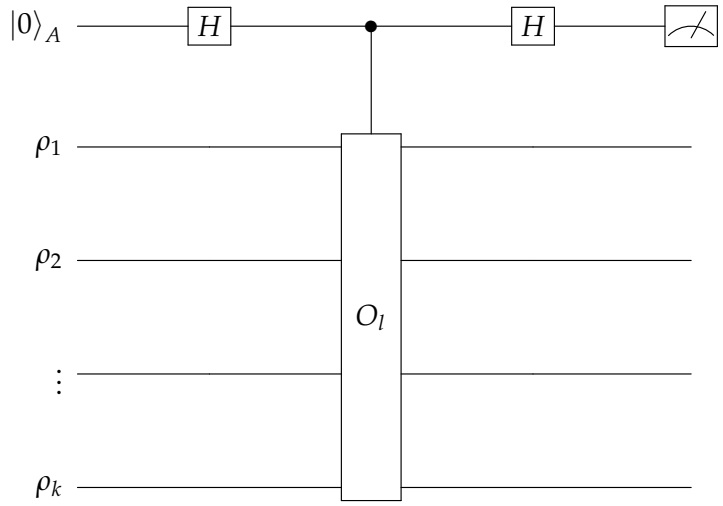

Figure 3.5: Circuit estimating $\mathrm{Tr}[O_l\rho_1 \otimes \rho_2 \otimes \ldots \otimes \rho_k] = v$. A Hadamard gate H is applied to the ancillary qubit, followed by a controlled-O_l gate acting on the overlap of states and then another Hadamard gate. Then, a measurement in the computational basis $\{|0\rangle, |1\rangle\}$ returns the visibility $v = p_0(\rho^{\mathrm{fin}}) - p_1(\rho^{\mathrm{fin}})$, which equals the expectation value of the operator O_l.

of the operator O_l on the dummy overlap $\rho_1 \otimes \rho_2 \otimes \ldots \otimes \rho_k$, as one can write $\mathrm{Tr}[O_l\rho_1 \otimes \rho_2 \otimes \ldots \otimes \rho_k] = v$. Hence, to quantify the degree of QC for an arbitrary two-qubit state ρ, this method requires nine independent measurements instead of the fifteen necessary for tomography [DG4].

There is still room for improvement. In particular, looking at [109], we may appreciably reduce the number of measurements and the complexity of the setting. We observe that $V^2 = \sum_{ij} |ij\rangle\langle ji| = \frac{1}{2}(\mathbb{I}_4 + \sum_k \sigma_k \otimes \sigma_k)$ (note that the V defined in [109] is twice ours). Then, let us introduce the quantities

$$\begin{aligned}
c_1 &= \mathrm{Tr}[(P^-_{A_1A_2} \otimes P^-_{B_1B_2})(\rho^{\otimes 2})] \\
c_2 &= \mathrm{Tr}[(P^-_{A_1A_2} \otimes \mathbb{I}_{B_1B_2})(\rho^{\otimes 2})] \\
c_3 &= \mathrm{Tr}[(\mathbb{I}_{A_1A_2} \otimes P^-_{B_1B_2})(\rho^{\otimes 2})] \\
c_4 &= \mathrm{Tr}[(P^-_{A_1A_4} \otimes P^-_{A_2A_3} \otimes P^-_{B_1B_2} \otimes P^-_{B_3B_4})(\rho^{\otimes 4})] \\
c_5 &= \mathrm{Tr}[(P^-_{A_1A_4} \otimes \mathbb{I}_{A_2A_3} \otimes P^-_{B_1B_2} \otimes P^-_{B_3B_4})(\rho^{\otimes 4})] \\
c_6 &= \mathrm{Tr}[(P^-_{A_1A_4} \otimes P^-_{A_2A_3} \otimes P^-_{B_1B_2} \otimes \mathbb{I}_{B_3B_4})(\rho^{\otimes 4})] \\
c_7 &= \mathrm{Tr}[(\mathbb{I}_{A_1A_4} \otimes P^-_{A_2A_3} \otimes P^-_{B_1B_2} \otimes \mathbb{I}^-_{B_3B_4})(\rho^{\otimes 4})],
\end{aligned} \tag{3.3.10}$$

where $P_{ij}^{-} = \frac{1}{2}(1 - V_{ij})$ is the projector on the antisymmetric subspace for a two-qubit state. Evaluating c_i is equivalent to measuring the quantities

$$\begin{aligned} d_1 &= \mathrm{Tr}[(V_{A_1A_2} \otimes V_{B_1B_2})(\rho^{\otimes 2})] \\ d_2 &= \mathrm{Tr}[(\mathbb{I}_{A_1A_2} \otimes V_{B_1B_2})(\rho^{\otimes 2})] \\ d_3 &= \mathrm{Tr}[(\mathbb{I}_{A_1A_4} \otimes V_{A_2A_3} \otimes V_{B_1B_2} \otimes V_{B_3B_4})(\rho^{\otimes 4})] \\ d_4 &= \mathrm{Tr}[(V_{A_1A_4} \otimes V_{A_2A_3} \otimes V_{B_1B_2} \otimes V_{B_3B_4})(\rho^{\otimes 4})]. \end{aligned} \tag{3.3.11}$$

Finally, one sees that

$$\begin{aligned} \mathrm{Tr}[S] &= 4c_1 - 2c_2 - c_3 + \frac{1}{2} = d_1 - \frac{1}{2}d_2 \\ \mathrm{Tr}[S^2] &= 16c_4 + 8(c_7 - c_5 - 2c_6) + c_3^2 + 4c_2^2 - c_3 - 2c_2 + \frac{1}{2} \\ &= d_4 - d_3 + \frac{1}{4}d_2^2. \end{aligned} \tag{3.3.12}$$

In conclusion, Q is a function of the expectation values of seven projective or, alternatively, just four swap measurements:

$$\begin{aligned} Q(\rho) &= \tilde{f}(\langle O_l^{\mathrm{OPT}} \rangle) \\ \{O_l^{\mathrm{OPT}}\} &= \{c_l\} \text{ or } \{d_l\}. \end{aligned} \tag{3.3.13}$$

We remark that geometric discord would require a rather more complex expression in terms of overlaps or alternatively measurements over six copies of the state [109], entailing a by far harder implementation.

Now, let us have a look at the extension to the $2 \otimes d$ case. We arguably say that the very same expressions hold, at least at formal level. We have to generalize the swap and the projectors to arbitrary finite dimension. A state of a d-dimensional system reads $\rho = \frac{1}{d}(\mathbb{I}_d + \sum_i x_i \tau_i)$, implying $\mathrm{Tr}[\rho^2] = \frac{1}{d}(1 + |\vec{x}|^2)$. Thus, in the most general fashion one obtains

$$V^2 = \frac{1}{d}(\mathbb{I}_{d^2} + \sum_i \tau_i \otimes \tau_i), \tag{3.3.14}$$

and consequently

$$P^- = \frac{1}{2d}\Big((d-1)\mathbb{I}_{d^2} - \sum_i \tau_i \otimes \tau_i\Big), \tag{3.3.15}$$

where the $\{\tau_i\}$ reduce to Pauli matrices in $d = 2$.

On the feasibility of a quantum optics experiment

It is remarkable that an optical setup would allow to detect QC by only seven projective or four swap measurements for any d in Eq. (3.3.12), but evaluating the expectation value of such operators appears to be challenging even with state-of-the-art technology [117]. Also, the optical implementation of projectors on $P_{B_iB_j}$, i.e. multiqubit projectors, is more complicated than the two-qubit case, see e.g. [20, 118]. A method to simplify the problem could be the following. If we restrict to the case of even d and pick for Bob's subsystem the basis considered in Eq. (3.3.18), such that V, P^- can be rewritten in terms of two-qubit operators, the necessary number of optical devices should increase polynomially with d as the number of measurements should increase linearly with d not compromising the scalability of the protocol. See also [119] for more a detailed analysis. Anyway, swaps and projectors on large dimensional systems seem of hard implementation. We leave for future investigations an extensive treatment of this issue.

3.3.2 NMR setting

For this Section, the main references are [104, 120]. For a critical assessment and an informative review on quantum information processing in NMR systems, refer to [17].

In NMR experiments, quantum states are realized by spin configurations of magnetic nuclei. A large ensemble ($\sim 10^{18}$ elements) of liquid-state molecules

is embedded in a strong magnetic field $B_z = 12\ T$. The nuclear spins align with B_z. Then, a second magnetic field (transverse to B_z) is applied by means of radio frequency pulses, inducing a precession of the spins around z with Larmor frequency $\omega_L = \mu B_z$. The spin precession generates an oscillatory current in a coil, which is then detected. The relaxation time of the nuclei (i.e. the time they take to realign with B_z) is remarkably large when compared to other qubit implementations (magnitude order of seconds). The dipole-dipole interaction between two spins (averaged over all the ensemble) characterizes the qubit. Indeed, the state of a spin-$\frac{1}{2}$ nucleus (for example, the proton in ^1H) reads $|\psi\rangle_{\text{NMR}} = e^{\frac{\omega_L t}{2}}|0\rangle + \mathrm{e}^{\frac{\omega_L t}{2}}|1\rangle$. At room temperature ($T = 25^oC$), the thermal energy is much higher than the energy difference between the states $|0\rangle, |1\rangle$ of the spins. Given an n-qubit state of a NMR system at equilibrium, $\rho = \frac{\mathbb{I}_{2^n}}{2^n}$, by applying appropriate rf pulses we can build the state

$$\rho = \frac{1}{2^n}\mathbb{I}_{2^n} + \varepsilon\Delta\rho, \tag{3.3.16}$$

where $\varepsilon = \hbar\omega_L/2^n K_B T \sim 10^{-5}$ and k_B is the Boltzmann constant [104]. Every manipulation is implemented by varying the deviation matrix $\Delta\rho$, which carries the information content of the state. The unitary operations over $\Delta\rho$ are implemented by the rf pulses as well (with an excellent control of the rotation angle and direction).

A peculiarity of the NMR setting is that there is negligible entanglement in the state of the system. In spite of that, quantum computational tasks as the Shor's algorithm have been studied and implemented by means of such a technique [17, 121].

It is legit to suppose that QC might be one of the key resources for supra-classical performances in NMR environments. Indeed, the DQC1 model of computation we discussed in Secs. 1.3.2, 3.2.2 was designed by thinking about the NMR implementation of quantum information processing, where one has necessarily to deal with highly mixed states [61]. As a result of this, NMR appears a well suited ground for investigating QC potentialities. On this purpose, mea-

sures of QC such as geometric discord and Q have been built by considering the density matrix of the two-qubit state in the Bloch form of Eq. (2.1.1) and its generalized version in Eq. (3.2.9). This theoretical framework was introduced in [76, 77] just for efficiently describing the resonance of magnetic nuclei under the influence of an external magnetic field. Thus, we can exploit this privileged interweaving between geometric quantification of QC and NMR techniques. An overview of the recent studies of QC in this setting can be found in [120].

In the NMR context, performing global and local spin measurements is the most convenient method for gaining information about a state. Tomography would definitely require the spin measurements necessary to retrieve *all* the $R_{ij} = \mathrm{Tr}[(\sigma_i \otimes \tau_j)\rho]$ coefficients, and thus the state. On the other hand, to evaluate geometric discord D_G and the lower bound Q, by definition, does not require to know the state of Bob's subsystem, then we drop the $d^2 - 1$ measurements related to the Bloch vector $\vec{y}$, with $y_j = \mathrm{Tr}[(\mathbb{I}_2 \otimes \tau_j)\rho]$. One has

$$\begin{aligned} \langle O_l^{\mathrm{NMR}} \rangle_\rho &= \mathrm{Tr}[\sigma_\nu \otimes \tau_\lambda \rho], \nu = 1, \ldots, 3, ; \lambda = 0, \ldots, d^2 - 1 \\ D_G(\rho) &= f(\langle O_l^{\mathrm{NMR}} \rangle_\rho) \\ Q(\rho) &= \tilde{f}(\langle O_l^{\mathrm{NMR}} \rangle_\rho). \end{aligned} \tag{3.3.17}$$

Thus, it is relatively easy to quantify QC in NMR setting [63, 64, 82, 103]. An experimental trick for further simplifying the considered procedure allows us to restate global spin measurements as local ones on Alice only, as detailed in next Section.

One could maintain that, when $d > 2$, the global spin measurements which estimate the expectation values of $\sigma_\nu \otimes \tau_\lambda$ as introduced in Eq. (3.2.9) seem extremely intricate, and the realization of the global rotation might be beyond the current technological possibilities. In such a case, at least for the paradigmatic instance in which Bob is a n-qubit subsystem (d is even), we can pick, as basis

$\{\tau_j\}$ for the d-dimensional subsystem, the tensor products of Pauli matrices

$$\{\tau_\lambda\} = \{\mathbb{I}_d, \sigma_1 \otimes \mathbb{I}_{d-2}, \sigma_2 \otimes \mathbb{I}_{d-2}, \sigma_3 \otimes \mathbb{I}_{d-2}, \mathbb{I}_2 \otimes \sigma_1 \otimes \mathbb{I}_{d-4}, \ldots, \sigma_3 \otimes \ldots \otimes \sigma_3\}, \tag{3.3.18}$$

thus reducing the detection of t_{ij} to local spin measurements on single qubits only. In summary, for the NMR set up, the QC quantification, by both geometric discord and the lower bound Q, demands $3d^2$ measurements, against the $4d^2 - 1$ required by full state reconstruction. Indeed, we are exempt from making local spin measurements on Bob's side.

3.4 The Experiment

In this Section, we report the results of the experiment carried out at the Brazilian Center for Research in Physics (CBPF, Rio de Janeiro). The reader can find a technical description of the implementation in [DG6]. Here, we focus on the (theoretical) analysis of the experimental data. The plots in Fig. 3.6, 3.7 are courtesy of I. Almeida-Silva and R. Auccaise.

3.4.1 Implementation of the quantum state and measurements

A two-qubit state of NMR system takes the form $\rho = \frac{1}{4}\mathbb{I}_4 + \varepsilon\Delta\rho$, where $\Delta\rho$ is the deviation matrix, with $\varepsilon = \hbar\omega_L/4K_BT \sim 10^{-5}$. The two qubits are implemented by the magnetization of the hydrogen ^1H and carbon ^{13}C nuclei in a (bulk of) $CHCl_3$ molecules. The precession frequencies are $\omega_L^H = 125\ MHZ, \omega_L^C = 500\ MHZ$, while $B = 11.6\ T$. It is worth remarking that, since in NMR experiments only the deviation matrix is detected, the coefficients of the density matrix are given in units of ε.

To investigate the dynamics of QC, we implement two Bell-diagonal states

$\rho^{\alpha=1,2}$ [17]:

$$\begin{aligned}\rho^{\alpha} &= \frac{1}{4}(\mathbb{I}_4 + \sum_{i=1}^{3} c_i^{\alpha}\sigma_i \otimes \sigma_i) \\ &= \frac{1}{4}\begin{pmatrix} 1+c_3^{\alpha} & 0 & 0 & c_1^{\alpha}-c_2^{\alpha} \\ 0 & 1-c_3^{\alpha} & c_1^{\alpha}+c_2^{\alpha} & 0 \\ 0 & c_1^{\alpha}+c_2^{\alpha} & 1-c_3^{\alpha} & 0 \\ c_1^{\alpha}-c_2^{\alpha} & 0 & 0 & 1+c_3^{\alpha} \end{pmatrix},\end{aligned} \tag{3.4.1}$$

where the coefficients are: $|c_1^1| = |c_2^1| = |c_3^1| = 0.2, |c_1^2| = 0.5, |c_2^2| = 0.06, |c_3^2| = 0.24$. Such states are obtained from thermal equilibrium by applying the pulse sequence for producing the state $|11\rangle$ [120].

After having prepared the initial state, the system is left to evolve. The decoherence process is theoretically described through the operator sum representation technique (see Sec. 1.1.2), in which the evolution of the density operator is given by [122]

$$\rho^{\alpha}(t) = \Phi(\rho^{\alpha}(0)) = \sum_{i,j}(M_{A,i} \otimes \mathbb{I}_B)(\mathbb{I}_A \otimes M_{B,j})\rho^{\alpha}(0)(\mathbb{I}_A \otimes M_{B,j})^{\dagger}(M_{A,i} \otimes \mathbb{I}_B)^{\dagger},$$

where the $\{M_i(t)\}$ are the Kraus operators.

NMR systems undergo two relaxation channels, namely the amplitude damping and the phase damping [17, 104]. The amplitude damping channel is described by the Kraus operators

$$\begin{aligned} M_0 &= \sqrt{\gamma}\begin{pmatrix} 1 & 0 \\ 0 & \sqrt{1-p} \end{pmatrix}, \quad M_1 = \sqrt{\gamma}\begin{pmatrix} 0 & \sqrt{p} \\ 0 & 0 \end{pmatrix}, \\ M_2 &= \sqrt{1-\gamma}\begin{pmatrix} \sqrt{1-p} & 0 \\ 0 & 1 \end{pmatrix}, \quad M_3 = \sqrt{1-\gamma}\begin{pmatrix} 0 & 0 \\ \sqrt{p} & 0 \end{pmatrix}, \end{aligned} \tag{3.4.2}$$

where, in the NMR context, $\gamma = 1/2 - \varepsilon/2$ and $p = 1 - \exp(-t/T_1)$, being T_1 the longitudinal relaxation time of the qubit under consideration. We observe that in our case the relaxation times are different for the two qubits, since they

have distinct Larmor frequencies: $T_1^H = 3.57\,s$, $T_1^C = 10.00\,s$.

For the phase damping channel, one has

$$M_4 = \sqrt{1-\frac{\lambda}{2}}\begin{pmatrix} 1 & 0 \\ 0 & 1 \end{pmatrix}, \quad M_5 = \sqrt{\frac{\lambda}{2}}\begin{pmatrix} 1 & 0 \\ 0 & -1 \end{pmatrix}, \tag{3.4.3}$$

where $\lambda = 1 - \exp(-t/T_2)$ and T_2 is the transverse relaxation time associated with the qubits. Again, two different values are associated to the qubits: $T_2^H = 1.20\,s$, $T_2^C = 0.19\,s$.

For arbitrary states, the column vectors $\vec{x}$ and $\vec{y}$ of the density matrix in Bloch form (Eq. 2.1.1) are proportional to the magnetization of each nuclear spin, $\vec{x} = 2\langle \vec{I} \otimes \mathbb{I}_2 \rangle$ and $\vec{y} = 2\langle \mathbb{I}_2 \otimes \vec{I} \rangle$, where $\vec{I} = \{I_x, I_y, I_z\}$ is the nuclear spin operator, which for spins -$\frac{1}{2}$ is $\vec{I} = \vec{\sigma}/2$. The elements of the correlation matrix follow accordingly: $t_{\nu\lambda} = \langle \sigma_\nu \otimes \sigma_\lambda \rangle = 4\langle I_\nu \otimes I_\lambda \rangle$ [104]. For Bell diagonal states, $\vec{x} = \vec{y} = \vec{0}$ and $T = C = \mathrm{diag}(c_1, c_2, c_3)$. We note that global measurements can be replaced by local ones [120]:

$$\begin{aligned} \mathrm{Tr}[(\sigma_\nu \otimes \sigma_\lambda)\rho^\alpha] &= \mathrm{Tr}[(\sigma_1 \otimes \mathbb{I}_d)\xi_{\nu\lambda}^\alpha] \\ \xi_{\nu\lambda}^\alpha &= U_{\nu\lambda}\rho^\alpha U_{\nu\lambda}^\dagger, \end{aligned} \tag{3.4.4}$$

where $U_{\nu\lambda} = K_{A\to B} R_{\phi_\nu,\phi_\lambda}(\theta_{\nu\lambda})$, for $R_{\phi_\nu,\phi_\lambda}(\theta_{\nu\lambda}) = R^A_{\phi_\nu}(\theta_{\nu\lambda}) \otimes R^B_{\phi_\lambda}(\theta_{\nu\lambda})$, being $R^{A(B)}_{\phi_{\nu(\lambda)}}(\theta_{\nu\lambda})$ a rotation by an angle $\theta_{\nu\lambda}$ over the direction $\phi_{\nu(\lambda)}$, the indexes $\nu, \lambda = 1, 2, 3$ refer to the rotations for measuring the C matrix elements and $K_{A\to B}$ represents the CNOT gate with subsystem A acting as the control qubit [17].

The experiment is run for each initial state in order to measure the magnetization $\langle I_1^H \rangle_{\xi_i}$ in the states ξ_i that leads to determine the two-point correlation functions $\langle I_i^H \otimes I_i^C \rangle_\rho$. The rotations for transforming the elements of the correlation matrix into expectation values of local magnetizations ($\langle I_i^H \otimes I_i^C \rangle_\rho \to \langle I_1^H \rangle_{\xi_{ii}}$)

are given by:

$$
\begin{aligned}
R_{\phi_1,\phi_1}(\theta_{11}) &= R_{xx}(0), & R_{\phi_2,\phi_2}(\theta_{22}) &= R_{zz}(\pi/2),\\
R_{\phi_3,\phi_3}(\theta_{33}) &= R_{yy}(\pi/2), & R_{\phi_1,\phi_2}(\theta_{12}) &= R_{xz}(3\pi/2),\\
R_{\phi_2,\phi_1}(\theta_{21}) &= R_{zx}(3\pi/2), & R_{\phi_1,\phi_3}(\theta_{13}) &= R_{xy}(\pi/2)\\
R_{\phi_3,\phi_1}(\theta_{31}) &= R_{yx}(\pi/2), & R_{\phi_2,\phi_3}(\theta_{23}) &= -R_{zy}(\pi/2),\\
R_{\phi_3,\phi_2}(\theta_{32}) &= -R_{yz}(\pi/2).
\end{aligned}
$$

This process allows us to reconstruct the deviation density matrix of the system at each instant of time, benchmarking its behaviour under the coupling with the environment.

3.4.2 Evaluation of QC

We monitor the QC of the state by evaluating from the experimental data the values of the geometric discord D_G, its lower bound Q, and the negativity of quantumness [105].

The expression for D_G and Q have been derived in Eqs. (3.2.6, 3.2.7), and, by exploiting Eq. (3.3.17), they are translated in functions of the expectation values of the correlation matrix elements $t_{\nu\lambda} = \langle \sigma_\nu \otimes \sigma_\lambda \rangle = \mathrm{Tr}[(\sigma_\nu \otimes \sigma_\lambda)\rho]$ and $\vec{x} = \langle \vec{\sigma} \otimes \mathbb{I}_2 \rangle$. By using the rotations described by Eq. (3.4.4) with a proper set of angles (Eq. 3.4.5), the evaluation of D_G and Q is reduced to a set of spin magnetization measurements on one of the qubits. This means that, after an appropriate set of rotations (rf pulses) applied to the prepared state, the geometric discord (and its lower bound) can be determined directly from the NMR signals (in units of the ε^2 factor), without having to know the state. We dub this procedure as *direct measurement*. The procedure is repeated until the thermal equilibrium state is re-established. The quantum state is also read-out by quantum state tomography, as described in [123, 124], in order to check the consistency of the results obtained by direct measurements. The negativity of quantumness Q_N^A is defined for $2 \otimes d$ systems as the minimum trace distance from the set of classical-quantum states (see [105] for other definitions and interpretations),

$Q_N^A(\rho) = \frac{1}{2} \min_{\chi} \|\rho - \chi\|_1$, where we remind that $\|A\|_1 = \mathrm{Tr}\left[\sqrt{A^\dagger A}\right]$ is the trace norm.

A partial knowledge of the state is instead required to evaluate Q_N^A. However, assuming (as *a posteriori* verified by tomography) that the state remains in Bell diagonal form during the evolution, then the direct method still suffices to extract the correct value of Q_N^A. To benchmark the effectiveness of the direct method, overall, we compare its outcomes with the results obtained for the corresponding measures of QC by evaluating them on the state reconstructed by complete tomography as well, as we do for D_G and Q.

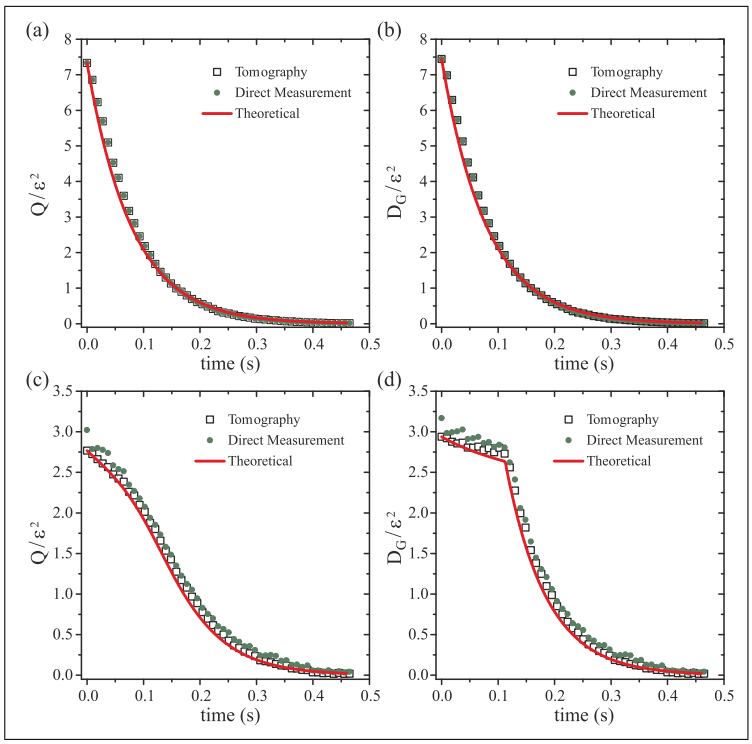

Figure 3.6: (Colours online). Time evolution of Q and D_G for the state ρ^1 in (a) and (b), and ρ^2 in (c) and (d). Two experiments have been carried out. In the first one, we performed only the measurements which are necessary to calculate D_G, Q. The second experiment allowed to reconstruct the full density matrix of the state and calculate from it the value of the QC measures. The black open squares corresponds to tomography results, the green dots represent the direct measurement, and the red lines depict the theoretical predictions. The relaxation times of the qubits retrieved from experimental data are: $T_1^H = 3.57\,s$ and $T_2^H = 1.20\,s$ for the hydrogen, and $T_1^C = 10.00\,s$ and $T_2^C = 0.19\,s$ for the carbon. QC measures are displayed in units of ε^2.

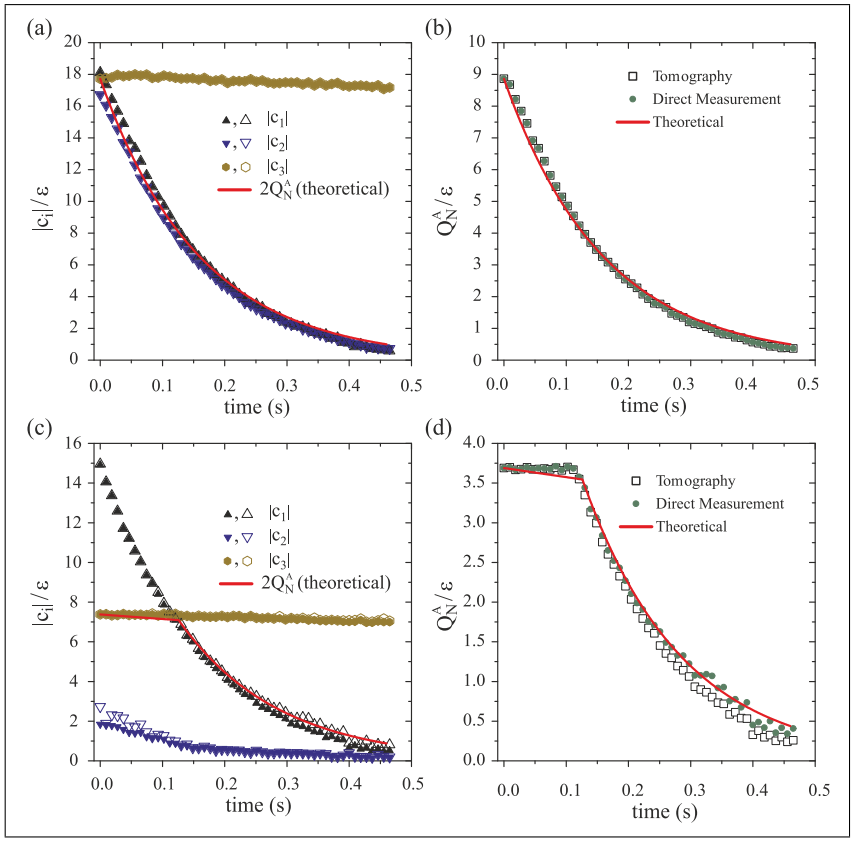

Figure 3.7: (Colours online) Time evolution of $|c_1|$ (upward triangle), $|c_2|$ (downward triangle) and $|c_3|$ (hexagon) for state ρ^1 in (a), and ρ^2 in (c). Again, two experiments have been realized. The open symbols represent the tomography results and the filled symbols represent the direct measurement. In (b), for the initial state ρ^1, and (d), for the initial state ρ^2, the green dots represent the direct measurement and the black squares represent the tomography results. The red lines are the theoretical predictions for Q_N^A. QC are displayed in units of ε.

Reminding Eqs. (3.2.6,3.2.7), for Bell-diagonal states one has

$$S = \frac{C^2}{4} = \text{diag}\{c_1^2/4, c_2^2/4, c_3^2/4\}. \tag{3.4.5}$$

The expressions for D_G and Q are easily obtained:

$$
\begin{aligned}
D_G(\rho^\alpha) &= \frac{1}{3}\left[\sum_i (c_i^\alpha)^2 - \sqrt{\sum_i (c_i^\alpha)^4 - \sum_{i<j}^{3} (c_i^\alpha)^2 (c_j^\alpha)^2}\cos\left(\frac{1}{3}\arccos K^\alpha\right)\right] \\
K^\alpha &= \left(\frac{2\sum_i (c_i^\alpha)^6 - 3\sum_{i\neq j}^{3} (c_i^\alpha)^4 (c_j^\alpha)^2 + 12 (c_1^\alpha)^2 (c_2^\alpha)^2 (c_3^\alpha)^2}{2\sqrt{(\sum_i (c_i^\alpha)^4 - \sum_{i<j,}^{3} (c_i^\alpha)^2 (c_j^\alpha)^2)^3}}\right) \\
Q(\rho^\alpha) &= \frac{1}{3}\left(\sum_i (c_i^\alpha)^2 - \sqrt{\sum_i (c_i^\alpha)^4 - \sum_{i<j,}^{3} (c_i^\alpha)^2 (c_j^\alpha)^2}\right). \qquad (3.4.6)
\end{aligned}
$$

Also, the negativity of quantumness is analytically computable [105, 125]. Denoting the ordered singular values of the Bloch correlation matrix C as $|c_i| \geq |c_j| \geq |c_k|$, where i, j, k are permutations of $1, 2, 3$, then the negativity of quantumness is given by half the intermediate one: $Q_N^A(\rho^\alpha) = |c_j|/2$.

3.4.3 Analysis of the results

While the quantity Q is manifestly smooth at any time during the evolution, D_G and Q_N^A may have a cuspid at a critical time. The phenomenon clearly depends on the peculiar form of the quantum state. As shown in [82, 103], and as we appreciate by calculating the QC of the states $\rho^\alpha(t)$, the QC of the initial state $\rho^1(t)$ should decay monotonically in time, while in the state $\rho^2(t)$ they are expected to exhibit a non-trivial evolution, a phenomenon known as freezing of QC, followed by a sudden transition to an exponential decay [54]. Such behaviour has been recently pinpointed as a further universal *bona fide* criterion for QC measures (indeed, all the known reliable QC quantifiers satisfy it) [107].

The results obtained for D_G and Q, by using the direct measurement (the ^1H nucleus has been detected) and tomography procedures as well as the theoretical predictions, are reported in Fig. 3.6 for both experimentally produced states. In Fig. 3.7, we present the results obtained for Q_N^A by direct measurements, tomography and theoretical predictions for both states. In particular, for the first time the negativity of quantumness is observed to undergo sudden transition in the same dynamical conditions as the geometric discord and the entropic dis-

cord [52, 106].

We highlight a satisfactory agreement between the direct measurements, the tomographic data, and the theoretical predictions. This demonstrates that we are able to directly quantify bipartite QC in unknown (or partially known in the case of Q_N^A) two-qubit states with our NMR setup. Indeed, the choice to prepare a Bell-diagonal state is convenient, but not compulsory: we stress again that our recipe for measuring bipartite QC of an unknown state would apply to arbitrary states of $2 \otimes d$ systems.

3.5 Summary of Chapter 3

- We showed that QC in a arbitrary two-qubit state ρ can be reliably quantified without any explicit optimisation and with no need to know the full shape of the state, if geometric quantifiers are adopted. We derived a state-independent expression for geometric discord of two-qubit states, and defined a QC measure Q which is a tight lower bound of geometric discord and still a function of the density matrix elements.

- Both D_G and Q are then expressed in terms of the expectation values of a set of observables $\{O_l\}$. Consequently, they could be evaluated by designing quantum circuits in optical setting by simulating the measurements of $\{\langle O_l^{\mathrm{OPT}} \rangle\}$. By adopting the alternative approach of [101, 102, 109], we have further seen that the quantity Q is less experimentally demanding than D_G, being measured by performing seven local projections or four swaps on up to four copies of the state ρ . Then, we extended our measure to capture bipartite QC in states of $2 \otimes d$ dimensional systems, finding that seven projective measurements are always sufficient to experimentally determine Q, i.e. the number of measurements required is independent of d. Unfortunately, an implementation in optical set-up appears to be hard even with cutting-edge technology.

- NMR systems are a natural arena for quantum information processing with

negligible entanglement, thus ideal testbeds for investigating dynamical properties of QC in open system dynamics. Our theoretical results allow one to implement optimized protocols by reducing the number of required measurements as compared to the full state reconstruction. Indeed, to know the full state would demand $4d^2 - 1$ spin measurements, while to compute D_G and Q one can get rid of $d^2 - 1$ local measurements on one the subsystems, as information on the Bloch vector of one of the subsystems is unnecessary. We have considered an NMR system and detected the QC of a two-qubit Bell diagonal state by measuring geometric discord, its lower bound, and the negativity of quantumness. We observed the sudden transition of geometric discord and negativity of quantumness under phase and amplitude damping channels. The sudden transition and the freezing [52], common to various measures of QC under particular decoherent evolutions, are certainly phenomena worthy of further theoretical and experimental investigation.

Acknowledgments

The circuits have been drawn by using the package *Q-circuit* written by B. Eastin and S. Flammia. I thank for fruitful discussions L. Amico, S. Bose, S. Clark, B. Dakic, R. Filip, S. Gharibian, V. Giovannetti, M. Guta, P. Horodecki, D. Jaksch, R. Jozsa, C.-F. Li, R. Lo Franco, S. Maniscalco, L. Mazzola, L. Mista, O. Moussa Jr., G. Passante, M. Piani, T. Short, D. Soares-Pinto, and T. Tufarelli.

CHAPTER 4

Rethinking Quantum Correlations

Here I build up an alternative point of view on QC by starting from the concept of quantum uncertainty. This chapter is based on [DG7] (T. Tufarelli and G. Adesso contributed to derive the technical results). I show that quantum mechanics predicts that even a single observable can be intrinsically uncertain on its own. In particular, quantum uncertainty is forced to appear on a single local observable in a system A whenever A shares QC with a second system B. The minimum achievable local uncertainty is a measure of QC as perceived by A. This result links in a novel way two apparently unrelated quantum features as (global) correlations of states and (local) uncertainty on observables, shedding a new light on the ultimate meaning of QC: they trigger local quantum uncertainty. Also, QC shared by the system under scrutiny affect the statistical accuracy of experimental data analysis and the measurability of quantum observables. The QC-induced uncertainty has an application in quantum metrology tasks, establishing a minimum guaranteed quantum enhancement in parameter estimation with noisy probes.

4.1 Quantum uncertainty and quantum correlations

4.1.1 Quantum uncertainty on single observables

Physicists investigate Nature by making measurements and predicting their outcomes. In a classical world, error bars are exclusively due to technological limitations, while quantum mechanics entails that two non-commuting observables cannot be jointly measured with arbitrary accuracy [126], even if one could access a flawless measurement device. The corresponding uncertainty relations have been linked to distinctive quantum features such as non-locality, entanglement and data processing inequalities [127–129].

Remarkably, even a single quantum observable may display an intrinsic uncertainty as a result of the probabilistic character of quantum mechanics. Let us consider for instance a composite system prepared in an entangled state [20], say the Bell state $|\phi^+\rangle = \frac{1}{\sqrt{2}}(|00\rangle + |11\rangle)$ of two qubits. This is an eigenstate of the global observable $\sigma_3 \otimes \sigma_3$, so there is no uncertainty on the result of such a measurement. On the other hand, the measurement of *local* spin observables of the form $\vec{a} \cdot \vec{\sigma} \otimes \mathbb{I}$ (where $\vec{a} \neq 0$ is a real vector) is intrinsically uncertain. Indeed, the state $|\phi^+\rangle\langle\phi^+|$, and in general any entangled state, cannot be eigenstates of a local observable. Only uncorrelated states of the two qubits, e.g. $|00\rangle$, admit at least one completely "certain" local observable.

Extending the argument to mixed states, one needs to filter out the uncertainty due to classical mixing, i.e. lack of knowledge of the state, in order to identify the genuinely quantum one. We say that an observable K on the state ρ is "quantum-certain" when the statistical error in its measurement is solely due to classical ignorance. By adopting a meaningful quantitative definition of quantum uncertainty, as detailed later, we find that K is quantum-certain if and only if $\rho = \rho_K$, where ρ_K is the density matrix of the state after the measurement of K. It follows that even on unentangled states (all but a null measure set thereof [38]) no local observable is quantum-certain. The only states left invariant by a local complete measurement are those described within classical probability

theory [49], i.e. embeddings of joint probability distributions.

The quantum uncertainty on local observables is then entwined to the concept of QC (see Fig. 4.1). In fact, the states ρ_K which admit a quantum-certain local observable K are the states with zero QC. In the following, an entire class of QC measures is defined, interpreted and analyzed within the framework of local quantum uncertainty.

4.1.2 Skew information and Local Quantum Uncertainty

There are several ways to quantify the uncertainty on a measurement, but we aim at extracting the truly quantum share. Entropic quantities or the variance, though used extensively as indicators of uncertainty [126, 128, 129], do not fit our purpose, since they are affected by the state mixedness. It has been proposed to isolate the quantum contribution to the total statistical error of a measurement as being due to the non-commutativity between state and observable: this may be reliably quantified via the *skew information* [130, 131]

$$\mathcal{I}(\rho, K) = -\frac{1}{2}\mathrm{Tr}\left[[\sqrt{\rho}, K]^2\right] \tag{4.1.1}$$

introduced in [130] and investigated in studies on uncertainty relations [131], quantum statistics and information geometry [131–134]. Referring to [130] for the main properties of the skew information, we recall the most relevant ones: it is non-negative, vanishing if and only if state and observable commute, and is convex, that is, non-increasing under classical mixing. Moreover, $\mathcal{I}(\rho, K)$ is always smaller than the variance of K:

$$\begin{aligned} \mathcal{I}(\rho, K) &= \mathrm{Tr}[\rho K^2] - \mathrm{Tr}[\sqrt{\rho} K \sqrt{\rho} K] \\ &\leq \mathrm{Tr}[\rho K^2] - \mathrm{Tr}[\rho K]^2 \\ &\equiv \mathrm{Var}_\rho(K), \end{aligned} \tag{4.1.2}$$

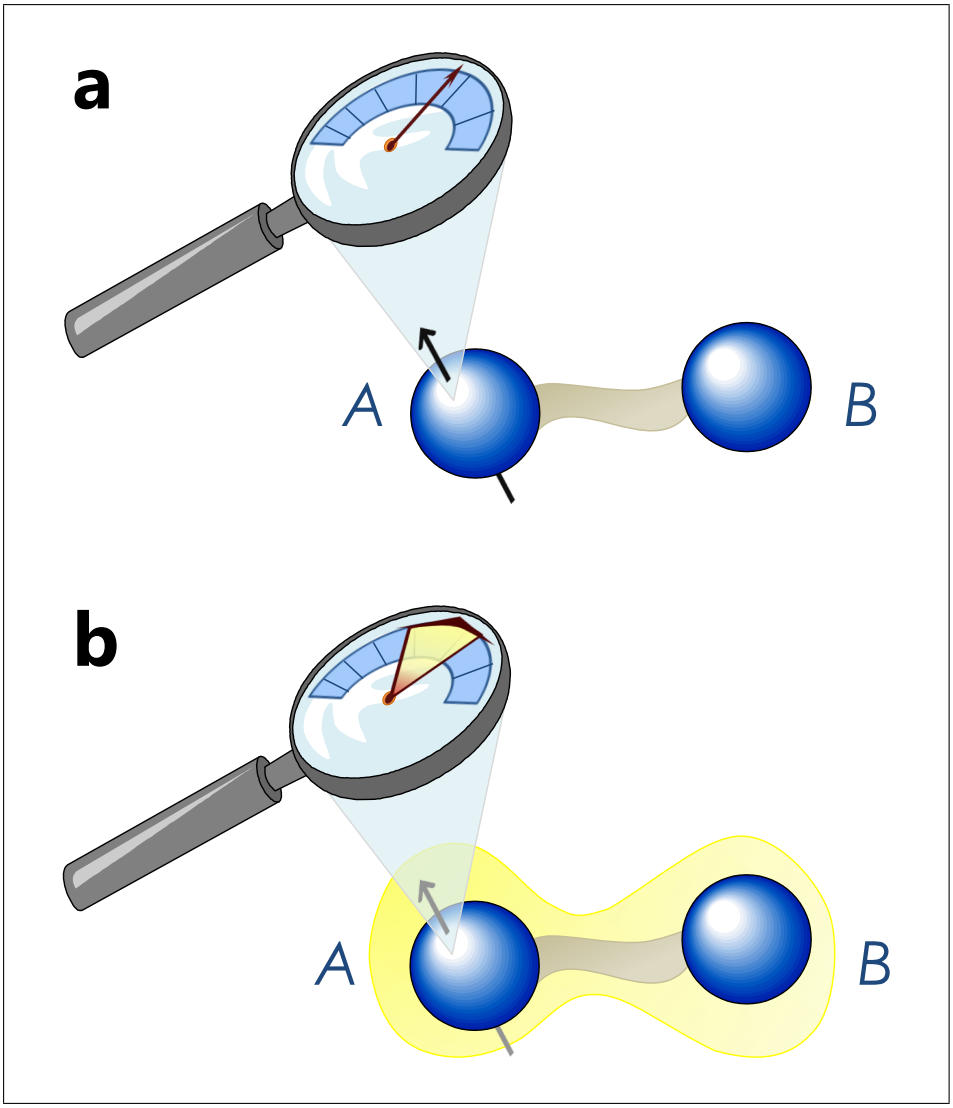

Figure 4.1: (Colours online) QC trigger local quantum uncertainty. Let us consider a bipartite state ρ. An observer on subsystem A is equipped with a *quantum meter*, a measurement device whose error bar shows the quantum uncertainty only (Note: in order to access such quantity, the measurement of other observables may be required, in a procedure similar to state tomography). (a) If ρ is uncorrelated or contains only classical correlations (brown shade), then ρ is of the form $\rho = \sum_i p_i |i\rangle\langle i|_A \otimes \rho_{B,i}$ (with $\{|i\rangle\}$ an orthonormal basis for A) [35, 37, 45], the observer can measure at least one observable on A without any intrinsic quantum uncertainty. (b) If ρ contains a non-zero amount of QC (yellow shade), as quantified by entanglement for pure states [20] and QC in general [45], any local measurement on A is affected by quantum uncertainty. The minimum quantum uncertainty associated to a single measurement on subsystem A can be used to quantify QC in the state ρ, as perceived by the observer on A. In this Chapter, we pick the Wigner-Yanase skew information [130] to measure the quantum uncertainty on local observables.

with equality reached on pure states ($\rho = \sqrt{\rho}$), where no classical ignorance occurs (see Fig. 4.2). Hence, we adopt the skew information as measure of quantum uncertainty and deliver a theoretical analysis in which we convey and discuss its operational interpretation.

As a central concept in our work, we introduce the *local quantum uncertainty* (LQU) as the minimum skew information achievable on a single local measurement. We remark that by "measurement" in this Chapter we always refer to a complete von Neumann measurement. Let $\rho \equiv \rho_{AB}$ be the state of a bipartite system, and let $K^{\Lambda} = K_A^{\Lambda} \otimes \mathbb{I}_B$ denote a local observable, with K_A^{Λ} a Hermitian operator on A with spectrum Λ. We require Λ to be non-degenerate, which corresponds to maximally informative observables on A. The LQU with respect to subsystem A, optimized over all local observables on A with non-degenerate spectrum Λ, is then

$$\mathcal{U}_A^{\Lambda}(\rho) \equiv \min_{K^{\Lambda}} \mathcal{I}(\rho, K^{\Lambda}). \tag{4.1.3}$$

Eq. (4.1.3) defines a family of Λ-dependent quantities, one for each equivalence class of Λ-spectral local observables over which the minimum skew information is calculated. In practice, to evaluate the minimum in Eq. (4.1.3), it is convenient to parametrize the observables on A as $K_A^{\Lambda} = V_A \mathrm{diag}(\Lambda) V_A^{\dagger}$, where V_A is varied over the special unitary group on A. In this representation, the (fixed) spectrum Λ may be interpreted as a standard "ruler", fixing the units as well as the scale of the measurement (that is, the separation between adjacent "ticks"), while V_A defines the measurement basis that can be varied arbitrarily on the Hilbert space of A.

In the following, we prove some qualitative properties of the Λ-dependent LQUs, which reveal their intrinsic connection with QC.

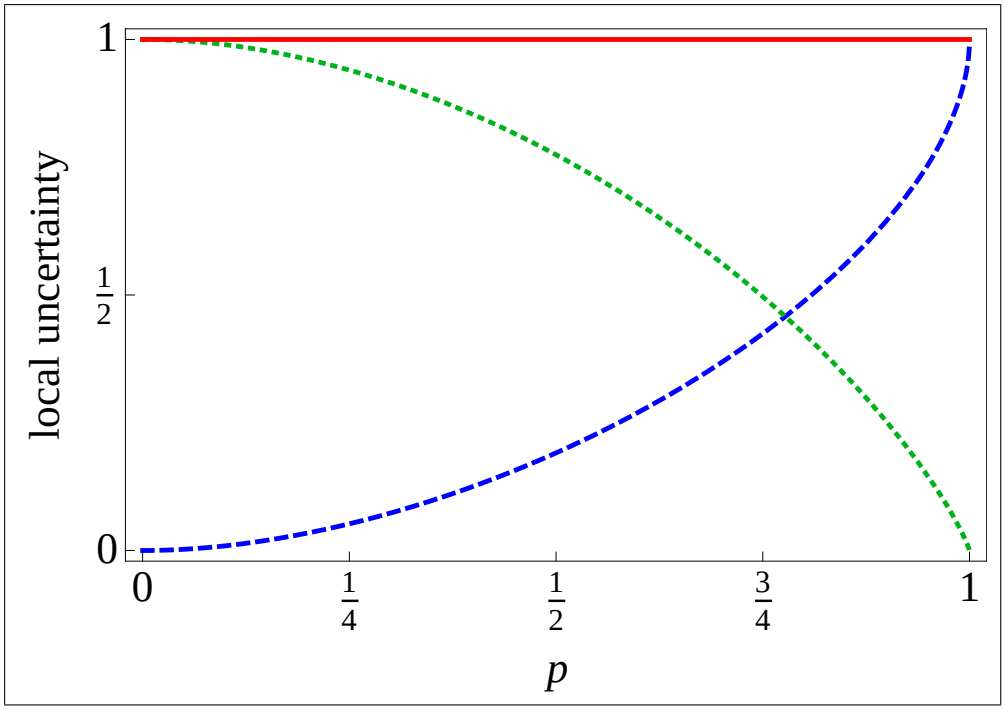

Figure 4.2: (Colours online) The plot shows different contributions to the error bar of spin measurements on subsystem A in a Werner state [20] $\rho = p|\phi^+\rangle\langle\phi^+| + (1-p)\mathbb{I}/4, p \in [0,1]$, of two qubits A and B. The red line is the variance $\mathrm{Var}_\rho(\sigma_3^A)$ of the σ_3^A operator, which amounts to the total statistical uncertainty. The blue dashed curve represents the local quantum uncertainty $\mathcal{U}_A(\rho)$, which in this case is $\mathcal{I}(\rho, \sigma_3^A)$ (any local spin direction achieves the minimum for this class of states). The green dotted curve depicts the (normalized) linear entropy $S_L(\rho) = \frac{4}{3}(1 - \mathrm{Tr}[\rho^2])$ of the global state ρ, which measures its mixedness. Notice that the Werner state is separable for $p \leq 1/3$ but it always contains QC for $p > 0$.

4.1.3 A class of QC measures

As anticipated, the non-existence of quantum-certain local observables characterizes a quantum correlated state. In fact, we find that each quantity $\mathcal{U}_A^\Lambda(\rho)$ defined in Eq. (4.1.3) is not only an indicator, but also a full fledged measure of bipartite QC (see Fig. 4.1) [135], as it meets all the known *bona fide* criteria for a QC quantifier stated in Sec. 1.3.2. Specifically, in Sec. 4.1.4 we prove that the Λ-dependent LQU (for any non-degenerate Λ) is invariant under local unitary operations, is non-increasing under local operations on B, vanishes if and only if ρ is a zero QC state with respect to measurements on A, and reduces to an entanglement monotone when ρ is a pure state.

If we now focus on the case of bipartite $2 \otimes d$ systems, we further find that quan-

tifying QC via the LQU is very advantageous in practice compared to quantum discord and other entropic measures [45], which typically involve formidably hard optimizations, not admitting a closed formula even for two-qubit states, as we seen in Ch. 2. The minimization in Eq. (4.1.3) can be expressed in closed form for arbitrary states ρ_{AB} of a qubit-qudit system defined on $\mathbb{C}^2 \otimes \mathbb{C}^d$, so that $\mathcal{U}_A^\Lambda$ admits a *computable* closed formula. Moreover notice that, when A is a qubit, all the Λ-dependent measures are equivalent up to a multiplication constant. Indeed, a non-degenerate qubit observable $K^A = K_A \otimes \mathbb{I}_B$ with fixed spectrum can be parametrized as $K_A = V_A(\alpha\sigma_{zA} + \beta\mathbb{I}_A)V_A^\dagger = \alpha\vec{n}\cdot\vec{\sigma}_A + \beta\mathbb{I}_A$, where α, β are constants ($\alpha \neq 0$) while $\vec{n}$ varies on the unit sphere. Then $\mathcal{I}(\rho, K^A) = \alpha^2\mathcal{I}(\rho, \vec{n}\cdot\vec{\sigma}_A \otimes \mathbb{I}_B)$, implying that all the $\mathcal{U}_A^\Lambda$ are proportional to each other. We thus drop the superscript Λ for brevity, and pick non-degenerate observables K_A on the qubit A of the form $K_A = V_A\sigma_{zA}V_A^\dagger = \vec{n}\cdot\vec{\sigma}_A$, with $|\vec{n}| = 1$. This choice corresponds to a LQU normalized to unity for pure, maximally entangled states. Eq. (4.1.3) can then be rewritten as the minimization of a quadratic form involving the unit vector $\vec{n}$, yielding simply

$$\mathcal{U}_A(\rho_{AB}) = 1 - \lambda_{\max}\{W_{AB}\}, \tag{4.1.4}$$

where $\lambda_{\max}$ denotes the maximum eigenvalue, and W_{AB} is a 3×3 symmetric matrix whose elements are

$$(W_{AB})_{ij} = \mathrm{Tr}\left[\sqrt{\rho_{AB}}\,(\sigma_{iA} \otimes \mathbb{I}_B)\,\sqrt{\rho_{AB}}\,(\sigma_{j_A} \otimes \mathbb{I}_B)\right],$$

with $i, j = x, y, z$. It is easy to check that, for a pure state $|\psi\rangle\langle\psi|_{AB}$, Eq. (4.1.4) reduces to the linear entropy of entanglement, $\mathcal{U}_A(|\psi\rangle\langle\psi|_{AB}) = 2(1 - \mathrm{Tr}[\rho_A^2])$. Qubit-qudit states represent a relevant class of states for applications in quantum information processing, and we present some pertinent examples in this work. The evaluation of the LQU for Werner states of two qubits is displayed in Fig. 4.2. A case study of the DQC1 model of quantum computation [61] is reported in Sec. 4.1.4, showing that our measure (evaluated in the one versus

n qubits partition) exhibits the same scaling as the canonical quantum discord [35, 62]. The computability of the LQU opens a range of possibilities to investigate analytically the role of QC in open dynamical evolutions and communication protocols [45]. More generally, the approach adopted in this Chapter provides a nice physical interpretation of QC as the minimum quantum contribution to the statistical uncertainty associated to the measurement of local observables in correlated quantum systems.

Interestingly, the LQU in a state ρ_{AB} of a $\mathbb{C}^2 \otimes \mathbb{C}^d$ system is reinterpreted geometrically as the minimum squared Hellinger distance between ρ_{AB} and the state after a least disturbing root-of-unity local unitary operation applied on the qubit A, in a spirit close to that adopted to define geometric QC measures based on other metrics [45, 80, 136, 137] as we discussed in Sec. 2.1.5. Let us recall that the squared Hellinger distance between density matrices ρ and χ is defined as $D_H^2(\rho,\chi) = \frac{1}{2}\mathrm{Tr}\left[(\sqrt{\rho}-\sqrt{\chi})^2\right]$ [138, 139]. Observing that, for qubit A, any generic non-degenerate Hermitian observable $K_A = \vec{n}\cdot\vec{\sigma}_A$ is a root-of-unity unitary operation, which implies $K^A f(\rho_{AB}) K^A = f(K^A \rho_{AB} K^A)$ for any function f, we have

$$\begin{aligned}\mathcal{I}(\rho_{AB}, K^A) &= 1 - \mathrm{Tr}\left[\sqrt{\rho_{AB}}K^A\sqrt{\rho_{AB}}K^A\right] = 1 - \mathrm{Tr}\left[\sqrt{\rho_{AB}}\sqrt{K^A\rho_{AB}K^A}\right] \\ &= D_H(\rho_{AB}, K^A\rho_{AB}K^A); \end{aligned} \tag{4.1.5}$$

this result highlights a geometric interpretation of the LQU, analytically computed in Eq. (4.1.4), in terms of Hellinger distance. The study of further connections between uncertainty on a single local observable and geometric approaches to quantumness of correlations, possibly in larger and multipartite systems, opens an avenue for future investigations.

4.1.4 Proof of the properties of LQU

We refer to [130–132] for a summary of the relevant properties of the skew information which constitute the main ingredients of the proofs. We also remind

that, for the classical-quantum states ρ_{CQ} defined in Eq (1.3.12), there exists at least one set of projectors $\{\Pi_i^A = \Pi_{A,i} \otimes \mathbb{I}_B\}$ such that $\rho_{CQ} = \sum_i p_i \Pi_i^A \rho_{CQ} \Pi_i^A$.

To prove that the classical-quantum states have vanishing LQU $\mathcal{U}_A^\Lambda$, it is sufficient to define the observable $K^{A,\Pi} = K_A^\Pi \otimes \mathbb{I}_B$ where K_A^Π is diagonal in the basis defined by $\{\Pi_{A,i}\}$, to obtain $[\rho_{CQ}, K^{A,\Pi}] = 0$ which means $\mathcal{U}_A^\Lambda(\rho_{CQ}) = \mathcal{I}(\rho_{CQ}, K^{A,\Pi}) = 0$. On the other hand, a vanishing LQU ensures the existence of a local observable $\tilde{K}^A$ such that $\mathcal{I}(\rho, \tilde{K}^A) = 0$. Hence $\tilde{K}^A$ commutes with the density matrix, and we can diagonalize them simultaneously. Since the observable is assumed non-degenerate, its eigenvectors define a *unique* basis on A (up to phases), say $\{|k_i\rangle\}$. Then, an eigenvector basis for $\tilde{K}^A$ will be simply $\{|k_i\rangle_A \otimes |\phi_{ij}\rangle_B\}$, and the state must necessarily be of the form $\rho_{K_A} = \sum_i p_{ij} |k_i\rangle\langle k_i|_A \otimes |\phi_{ij}\rangle\langle\phi_{ij}|_B$, which is classical-quantum state. This proves that $\mathcal{U}_A^\Lambda(\rho)$ vanishes if and only if $\rho = \rho_{CQ}$, thus $\mathcal{U}_A^\Lambda$ is a faithful QC measure.

Let us now show that the LQU is invariant under local unitary transformations. We have

$$\begin{aligned} & \mathcal{U}_A^\Lambda \left((U_A \otimes U_B)\rho(U_A \otimes U_B)^\dagger \right) = \\ = \; & \min_{K^A} \mathcal{I} \left((U_A \otimes U_B)\rho(U_A \otimes U_B)^\dagger, K_A \otimes \mathbb{I}_B \right) \\ = \; & \min_{K^A} \mathcal{I} \left(\rho, (U_A \otimes U_B)^\dagger (K_A \otimes \mathbb{I}_B)(U_A \otimes U_B) \right) \\ = \; & \min_{K^A} \mathcal{I} \left(\rho, (U_A^\dagger K_A U_A) \otimes \mathbb{I}_B \right) = \mathcal{U}_A^\Lambda(\rho), \end{aligned} \tag{4.1.6}$$

as minimizing over the local observables K^A is obviously equivalent to do it over the ones rotated by U_A.

We then note that the skew information $\mathcal{I}(\rho, K^A)$ is contractive under completely positive and trace-preserving maps Φ_B on B, $\mathcal{I}(\rho, K_A \otimes \mathbb{I}_B) \geq \mathcal{I}\big((\mathbb{I}_A \otimes \Phi_B)\rho, K_A \otimes \mathbb{I}_B\big)$. Consequently, the LQU inherits this property. Denoting as $\tilde{K}_A$ the most certain observable for ρ, we have

$$\mathcal{U}_A^\Lambda(\rho) = \mathcal{I}(\rho, \tilde{K}_A \otimes \mathbb{I}_B) \geq \mathcal{I}\left((\mathbb{I}_A \otimes \Phi_B)\rho, \tilde{K}_A \otimes \mathbb{I}_B\right) \geq \mathcal{U}_A^\Lambda\big((\mathbb{I}_A \otimes \Phi_B)\rho\big). \tag{4.1.7}$$

Finally, we remind that for pure states $\rho = |\psi\rangle\langle\psi|$, the LQU reduces to the variance of K^A minimized over all local observables K^A. In the next Section, we present a proof (which may be of independent interest) that such a quantity decreases monotonically under local operations and classical communication (LOCC), so that the LQU, alias minimal local variance, reduces to an entanglement measure on pure states.

Proof of LOCC monotonicity of LQU for pure states

Lemma 1. *Consider a N-dimensional density matrix ρ, and the set $\{K\}$ of all observables with fixed spectrum $\Lambda = (\lambda_1, ..., \lambda_N)$. Then, the variance $Var_\rho(K) \equiv \mathcal{V}(\rho, K) = Tr[\rho K^2] - Tr[\rho K]^2$ is minimized by an observable K_0 commuting with ρ.*

Proof. Working in the eigenbasis of the density matrix, one has the representation $\rho = \text{diag}(p_1, ..., p_N)$. An observable in the considered set can then be expressed as $K = V\text{diag}(\lambda_1, ..., \lambda_N)V^\dagger$, where V is a unitary transformation. The variance of K on the state ρ reads ($V_{ij} \equiv \langle i|V|j\rangle$)

$$\begin{aligned} \mathcal{V}(\rho, K) &= \sum_{i,j} p_i \lambda_j^2 |V_{ij}|^2 - \left(\sum_{i,j} p_i \lambda_j |V_{ij}|^2 \right)^2 \equiv \text{Tr}[PB] - \text{Tr}[QB]^2 \\ P_{ij} &\equiv p_i \lambda_j^2,\ Q_{ij} \equiv p_i \lambda_j,\ B_{ij} \equiv |V_{ij}|^2. \end{aligned} \tag{4.1.8}$$

Note that B is a unistochastic matrix, and in fact, any unistochastic matrix is expressible as $B_{ij} = |V_{ij}|^2$ for some unitary V. Hence, the problem of minimizing the variance is equivalently formulated as a minimization of the right hand side of Eq. (4.1.8) over the set of unistochastic matrices. Since every unistochastic matrix is also bistochastic (but not vice versa), one has

$$\min_{\{K\}} \mathcal{V}(\rho, K) \geq \min_{B \in \mathcal{B}} \left[\text{Tr}[PB] - \text{Tr}[QB]^2 \right], \tag{4.1.9}$$

where $\mathcal{B}$ is the set of all $N \times N$ bistochastic matrices. One now exploits the Birkhoff-von Neumann theorem, and express a generic bistochastic matrix as a

convex sum of permutations of the form $B = \sum_k q_k S_k$, where the q_k's are probabilities and $\{S_k\}$ is the set of permutation matrices in dimension N, which has $N!$ elements. Then,

$$\begin{aligned}\min_{B\in\mathcal{B}}\Big[\mathrm{Tr}[PB]-\mathrm{Tr}[QB]^2\Big] &= \min_{\{q_k\}}\Big[\sum_k q_k\mathrm{Tr}[PS_k]-\Big(\sum_k q_k\mathrm{Tr}[QS_k]\Big)^2\Big]\\ &\geq \min_{\{q_k\}}\Big[\sum_k q_k\Big(\mathrm{Tr}[PS_k]-\mathrm{Tr}[QS_k]^2\Big)\Big]\\ &\geq \sum_k q_k\Big(\mathrm{Tr}[PS_{\min}]-\mathrm{Tr}[QS_{\min}]^2\Big)\\ &= \mathrm{Tr}[PS_{\min}]-\mathrm{Tr}[QS_{\min}]^2, \end{aligned} \tag{4.1.10}$$

where we have exploited the convexity of the square, and $S_{\min}$ is a particular permutation that minimises the expression $\mathrm{Tr}[PS_k]-\mathrm{Tr}[QS_k]$. Such minimizing permutation can always be found since $\{S_k\}$ is a finite set. Noting that permutations are also unistochastic matrices, the above steps imply that the equality sign in Eq. (4.1.9) can be always achieved:

$$\min_{\{K\}}\mathcal{V}(\rho,K)=\mathrm{Tr}[PS_{\min}]-\mathrm{Tr}[QS_{\min}]^2=\sum_i p_i\lambda^2_{\mathcal{P}(i)}-\left(\sum_i p_i\lambda_{\mathcal{P}(i)}\right)^2, \tag{4.1.11}$$

where $\mathcal{P}$ indicates the permutation of the indices associated to the matrix $S_{\min}$. This implies that the variance is minimized by an observable which takes the form $K_0 = \mathrm{diag}(\lambda_{\mathcal{P}(1)},...,\lambda_{\mathcal{P}(N)})$, which commutes with ρ. □

Lemma 2. *Let $d_{A,B} \equiv dim(\mathcal{H}_{A,B})$. Suppose that $d_A \leq d_B$. Under local operations on subsystem A, a globally pure state $|\psi\rangle$ evolves within a subspace $\mathcal{H}_A \otimes \tilde{\mathcal{H}}_B$, where $\tilde{\mathcal{H}}_B$ is a d_A-dimensional subspace of $\mathcal{H}_B$.*

Proof. We suppose that $|\psi\rangle$ is in Schmidt form:

$$|\psi\rangle = \sum_j^{d_A} c_i|i\rangle_A|i\rangle_B, \tag{4.1.12}$$

Clearly, $|\psi\rangle \in \mathcal{H}_A \otimes \tilde{\mathcal{H}}_B$, where $\tilde{\mathcal{H}}_B$ is spanned by the d_A orthonormal vectors $\{|i\rangle_B\}$. A local operation on A is described via Kraus operators of the form

$M^A = M_A \otimes \mathbb{I}_B$. Applying the operator on the state, one has:

$$M^A|\psi\rangle = \sum_j^{d_A} c_i (M_A|i\rangle_A)|i\rangle_B, \tag{4.1.13}$$

which is still a vector with support in $\mathcal{H}_A \otimes \tilde{\mathcal{H}}_B$. □

Corollary. *When applying operations on A to a pure state, we suppose $d_A \geq d_B$. A proof of monotonicity in this particular case will then be sufficient.*

Lemma 3. *Suppose $d_A \geq d_B$, and the (non-degenerate) spectrum of the A-observables is fixed as $\Lambda(K_A) = \{\lambda_1, ..., \lambda_{d_A}\}$. One has,*

$$\mathcal{U}_A^\Lambda(|\psi\rangle\langle\psi|) = \min_{K_B \in \mathcal{K}_B} \mathcal{I}(|\psi\rangle\langle\psi|, \mathbb{I}_A \otimes K_B), \tag{4.1.14}$$

where $\mathcal{K}_B$ is the set of B-observables whose d_B eigenvalues are non-degenerate and are a subset of $\Lambda(K_A)$: $\Lambda(K_B) = \{\mu_1, ..., \mu_{d_B} | \mu_j \in \Lambda(K_A), \mu_i \neq \mu_j (i \neq j)\}$.

Proof. We start by noting that

$$\mathcal{U}_A^\Lambda(|\psi\rangle\langle\psi|) \leq \min_{K_B \in \mathcal{K}_B} \mathcal{I}(|\psi\rangle\langle\psi|, \mathbb{I}_A \otimes K_B). \tag{4.1.15}$$

In fact, by rotating $|\psi\rangle$ to the Schmidt form, we see that the variance of any observable $K_B \in \mathcal{K}_B$ is achieved by an operator K_A on A. Given K^B such that $K^B|\psi\rangle = \sum_{ij} c_i (K_B)_{ij} |i\rangle_A |j\rangle_B$, it is sufficient to choose K^A such that $K^A|\psi\rangle = \sum_{ij} c_i (K_A)_{ij} |j\rangle_A |i\rangle_B = \sum_{ij} c_i (K_A)_{ij} |i\rangle_B |j\rangle_A$. The two operators yield the same variance, since the labels A, B do not affect its calculation. Note that it is always possible to pick K^A in the above form since the operators on A restricted to a d_B-dimensional subspace can assume the same form as any operator in $\mathcal{K}_B$.

Reminding that the skew information equals the variance for pure states, we now show that the inequality

$$\mathcal{U}_A^\Lambda(|\psi\rangle\langle\psi|) \geq \min_{K_B \in \mathcal{K}_B} \mathcal{I}(|\psi\rangle\langle\psi|, \mathbb{I}_A \otimes K_B) \tag{4.1.16}$$

is also verified, and equality must hold. The most certain observable on A has

to commute with the reduced state ρ_A (Lemma 1). Hence, if the latter has eigenvalues p_j, $j \leq d_B$, there is an appropriate permutation $\mathcal{P}$ such that:

$$\mathcal{U}_A^{\Lambda}(\psi) = \sum_{j=1}^{d_B} p_j (\lambda_{\mathcal{P}(j)})^2 - \left(\sum_{j=1}^{d_B} p_j \lambda_{\mathcal{P}(j)} \right)^2 = \mathcal{I}(|\psi\rangle\langle\psi|, \mathbb{I}_A \otimes \tilde{K}_B). \tag{4.1.17}$$

The latter equality is obtained by choosing $\tilde{K}_B$ diagonal in the same basis as ρ_B, with eigenvalues $\mu_j = \lambda_{\mathcal{P}(j)}$, and by noting that ρ_A and ρ_B have the same eigenvalues. □

Theorem. *The LQU is an entanglement monotone for pure states.*

Proof. By Lemma 2, we suppose $d_A \geq d_B$. We already have proven the invariance under local unitary transformations and contractivity under local operations on B. To complete the proof we need to show that, on average, the LQU of $|\psi\rangle$ is non-increasing under operations on A. Let $\{M_i^A\}$ be the Kraus operators on Alice: $\sum_i M_i^{A\dagger} M_i^A = \mathbb{I}$. The output ensemble is given by $\{p_i, |\phi_i\rangle\}$, where

$$\sqrt{p_i}|\phi_i\rangle = M_i^A|\psi\rangle. \tag{4.1.18}$$

We want to prove that $\sum_i p_i \mathcal{U}_A^{\Lambda}(|\phi_i\rangle\langle\phi_i|) \leq \mathcal{U}_A^{\Lambda}(|\psi\rangle\langle\psi|)$. Suppose that $K_0 \in \mathcal{K}_B$ is such that $\mathcal{U}_A^{\Lambda}(|\psi\rangle\langle\psi|) = \mathcal{I}(|\psi\rangle\langle\psi|, \mathbb{I}_A \otimes K_0)$, as given by Lemma 3. Then, by using Lemma 3 and the concavity of the variance, we have

$$\begin{aligned}
\sum_i p_i \mathcal{U}_A^{\Lambda}(|\phi_i\rangle\langle\phi_i|) &= \sum_i p_i \min_{K_i \in \mathcal{K}_B} \mathcal{I}(|\phi_i\rangle\langle\phi_i|, \mathbb{I}_A \otimes K_i) \leq \sum_i p_i \mathcal{I}(|\phi_i\rangle\langle\phi_i|, \mathbb{I}_A \otimes K_0), \\
&= \sum_i p_i \mathcal{V}(|\phi_i\rangle\langle\phi_i|, \mathbb{I}_A \otimes K_0) \leq \mathcal{V}\left(\sum_i p_i |\phi_i\rangle\langle\phi_i|, \mathbb{I}_A \otimes K_0 \right) \\
&= \sum_i p_i \langle\phi_i|\mathbb{I}_A \otimes K_0^2|\phi_i\rangle - \big(\sum_i p_i \langle\phi_i|\mathbb{I}_A \otimes K_0|\phi_i\rangle \big)^2 \\
&= \sum_i \langle\psi|M_i^A(\mathbb{I}_A \otimes K_0^2)M_i^{A\dagger}|\psi\rangle - \big(\sum_i \langle\psi|M_i^A(\mathbb{I}_A \otimes K_0)M_i^{A\dagger}|\psi\rangle \big)^2 \\
&= \langle\psi| \sum_i M_{iA}^\dagger M_{iA} \otimes K_0^2 |\psi\rangle - \big(\langle\psi| \sum_i M_{iA}^\dagger M_{iA} \otimes K_0 |\psi\rangle \big)^2 \\
&= \langle\psi|\mathbb{I}_A \otimes K_0^2|\psi\rangle - \big(\langle\psi|\mathbb{I}_A \otimes K_0|\psi\rangle \big)^2 \\
&= \mathcal{I}(|\psi\rangle\langle\psi|, \mathbb{I}_A \otimes K_0) = \mathcal{U}_A^{\Lambda}(|\psi\rangle\langle\psi|),
\end{aligned} \tag{4.1.19}$$

which proves the theorem. □

Example: LQU in the DQC1 model

We calculate LQU for the bipartition ancilla-system in the final state of the DQC1 model introduced Sec. 1.3.2 and discussed in Sec. 3.2.2. We consider the protocol in the full generality: the ancilla is quantum correlated with a n-qubit maximally mixed state. The task is to estimate the normalized trace of the $2n \times 2n$ unitary matrix U.

Remark. *The local quantum uncertainty for the output state of the DQC1 model calculated via Eq. (4.1.4), for large n and unitaries with eigenvalues uniformly distributed, yields:*

$$\mathcal{U}_A(\rho^{out}) \simeq \frac{1}{2}\left(1 - \sqrt{1-\mu^2}\right). \tag{4.1.20}$$

Proof. We choose the basis $\{|k\rangle\}$ on B which diagonalizes U: $U|k\rangle = \mathrm{e}^{-i\varphi_k}|k\rangle$. We may then rewrite the output state as $\rho^{\mathrm{out}} = 2^{-n}\sum_k \rho_k \otimes |k\rangle\langle k|$, where $\rho_k = 1/2(\mathbb{I}_A + \vec{\mu}_k \cdot \vec{\sigma})$ and $\vec{\mu}_k = \mu(\cos\varphi_k, \sin\varphi_k, 0)$. The square root of the density matrix is then expressed as $\sqrt{\rho^{\mathrm{out}}} = 2^{-n/2}\sum_k r_k \otimes |k\rangle\langle k|$, where $r_k = 2^{-1/2}(v_0\mathbb{I}_A + \vec{v}_k \cdot \vec{\sigma})$, where $\vec{v}_k = v(\cos\varphi_k, \sin\varphi_k, 0)$ and the pair v_0, v verify $v_0^2 + v^2 = 1$ and $2v_0v = \mu$. Both v_0 and $v \equiv |\vec{v}_k|$ do not depend on k, while $\vec{v}_k$ does. The elements of the matrix W_{AB} are then given by

$$\begin{aligned}(W_{AB})_{ij} &= \frac{1}{2^n}\sum_k \mathrm{Tr}[r_k\sigma_i r_k \sigma_j] \\ &= v_0^2\delta_{ij} + 2^{-(n+1)}\sum_{k,l,m}(\vec{v}_k)_l(\vec{v}_k)_m \mathrm{Tr}[\sigma_i\sigma_l\sigma_j\sigma_m].\end{aligned} \tag{4.1.21}$$

Now, we see that $\mathrm{Tr}[\sigma_i\sigma_l\sigma_j\sigma_m] = 2(\delta_{il}\delta_{jm} - \delta_{ij}\delta_{lm} + \delta_{im}\delta_{jl})$. Hence,

$$(W_{AB})_{ij} = (v_0^2 - v^2)\delta_{ij} + \frac{2}{2^n}\sum_k (\vec{v}_k)_i(\vec{v}_k)_j. \tag{4.1.22}$$

Substituting the explicit expressions for the components of $\vec{v}_k$, Eq. (4.1.22) requires evaluation of the sums $2^{-n}\sum_k \cos^2\varphi_k$, $2^{-n}\sum_k \sin^2\varphi_k$, and

$2^{-n}\sum_k \sin\varphi_k \cos\varphi_k$. We observe that for large n and unitary matrices where the phases φ_k are uniformly distributed [62], we can approximate those sums with integral averages of the trigonometric functions over the interval $\varphi \in [0, 2\pi]$: $\langle\cos^2\rangle \simeq \langle\sin^2\rangle \simeq 1/2$, $\langle\sin\cos\rangle \simeq 0$. Then,

$$W_{AB} \simeq \mathrm{diag}\{v_0^2, v_0^2, v_0^2 - v^2\} \Rightarrow \lambda_{\max}(W_{AB}) = v_0^2. \tag{4.1.23}$$

Finally, the conditions given above on v_0, v are used to express v_0 in terms of the qubit initial polarization, as $v_0^2 = 1/2(1+\sqrt{1-\mu^2})$. Substituting this in Eq. (4.1.4) yields the anticipated result of Eq. (4.1.20). As expected, the expression increases monotonically with the ancilla polarization and is independent of the number of qubits in the register. This is in agreement with what predicted by using the quantum discord in Sec. 3.2.2. □

4.2 Applications to quantum metrology

4.2.1 Classical and quantum parameter estimation

Quantum effects were long deemed as detrimental for the accuracy of a measurement, e.g. by implying uncertainty on non-commutative observables. Nowadays, we have developed methods to take *advantage* of quantumness for improving the performance of our devices. Quantum Metrology is the discipline that studies how to exploit quantum mechanics to gain accuracy in a measurement. Its range of applications is impressive (lossy optical interferometry, atomic spectroscopy, gravitometry). We refer to a recent review [140]. Here we discuss the paradigm of parameter estimation (the single parameter case) [141].

Classical parameter estimation

Let us consider a random variable X[1]. We make a set of n independent measurements of X, which give outcomes $\{x_1, x_2, \ldots x_n\}$. We want to find the prob-

[1]We treat the discrete case only, the results apply to continuous variables straightforwardly.

ability density function $f(X) \equiv f(x_1, x_2, \dots x_n) = \Pi_{i=1}^{n} f(x_i)$ underlying the outcomes we obtained. In the set of all the possible functions, we can employ a parameter φ, which is usually not measurable, as a coordinate: $f(X) \equiv f_\varphi(X)$. Therefore, the task is to estimate the value of φ. A well developed method for estimating a parameter is the maximum-likelihood estimation. The variable X takes values $x_i = x_i(\varphi)$ with probabilities $p_\varphi(x_i) \equiv p(x_i|\varphi)$. The likelihood function is defined as $l(\varphi|X) \equiv l(\varphi|x_1, x_2, \dots x_n) = f_\varphi(X)$. To clarify: the probability that the variable X has value x_i given the value φ_j of the parameter φ is equal to the likelihood of the value φ_j for φ given that X takes the value x_i. Since the parameter is not measurable, we cannot obtain $l(\varphi|X)$ and then the density function directly, but we can find an *observable* parameter $\hat{\varphi}$ such that the correspondent function $f_{\hat{\varphi}}(X)$ is a reliable characterization of the statistics of the experiment. The maximum likelihood method identifies the best estimator $\hat{\varphi}_{\text{best}}$ as the one such that $\max_{\hat{\varphi}} \ln l(\hat{\varphi}|X) = \ln l(\hat{\varphi}_{\text{best}}|X)$ (the logarithm is just a convention). This means that the function $f_{\varphi_{\text{best}}}(X)$ is the best function to describe the statistics of the outcomes. Let us suppose that any estimator is unbiased, i.e. its average value is the true value of the parameter: $\langle \hat{\varphi} \rangle_X = \varphi$. From now on, let us fix $X \equiv X_\varphi$, as the statistics of X is determined by the parameter. There is a fundamental theoretical limit to the uncertainty on the value of any estimator, that one measures with the variance $\text{Var}_{X_\varphi}(\hat{\varphi})$, determined as follows. Let us observe that one is interested to know how the likelihood function changes with the value of the parameter φ. This measures how much information on φ we can infer from the measurements of X_φ. If it does not change a lot, then the estimation is hard, while a large variation would imply that a lot of information on the parameter can be retrieved by sampling X_φ. On this purpose, the score function related to the true parameter reads: $s(\varphi) = \frac{\partial \ln l(\varphi|X_\varphi)}{\partial \varphi}$. This function has mean value zero. Consequently, for quantifying the information carried by the variable X_φ on φ, one has to study the second moment, i.e. the mean value of the square of the score, which equals its variance. The quantity

is called Fisher Information:

$$F(X_\varphi) = \mathrm{Var}_{X_\varphi}(s(\varphi)) = \sum_i p(x_i|\varphi) \left(\frac{\partial \ln p(x_i|\varphi)}{\partial \varphi} \right)^2 . \tag{4.2.1}$$

There is an important limitation to the ability of an experimenter to estimate the parameter, known as the Cramér-Rao bound [142]:

$$\mathrm{Var}_{X_\varphi}(\hat{\varphi}) \geq \frac{1}{\nu F(X_\varphi)}, \tag{4.2.2}$$

where ν denotes the number of times the estimation is repeated (i.e., the sequence of independent measurements are done). Thus, the Fisher information acts as the figure of merit of a phase estimation protocol. Note that the Cramér-Rao bound is saturated by the best estimator $\hat{\varphi}_{\mathrm{best}}$:

$$\mathrm{Var}_{X_\varphi}(\hat{\varphi}_{\mathrm{best}}) = \frac{1}{\nu F(X_\varphi)}. \tag{4.2.3}$$

Quantum phase estimation

In the quantum case, the information on the parameter is encoded in the quantum state: $\rho = \rho(\varphi) \equiv \rho_\varphi$. For example, given a (pure or mixed) bipartite state ρ used as a probe, the system undergoes a unitary transformation (specifically, a phase shift) so that the global state changes to $\rho_\varphi = U_\varphi \rho U_\varphi^\dagger$, where $U_\varphi = \mathrm{e}^{-i\varphi H}$, with H being the Hamiltonian. The goal is still to estimate the unobservable parameter φ.

Noting that $\sum_i p(x_i|\hat{\varphi}) \left(\frac{\partial \ln p(x_i|\hat{\varphi})}{\partial \hat{\varphi}} \right)^2 = 4 \sum_i \left(\left(\frac{\partial \sqrt{p(x_i|\hat{\varphi})}}{\partial \hat{\varphi}} \right)^2 \right)$, one is tempted to write a formal definition for the Fisher information in the quantum domain [132]:

$$F(\rho_\varphi) = 4\mathrm{Tr}\left[\left(\frac{\partial \sqrt{\rho_\varphi}}{\partial \varphi} \right)^2 \right] = 8\mathcal{I}(\rho_\varphi, H), \tag{4.2.4}$$

where $\frac{\partial \sqrt{\rho_\varphi}}{\partial \varphi} = -i[H, \sqrt{\rho_\varphi}]$ is exploited. However, in the quantum case, a further optimization on the measurement must be considered. Reminding the Born

rule, one has: $p(x_i|\varphi) = \mathrm{Tr}[\rho_\varphi M_i^x]$, where $\{M_i^x\}$ is a POVM. Thus, the Fisher information has to be rewritten as

$$F(\rho_\varphi) = \sum_i \frac{1}{\mathrm{Tr}[\rho_\varphi M_i^x]} \left(\mathrm{Tr}[\partial_\varphi \rho_\varphi M_i^x]\right)^2. \tag{4.2.5}$$

The quantum protocol, which has wide-reaching applications [140, 143], is optimized by picking the most informative measurement, the best estimator $\hat{\varphi}$ and the best probe state ρ. First, the Fisher information is majorized by finding the optimal POVM. It has been proven that $F(\rho_\varphi) \leq \mathrm{Tr}[\rho_\varphi L_\varphi^2]$, where L_φ is the symmetric logarithmic derivative, an operator which is defined implicitly by $2\partial_\varphi \rho_\varphi = L_\varphi \rho_\varphi + \rho_\varphi L_\varphi$ [144]. The Quantum Fisher Information (QFI) then reads [143, 145]:

$$\mathcal{F}(\rho_\varphi) = \mathrm{Tr}[\rho_\varphi L_\varphi^2], \tag{4.2.6}$$

and the quantum Cramér-Rao bound takes the form [144]:

$$\mathrm{Var}_\rho(\hat{\varphi}) \geq 1/[\nu \mathcal{F}(\rho_\varphi)]. \tag{4.2.7}$$

For any probe state ρ, the measurement of the best estimator saturates asymptotically the quantum Cramér-Rao bound. We have $\hat{\varphi}_{\mathrm{best}} = \varphi \mathbb{I} + \frac{L_\varphi}{\mathcal{F}(\rho_\varphi)}$ obtained from the optimal measurement strategy, so that

$$\mathrm{Var}_\rho(\hat{\varphi}_{\mathrm{best}}) = 1/[\nu \mathcal{F}(\rho_\varphi)]. \tag{4.2.8}$$

Finally, we focus on the optimization of the input state. In practical conditions, e.g. when the engineering of the probe states occurs within a thermal environment or with a reduced degree of control, it may not be possible to avoid some degree of mixing in the prepared probe states. It is then of fundamental and practical importance to investigate the achievable accuracy when the phase estimation is performed within specific noisy settings [146, 147]. In particular, one could ask if QC offer any advantage for the protocol.

4.2.2 QC in parameter estimation

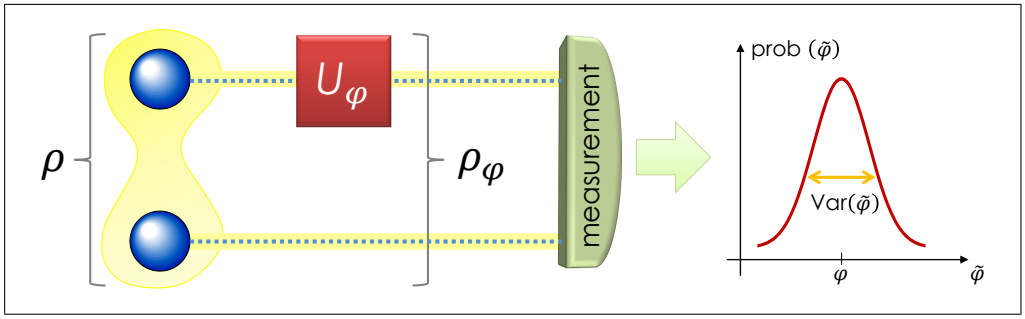

Figure 4.3: (Colours online) QC-assisted parameter estimation. A probe state ρ of a bipartite system AB is prepared, and a local unitary transformation depending on an unobservable parameter φ acts on subsystem A, transforming the global state into ρ_φ. By means of a suitable measurement at the output one construct an (unbiased) estimator $\hat{\varphi}$ for φ. The quality of the estimation strategy is benchmarked by the variance of the estimator. For a given probe state ρ, the optimal measurement at the output returns an estimator $\hat{\varphi}_{\text{best}}$ for φ with the minimum allowed variance given by the inverse of the QFI $\mathcal{F}(\rho_\varphi)$, according to the quantum Cramér-Rao bound [144]. In the prototypical case of optical phase estimation, the present scheme corresponds to a Mach-Zender interferometer. Restricting to pure inputs, research in quantum metrology [140] has shown that in this case entangled probes allow to beat the *shot noise* limit $\mathcal{F} \propto n$ (n being the input mean photon number) and reach ideally the Heisenberg scaling $\mathcal{F} \propto n^2$. However, recent investigations have revealed how in presence of realistic imperfections the achieved accuracy quickly degrades to the shot noise level [146, 147]. For mixed bipartite probes, we show that the QFI is bounded from below by the amount of QC in the probe state ρ as quantified by the LQU.

We now highlight the operative role that QC, as quantified by the LQU, plays in the paradigmatic scenario of phase estimation in quantum metrology [140]. We focus on an "interferometric" setup employing bipartite probe states, as sketched in Fig. 4.3. See also [68] for a study of multipartite QC as a resource for parameter estimation in a different setting. The unitary evolution is now $U^A = U_A \otimes \mathbb{I}_B$, so that the state changes to $\rho_\varphi = U^A_\varphi \rho U^{A\dagger}_\varphi$, where $U^A_\varphi = e^{-i\varphi H^A}$, with H^A a local Hamiltonian on A, which we assume to have a non-degenerate spectrum $\bar{\Lambda}$. We assess whether and how QC in the (generally mixed) state ρ play a role in determining the sensitivity of the estimation. Notice that the remaining steps of the estimation process are assumed to be noiseless (the unknown transformation U_φ is unitary and the output measurement is the ideal

one defined above). The key observation stems from the relation between the Wigner-Yanase and the Fisher metrics Eq. (4.2.4), which implies that the skew information of the Hamiltonian is majorized by the QFI [131, 148]. As H_A is not necessarily the most certain local observable with spectrum $\bar{\Lambda}$, the $\bar{\Lambda}$-LQU itself fixes a lower bound to the QFI:

$$\mathcal{U}_A^{\bar{\Lambda}}(\rho) \leq \mathcal{I}(\rho, H^A) = \mathcal{I}(\rho_\varphi, H^A) \leq \tfrac{1}{4}\mathcal{F}(\rho_\varphi). \tag{4.2.9}$$

Then, for probe states with any non-zero amount of QC, and for $\nu \gg 1$ repetitions of the experiment, the optimal detection strategy which asymptotically saturates the quantum Cramér-Rao bound produces an estimator $\hat{\varphi}_{\text{best}}$ with necessarily limited variance, scaling as

$$\text{Var}_\rho(\hat{\varphi}_{\text{best}}) = \frac{1}{\nu\mathcal{F}(\rho_\varphi)} \leq \frac{1}{4\nu\mathcal{U}_A^{\bar{\Lambda}}(\rho)}. \tag{4.2.10}$$

Hence, we established on rigorous footings that the QC measured by LQU, though not necessary [68, 149, 150], are a sufficient resource to ensure a fixed lower bound on the accuracy of optimal phase estimation with mixed probes.

We now provide a simple example to clarify the above discussion. Suppose system A is a spin-j particle undergoing a phase rotation $U_\varphi = \exp(-i\varphi J_z)$, where J_z is the third spin component, and φ the phase to be estimated. In this case the estimation accuracy is bounded by the so-called *Heisenberg limit* $\mathcal{F}_{\max} = 4j^2$ [140, 151]. A typical scheme achieving this limit can be outlined. Assume that system B is simply a qubit with states $|0\rangle_B, |1\rangle_B$. The AB system is initially prepared in the product state $|j\rangle_A|+\rangle_B$, where $|m\rangle_A$ are the eigenstates of J_z with eigenvalues $m = -j, -j+1, ..., j$, and $|\pm\rangle_B = \frac{1}{\sqrt{2}}(|0\rangle_B \pm |1\rangle_B)$. Then, a "control-flip" operation $\propto \exp(i\pi J_{xA}|1\rangle\langle 1|_B)$ is applied, so that the system evolves to $|\psi\rangle_{AB} = \frac{1}{\sqrt{2}}(|j\rangle_A|0\rangle_B + |{-j}\rangle_A|1\rangle_B)$. One sees that the entangled state $|\psi\rangle_{AB}$ used as a probe achieves the Heisenberg limit. This treatment allows us to study quantitatively the effect of noise on the estimation power of the bipartite state $|\psi\rangle_{AB}$. Suppose now that the probe state, ideally $|\psi\rangle_{AB}$, is prepared in a noisy

environment, which induces partial dephasing in the basis $|m\rangle_A$. Then, our probe state is given by

$$\rho_{AB} = \tfrac{1}{2}\left[|j,0\rangle\langle j,0| + |-j,1\rangle\langle -j,1| + r\left(|j,0\rangle\langle -j,1| + \text{h.c.}\right)\right], \tag{4.2.11}$$

where $0 \leq r \leq 1$ quantifies the degree of residual coherence, and $|m,\phi\rangle \equiv |m\rangle_A|\phi\rangle_B$. As this is effectively a 2-qubit state, we restrict our analysis to a truncated 2×2 Hilbert space. The restriction of J_z has the spectrum $\bar{\Lambda} = (-j, j)$. We thus calculate the $\bar{\Lambda}$-LQU in this effective 2×2 Hilbert space, obtaining $\mathcal{U}_A^{\bar{\Lambda}} = j^2(1-\sqrt{1-r^2})$. For any j, notice that the QC is a monotonically increasing function of the coherence r. Hence, from Eq. (4.2.9) one has $\mathcal{F}(\rho_{AB}^{\varphi}) \geq 4\mathcal{U}_A^{\bar{\Lambda}}(\rho_{AB}) = 4j^2(1-\sqrt{1-r^2})$. For large j, this guarantees that the classical scaling $\mathcal{F} \sim 2j$ (the so-called *shot noise limit* [140]) can still be beaten provided that $r \gtrsim 1/\sqrt{j}$.

The connection between the LQU and the sensitivity of parameter estimation can also be appreciated in more abstract geometrical terms, without the need for invoking the Fisher information. As shown by Brody [133], the skew information $\mathcal{I}(\rho_\varphi, H^A)$ of the Hamiltonian H^A determines the squared speed of evolution of the density matrix ρ under the unitary $U_\varphi^A = \mathrm{e}^{-i\varphi H^A}$. This provides another geometric interpretation for the LQU: The observable K_A which achieves the minimum in Eq. (4.1.3) is the local observable with the property that the resulting local unitary operation $\mathrm{e}^{-i\varphi K^A}$ makes the given state ρ of the whole system evolve as slowly as possible (the observable K_A is the least disturbing in this specific sense). Since a higher speed of state evolution under a change in the parameter φ means a higher sensitivity of the given probe state to the estimation of the parameter, our result can be interpreted as follows: The amount of QC (LQU) in a mixed correlated probe state ρ used for estimation of a parameter φ bounds from below the squared speed of evolution of the state under any local Hamiltonian evolution $\mathrm{e}^{-i\varphi H^A}$, and consequently the sensitivity of the given probe state ρ to a variation of φ, which is a measure of accuracy for the considered metrological task.

4.3 Other results on quantum uncertainty

4.3.1 Fine-tuned uncertainty relation for local observables

It is interesting to discuss the connections between the quantum uncertainty on a single observable and conventional Heisenberg uncertainty relations on pairs of incompatible observables [126]. Let us consider a bipartite state ρ_{AB} and let us pick a set of n local observables $\{K_j^A\}$ on A, with $j = 1, \ldots, n$. Then by definition of skew information and by using Eq. (4.1.3) we have $\prod_j \mathrm{Var}_{\rho_{AB}}(K_j^A) \geq \prod_j \mathcal{I}(\rho_{AB}, K_j^A) \geq [\mathcal{U}_A(\rho_{AB})]^n$. In the specific case of a pair of local measurements, $n = 2$, the previous inequality can be regarded as an alternative uncertainty relation, arising from the QC in the state rather than from the non-commutativity of the chosen observables. This induces a refinement of the Heisenberg principle on pairs of local observables, which is rewritten as

$$\mathrm{Var}_{\rho_{AB}}(K^A)\mathrm{Var}_{\rho_{AB}}(L^A) \geq \max\left[\frac{1}{4}\left|\left\langle [K^A, L^A]\right\rangle_{\rho_{AB}}\right|^2, \mathcal{U}_A^2(\rho_{AB})\right]. \tag{4.3.1}$$

For all the bipartite states and pairs of local observables K^A, L^A such that the amount of QC on A, measured by the LQU, is strong enough, namely $\mathcal{U}_A \geq \frac{1}{2}|\langle [K^A, L^A]\rangle|$, then such amount (squared) yields a tighter quantitative bound on the product of the variances of the chosen observables, compared to the Heisenberg one. This is the case, for instance, of pairs of local spin measurements on two-qubit Werner states (see Fig. 4.2), where the variance is one and the mean value is zero for any local observable. The right hand side of the conventional uncertainty relation would be then trivially vanishing, while the LQU is non-zero and increases with the purity of the state.

4.3.2 Quantum uncertainty and Superselection Rules

A superselection rule (SSR) can emerge not only from first principles, as it is the case for the electric charge, but also due to practical constraints: for exam-

ple, the typical energy scales involved in a quantum optics experiment imply that the number of atoms in a cavity is a supercharge, and it may only fluctuate as a result of classical ignorance. We remind the technical definition of SSR [152, 153]. A G-SSR for a quantity Q (supercharge) is defined as a law of invariance of the system with respect to a transformation group G. Given a G-SSR and a unitary representation $U(g) = e^{igQ}, g \in G$ of the group, any physical operation $\mathcal{E}_{\text{phys}}$ on a quantum system must satisfy $\mathcal{E}_{\text{phys}}(U(g)\rho U(g)^\dagger) = U(g)\mathcal{E}_{\text{phys}}(\rho)U(g)^\dagger$. This entails that there is no way to distinguish by means of a physical operation, without violating the SSR, between $U(g)\rho U(g)^\dagger$ and ρ. Thus, for finite groups, the physical quantum states are described by the density matrices $\rho_{\text{phys}} = \frac{1}{\dim G}\sum_{g\in G} U(g)\rho U(g)^\dagger$ (an equivalent definition holds for Lie groups). A physical state ρ_{phys} is either eigenstate $|q\rangle$ of Q or mixture of its eigenstates $\sum_q c_q|q\rangle\langle q|$. Any state represented by a density matrix ρ with off-diagonal entries (coherences) in the basis of the eigenstates of Q, even an entangled state, is projected by the average over the group transformations into a ρ_{phys}. Consequently, it cannot be distinguished, by allowed physical operations, from (a mixture of) such eigenstates, and cannot be exploited for quantum information tasks unless one could overcome the limitations imposed by the SSR, e.g. by accessing ancillary systems not obeying the SSR [153–155].

We then find

Remark. *In presence of a local G-SSR for a supercharge Q^A, one has $\mathcal{U}_A(\rho_{phys}) = 0$.*

This is proven by observing that a quantum G-SSR for Q are expressed by the condition $\mathcal{I}(\rho_{\text{phys}}, Q) = 0$ [154]. Focusing on one subsystem of a bipartite system, a *local* G-SSR for the supercharge $Q^A = Q_A \otimes \mathbb{I}_B$ entails the existence of a privileged local basis on A on which all the local physical observables diagonalise. Therefore, one has $\mathcal{U}_A(\rho_{\text{phys}}) = 0$. We find that a local SSR on subsystem A implies that any observable K^A, which is forced to commute with the supercharge Q^A, is quantum-certain on physical states: $\mathcal{I}(\rho_{\text{phys}}, K^A) = \mathcal{U}_A(\rho_{\text{phys}}) = 0$. The quantum uncertainty is then a signature of asymmetry, and the LQU can be read as "measure" of the local quantum symmetry of the system.

4.4 Summary of Chapter 4

- Conventional uncertainty on measurements of pairs of observables, as in the Heisenberg uncertainty principle, has been widely studied, whilst it is taken for granted that a single physical quantity can be always measured without any quantum limitation. We find that even the measurement of one observable can display truly quantum uncertainty. We study when and how quantum uncertainty manifests itself, proving a striking entwinement between two apparently unrelated quantum features as QC of states and uncertainty on observables.

- Quantum uncertainty is a measure of QC. Indeed, whenever we carry out a measurement on a subsystem of a bipartite system whose state possesses QC, quantum uncertainty is guaranteed to appear. The (minimum) quantum uncertainty on a single local measurement is itself a quantifier of QC. The exploration of this concept allowed us to define and investigate a class of measures of bipartite QC, which are physically insightful and mathematically rigorous. In particular, for qubit-qudit states a unique measure is defined (up to normalization), and it is computable in closed form. QC manifest in the fact that any single local observable displays an intrinsic quantum uncertainty.

- QC in mixed probe states, measured by the local quantum uncertainty, are further proven to guarantee a minimum accuracy in the protocol of optimal phase estimation in an interferometric setting. First, we showed that QC measured by the local quantum uncertainty are a lower bound of the uncertainty on the Hamiltonian governing the dynamics of the system, and therefore of the quantum Fisher information, which measures the accuracy of any metrological scheme for the estimation of an unknown parameter (e.g. phase in optical interferometry, which is at the heart of quantum-enhanced sensing, gravitometry, and navigation). The variance of the best estimator is, by definition, the inverse of the quantum Fisher information. Thus, it is necessary lower than the inverse of the QC. This provides a universal setting demon-

strating the resource value of those correlations, ready for immediate experimental exploitation. Currently, we are collaborating with research groups in Sao Paulo and Rio de Janeiro for implementing a related proposal in the NMR setting.

- Uncertainty due to non-commutativity of local observables is lower bounded by QC. We show that the theoretical framework delivered in the paper highlights an Heisenberg-like uncertainty relation where the product of the variances of non-commuting observables is lower bounded by the QC that the system under scrutiny shares with a second system. Also, we showed that a local superselection rule excludes QC.

Acknolewdgements

I warmly thank L. Correa for extensive comments on [DG7], and A. Balyuk, M. Ahmadi, V. P. Belavkin, D. Brody, J. Calsamiglia, F. Ciccarello, P. J. Coles, A. Datta, M. G. Genoni, V. Giovannetti, S. Girolami, M. Guta, F. Illuminati, M. S. Kim, L. Maccone, S. Pascazio, M. Piani, T. Rudolph for fruitful discussions.

CHAPTER 5

Conclusions and future developments

In this thesis, I presented and discussed the results of the research carried out during my PhD. Here I summarise my original contributions, which represented the core content of the manuscript. Then, I collect and discuss some lines of thinking about future developments in the field of QC. I have not had the time nor the ability to explore them and draw final conclusions on their relevance, but I still believe their potential implications to be worthy of future investigations.

5.1 Summary of the main results

The first part of the work has been dedicated to study the computability of QC measures in bipartite states of finite dimensional systems. In particular:

- We developed a reliable prescription to evaluate quantum discord for general two-qubit states, amending and extending an approach recently put forward for the subclass of X states. A closed expression for the discord of arbitrary states of two qubits cannot be obtained, as the optimization problem for the conditional entropy requires the solution to a pair of transcendental equations in the state parameters. Subsequently, we applied the algorithm to run a numerical comparison between quantum discord and an alternative, computable measure of QC, namely the geometric discord. We identified the most quantum-correlated two-qubit states according to the (normalized) geometric discord, at fixed value of the entropic quantum discord, and vice versa. The latter does not exceed the square root of the former for systems of two qubits **[Chapter 2]**;

- The interplay between QC and entanglement is still not completely understood. We investigated this issue focusing on computable and observable measures of such correlations: entanglement is quantified by the negativity N, while general QC are measured by the (normalized) geometric discord D_G. For two-qubit states, we found that the geometric discord reduces to the squared negativity on pure states, while the relationship $D_G \geq N^2$ holds for arbitrary mixed states. The latter result is rigorously extended to pure states of two-qudit systems for arbitrary d. The results establish an interesting hierarchy, between two relevant and experimentally friendly QC indicators. This ties in with the intuition that general QC should at least contain and in general exceed entanglement on mixed states of composite quantum systems **[Chapter 2]**;

- To overcome the asymmetry of quantum discord and the unfaithfulness of measurement-induced disturbance (severely overestimating QC), we intro-

duced the AMID (ameliorated measurement-induced disturbance) as a QC indicator, optimized over joint local measurements. We studied its analytical relation with discord, and characterized the maximally quantum-correlated mixed states, that simultaneously have extreme values of both quantifiers at given von Neumann entropy: among all two-qubit states, these ones possess the most robust QC against noise **[Chapter 2]**.

Then, we provided theoretical recipes to evaluate the QC of an unknown bipartite state in the laboratory:

- We introduced a measure Q (lower bound of geometric discord) of bipartite QC for arbitrary two-qubit states, expressed as a state-independent function of the density matrix elements. The amount of QC can be quantified experimentally by measuring the expectation value of a small set of observables on up to four copies of the state, without the need for a full tomography. We extended the measure to $2 \otimes d$ systems, providing its explicit form in terms of observables and applying it to the relevant class of multiqubit states in the DQC1 (deterministic quantum computation with one qubit) model. The number of required measurements to determine Q in our scheme does not increase with d. My results provided an experimentally friendly framework to estimate quantitatively the degree of general QC in composite systems. Then, we took in exam the specifics of the required experimental architecture in optical and nuclear magnetic resonance settings **[Chapter 3]**;

- We contributed to the experimental measurement of bipartite QC of an unknown two-qubit state. Using a liquid state Nuclear Magnetic Resonance (NMR) setup, we evaluated the QC (measured by the geometric discord and Q) of a state without resorting to prior knowledge of its density matrix. The negativity of quantumness was measured as well for reference. We also observed the phenomenon of sudden transition of QC when local phase and amplitude damping channels are applied to the state **[Chapter 3]**.

Finally, we contributed to outline the foundational stand of QC, unveiling a connection to the concept of quantum uncertainty:

- Quantum mechanics predicts that measurements of incompatible observables carry a minimum uncertainty which is independent of technical deficiencies of the measurement apparatus or incomplete knowledge of the state of the system. Nothing yet seems to prevent a single physical quantity, such as one spin component, from being measured with arbitrary accuracy. We showed that an intrinsic quantum uncertainty on a single observable is unavoidable in a number of physical situations. When revealed on local observables of a bipartite system, such uncertainty defines an entire class of *bona fide* measures of QC. For the case of $2 \otimes d$ systems, we found that a unique measure is defined, which has been evaluated in closed form. We then discussed the role that QC might play in the context of quantum metrology. In particular, the amount of discord present in a bipartite mixed probe state guarantees a minimum accuracy, as quantified by the quantum Fisher information, in the optimal phase estimation protocol **[Chapter 4]**.

5.2 Proposals for future research

5.2.1 Big Picture

We still believe QC to be an appealing research line, for two main reasons. First, they introduce a brand new quantum paradigm, a genuinely quantum statistical concept without any classical analogue. The meaning of QC in quantum information theory, and in particular their interplay with entanglement, still needs to be clarified,while they appear the most natural generalisation of quantum coherence applicable to multipartite systems [69]. Also, we may exploit them as an alternative resource for large scale implementations of quantum-based technology. Indeed, QC are easier to create and more robust than entanglement under dissipative dynamics. A number of results in literature confirmed that QC can even be created and controlled by interaction of quantum

systems with external environments, definitely harnessing noise as a performance enhancer, once that tasks in which QC are the figure of merit have been identified.

We would like to assess the potential of QC as a resource for delivering quantum technology and describing quantum effects in complex systems. The big aim is to discriminate QC-ruled processes in Nature and pave the way to build QC-based quantum devices. We would investigate open problems in quantum metrology, open quantum systems and complexity science in which we believe that QC take centre stage as benchmark of quantumness and definitely as a resource. This could lead to conceive new ways of exploiting quantum physics for delivering entanglement-free quantum technology and provide conceptual advances for the understanding of complex systems. In particular, we identify three main open questions in which QC play a critical role, as detailed in the following.

5.2.2 Quantum Metrology with mixed states

The first proposal is about quantum metrology. We have seen in Ch. 4 that QC affect the measurement process. We remind that for pure states, standard limits imposed on classical measurements have been overcome by employing quantum strategies which exploit entanglement [140], while a generalisation/no-go theorem for real world, mixed states is missing. We plan to establish the best possible accuracy we are able to reach without entanglement in such a case. We hypothesise that QC are sufficient to beat classical limits in a number of protocols: the assertion is supported by the surprising link between QC in probe states and accuracy of parameter estimation that we reported in [68] and in Ch. 4. Specifically, we would tackle two main questions:

- **Parameter estimation with noisy probes**

  Given an initial state (the probe) undergoing a unitary evolution depending on a parameter, e.g. a phase ϕ. As in Ch 4, the aim is to estimate the value of such unobservable phase with the best possible accuracy, provided a num-

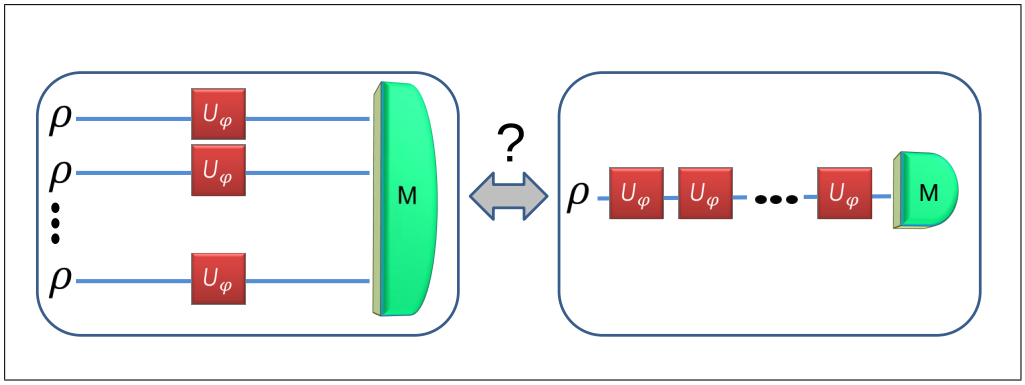

Figure 5.1: Two strategies for parameter estimation. On the left, the parallel one: N uncorrelated copies of the probe undergo a unitary evolution U_ϕ. At the end of the protocol, a measurement is performed with uncertainty $(\Delta\phi)^2_{\text{parUNC}} \sim \mathcal{O}(\frac{1}{N})$. On the right, the sequential strategy: a sequence of N unitary transformations is applied to a single probe. Every time quantum coherence is created in an appropriate basis, the measurement allows us to estimate the parameter by a smaller uncertainty $(\Delta\phi)_{\text{seq}} \sim \mathcal{O}(\frac{1}{N^2})$. For pure states, entanglement between the probes is necessary to reach the accuracy of the sequential strategy: $(\Delta\phi)^2_{\text{parENT}} \sim \mathcal{O}(\frac{1}{N^2})$[156], while a conclusive study for mixed probes is missing. We would like to determine the source of quantum enhancement when probes have fixed mixedness, and then to extend the analysis to general quantum channels.

ber n of copies of the state. The two strategies conventionally adopted, the parallel and the sequential one, are detailed in Fig. 5.1. For pure states in the parallel strategy, the best attainable classical accuracy (the shot noise limit) scales with the number of probes (copies of the state), while to exploit entangled copies allows us a scaling with the square of the number of probes. We plan to assess QC as a resource for parameter estimation when the probe states have a fixed, unavoidable degree of mixedness. A way to improve accuracy in phase estimation is by increasing uncertainty (as measured by the Wigner-Yanase information) on the generator of the evolution, the Hamiltonian H, which it is still a lower bound of the figure of merit of the protocol, the Quantum Fisher Information (QFI). In Ch. 4, we have proven that the uncertainty-based measure QC in the probe states is a lower bound of the quantum uncertainty on H [DG7] when the available resources are one probe state and an ancillary system: QC measure $\leq$ uncertainty on $H \leq$ QFI. Other pilot studies suggest that QC, and not entanglement, may be sufficient to beat

classical limits [68]. We will generalise the chain of inequalities to an arbitrary number of copies, showing that QC activate quantum enhancement, being a *monotone* lower bound of QFI. We will consider both qudits and Gaussian states of continuous variables systems as probes.

- **Parameter estimation with noisy probes and general quantum channels**
  We will extend the analysis to non-unitary evolutions, keeping fixed the mixedness of the probes. This generalisation is compelling, as the system of interest may be interacting with an environment and its dynamics would be then driven by a general quantum channel [17]. It is known that for pure states even a small amount of noise quickly degrades to the shot noise limit for the accuracy of the estimation. Nevertheless, quantum enhancement can be obtained by devising channel-dependent strategies [147, 157]. We will study the most general setting, characterized by mixed states and noisy channels. We expect to find that QC and coherence sustain quantum-enhancement for specific channels (no Hamiltonian here, we will directly prove that QC (coherence) $\leq$ QFI), thus deriving channel-dependent conditions for beating classical limits in both sequential and parallel schemes.

We expect to provide an operational interpretation of QC in the context of quantum metrology. We will adopt well developed tools from quantum estimation theory to determine the figure of merit (the QFI), for parameter estimation of both parallel and sequential strategies with probes at fixed mixedness (thus simulating a realistic condition), for unitary evolutions as well as quantum channels, for discrete and continuous variable systems. Then, we will evaluate coherence and QC by means of a multipartite extension of the bipartite uncertainty-based QC measure that we introduced in Ch. 4. We will prove that it is a monotone lower bound of the QFI, which means that QC yield a guaranteed improvement of accuracy over classical schemes. We have seen that is possible to interpret quantum uncertainty as the quantum contribution to the statistical error of a measurement (Fig 4.2). In this context, a striking relation with the variance on measurement outcomes has been provided, paving the

way to an experimental corroboration of the results in both optical and NMR systems, where high temperature regime imposes to deal with highly mixed states and vanishing entanglement.

5.2.3 Universal characterisation of quantum coherence in open quantum systems

It has been proven that QC are the cheapest signature of quantum coherence in multipartite systems. At macroscopic scales, we do not directly reveal more than what is prescribed by classical physics. This is not only due to our "classical" intuition, but also to the fragility of the quantum feature we usually investigate. Absence of entanglement does not entail classicality, whilst coherence is a non-negotiable fingerprint of quantumness, hence we should focus on the latter. Entanglement is not necessary to ensure coherence in such scenario, as we discussed in Ch. 1 and has been proven in [51]. On this hand, it is reasonable to think that both biological systems and biologically-inspired quantum devices should be optimized to catch and exploit the available quantum resources. Even small improvements in sustaining coherence time may make the difference between success and failure of a protocol. Such a situation is effectively represented by the open quantum system paradigm: the system of interest S is forced to interact with an external environment E (another physical system) (see Fig. 1.4), which, while usually destroying coherence and useful quantum properties in S, can be an additional resource by means of back-flow of information to S. A pivotal question is to develop universal efficient tools to describe the exchange of (quantum) information between system and environment [17, 158, 159]. As pointed out above, QC are the fingerprint of coherence in multipartite systems, thus are the quantum feature to investigate. Unfortunately, the dynamics of an open quantum system is notoriously difficult to model, and full information on the state of the system is rarely accessible [18]. We propose to attack the problem as follows: the information stored in the full density matrix is unnecessary to evaluate its truly quantum character. We are

only interested in the quantum properties of the system and how they evolve in time. Thus, we aim to describe open quantum system dynamics in terms of the evolution of a model-independent benchmark of QC and quantum coherence. We foresee two milestones:

- **Geometry of quantum coherence in open quantum systems**

  Any quantum process is described by a quantum channel acting on the state of the system. Information geometry allows us to represent such a channel as a curve linking two points on a statistical manifold, where the density matrices of the physical states represent coordinates on it [160]. We shall relate the dynamics of the quantumness of the system to geometric properties of the path determined by the channel. Such an approach has been adopted in [161]: singularities of the metric tensor along a path describing an adiabatic transformation correspond to quantum phase transition. Thus, to employ differential geometry techniques sounds promising: all the information carried by statistical distributions is encoded in their geometry. On the same hand, we conjecture that high order geometric tensors, as the intrinsic slope/curvature tensors of the path associated with the channel, contain *all* the relevant information about the dynamics of the interesting quantum properties (QC and coherence) of the system. We anticipate development of a general framework to describe open quantum system dynamics in terms of model-independent geometric properties of the quantum channels, corroborated by analytical and/or numerical evidences in relevant case studies (realistic noisy channels as phase and amplitude damping, and depolarising channels [17]).

- **Quantum memory effects**

  The back-flow of information from environment is not always useful. We would use the information on the geometry of the path to discriminate the *exploitable* quantum memory effects emerging in non-Markovian dynamics. There is a theoretical and experimental run to discover how to harness such effects for quantum technology [162, 163]. While there is neither a master

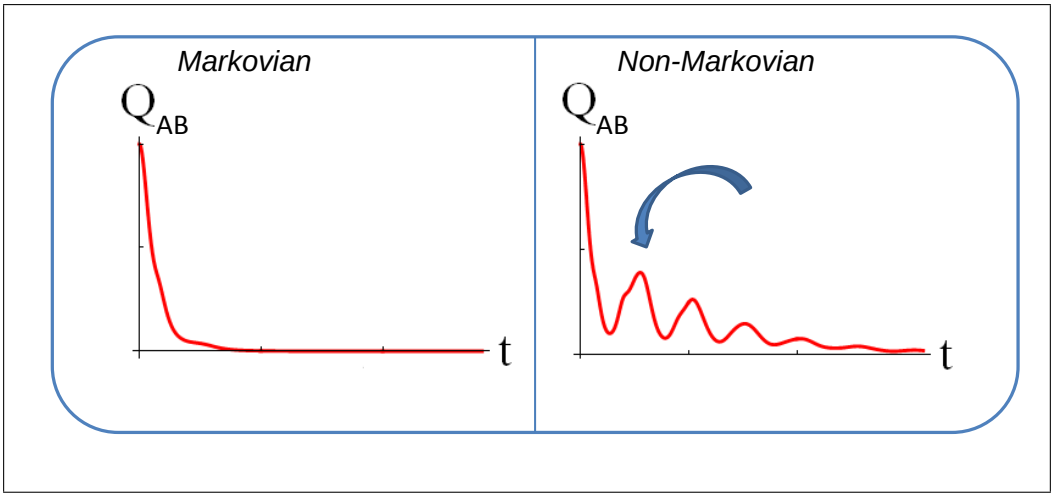

Figure 5.2: Non-Markovian processes occur whenever the environment fluctuations display correlation times longer than the relaxation time of the system under scrutiny. Revivals in time of QC (quantified by Q_{AB} as defined in Eq. (3.2.7)) *between parts of the system S* (pointed by the blue arrow), witness the non-Markovian deviations from exponential decay. The plot refers to a pilot study, in which a two-qubit system is coupled to a bosonic bath (Jaynes-Cummings model). On the left, the $S-E$ coupling is weak and no revivals are detected; on the right, the strong coupling condition is detected by QC revivals. We want to determine what geometric properties of the channel induce useful noise by favouring the revival of quantum coherence and QC.

equation nor even a general coherent fashion for describing a non-Markovian process (even how to evaluate the degree of quantum non-Markovianity of a map is still disputed) [18], theoretical and experimental studies confirmed that non-Markovianity can increase coherence time and the efficiency of energy transport in biological complexes [164, 165]. The QC have shown a peculiar behaviour under specific non-Markovian dynamics in specific model-dependent studies, but a theoretical underpinning for the phenomenon is missing. We aim to introduce a qualitative and quantitative distinction between useful and detrimental noise by observing QC dynamics in the system (see Fig. 5.2). Going beyond the plain dichotomy Markovian/non-Markovian, we expect to identify the geometric properties of the channels related to quantum memory effects. It will be then possible to devise strategies to maintain the supra-classical performance of a given quantum protocol by studying the geometry of the channel, e.g. by injecting supplemental noise with appropri-

ate geometry.

Specifically, we plan to adopt the following methodology. On a statistical manifold, density matrices are points and quantum evolutions are paths: two different points in the path are two distinguishable quantum states. This information is redundant, and a shift from a set in stone paradigm is needed. State distinguishability is the founding principle of quantum statistical inference, but two states can be distinguishable, even orthogonal, yet carry the same operational power (think about states $|0\rangle$ and $|1\rangle$). We will introduce a measure of *quantum* state distinguishability, i.e. a geometric quantifier of how much two states differ in their quantum properties. We will show that a measure of quantum distinguishability in the neighbourhood of a state corresponds to a measure of quantum uncertainty (on the generator of the evolution) and is consequently linked to the quantum character of the state. Then, we will monitor quantum memory effects by investigating the dynamics of such quantity. To extract the very quantum back-flow of information from E, detrimental noise (the noise which reduces quantum distinguishibility on the state of S) must be filtered out. Convex (thus, not entropic) Fisher information-like measures, e.g. a quantum version of the "Fisher memory matrix" introduced in [166], are ideal candidates for the purpose.

5.2.4 Assessing complexity in quantum systems

The term *Complexity* has both wide extent and content. More than a unique definition of complexity (a recent review counts forty-two measures of complexity! [167]), it is appropriate to refer to complexity signatures tailored to a specific domain of investigation: e.g. computer scientists call *computational complexity* a measure of how difficult is (how many resources/time are needed) to perform a certain calculation, and *algorithmic complexity* the length of the shortest description of a message [168]. We will address the complexity yielded by the degree of organisation of a given physical system [169]. A way to measure it is by introducing the concept of *statistical complexity* [170]: the complexity (organi-

sation) of a system is given by the amount of information on the system needed to predict its future dynamics. We hypothesise that quantum mechanical effects entails a peculiar statistical complexity which implies a supplemental degree of organisation in a system. The assertion is sustained by recent findings reported in [171]: in order to simulate a stochastic process by means of the dynamics of a physical system (e.g. a sequence of coin tosses), whenever this simulator has quantum properties and undergoes a quantum dynamics, less initial data are necessary to predict future measurement outcomes. Intuitively, this is due to the fact that a quantum state encodes more information than a classical one.
We aim to define the quantum complexity of states of multipartite systems, its main properties and the potential as a resource. Specifically: how complexity is related to the (quantum) information content of the state, how it affects (quantum) information processing, how it is linked to QC and coherence, if it is observer dependent, i.e. if it depends on the properties of a system acting as observer and/or on the observable we are measuring, how complexity behaves under decoherence and if memory effects affect it, if a system tends to evolve so as to maximize or minimize complexity and, definitely, if the complexity given by the structure of the system is *functional*, i.e. is an asset for quantum technology, as it seems to be for the efficiency of living systems. This is a promising and well motivated venture: to build quantum appliances by studying and imitating macroscopic systems granted by Nature, which may hardly be in pure entangled states yet are complex, the relation between quantumness and complexity must be clarified. We envisage two cornerstones:

- **Linking quantum correlations and complexity measures**
  In a multipartite system, interdependence between parts is expressed in terms of statistical correlations. However, to date, no results have been reported on the interplay between complexity and quantum correlations. We will introduce a measure of quantum complexity (a quantum version of statistical complexity [170]) and compare it with QC and entanglement in a number of case studies. This will establish the foundational value of complexity by

clarifying what role it takes in the quantum picture. Then, we will determine how complexity is affected by decoherence and dissipation by investigating its behaviour in the open quantum system framework. The goal is to assess the robustness of quantum-induced complexity in a realistic setting. Finally, we will devise an experimental set up to measure for the first time the quantum complexity of a system, bridging the gap between an inherent blue-skies research and the experimental necessity of having laboratory-friendly signatures or even measures of complexity.

- **Exploring the interplay between micro and macro-Complexity**
  Statistical complexity tells us about interactions in a compound system: the whole matters more than the sum of its parts [172]. We want to determine if macroscopic forms of organisations and complexity originate from microscopic interactions described by quantum mechanics (by quantum complexity and QC). We conjecture that macroscopic systems increase or decrease in complexity in order to adapt themselves to the environment. Organisation has to be a form of self-control, thus complexity is the way in which a system self-regulates and takes advantage of the interaction with other systems. The ability of a system to self-regulate and adapt to the action of external agents is quantified through an entropic inequality called Law of Requisite Variety (LRW), introduced in [173] and rediscovered in [174]. Our second conjecture is that quantum strategies have been developed by complex systems to improve their ability to adapt themselves to the environment, e.g. light-harvesting complexes have developed quantum coherence-based methods to trigger photosynthesis and discourage energy loss. We will translate the LRW in the quantum domain. We expect to find that a macro-system which exploits quantum complexity self-regulates better. More generally, we will quantify the maximum degree of control achievable by a quantum system given a fixed amount of noise and disorder (mixedness). Then, we hope to prove the advantage of quantum strategies in terms of energetic principles, hence unveiling the interplay between complexity and thermodynamics. We

wish to determine if there exists a thermodynamic limit to the amount of complexity which can be stored in a system of given dimension.

Research on quantumness and complexity will take a significant amount of time, as demands to acquire proficiency in advanced mathematical techniques and deep concepts of computational mechanics and information theory [17, 169]. First of all, we will introduce a measure of quantum complexity. There is just a loose agreement about what characteristics a complex systems should exhibit and a measure of complexity should evaluate: complexity vanishes for completely ordered (a crystal) and completely random systems (a gas in a box in thermal equilibrium) reaching its maximum at some point in the middle [169]. Information geometry will provide a common language for QC and complexity: a geometric quantifier of complexity will be derived by the (entropic) *statistical complexity* introduced in [170]. While this is a more speculative research line, we will endeavour to propose an experimentally appealing measure of complexity, being expressed as a function of observable quantities (for NMR: spins/polarizations, for optics: swap operators and projectors). A Fisher Information-inspired measure appears to fit for such requirement. Then, the quantum version of the Law of Requisite Variety, which somehow generalises the Shannon channel-correction theorem [173] to a universal condition for efficient quantum control, will be obtained by exploiting tools from *one shot quantum information theory* (OSQIT). Finally, we will study the role of quantum complexity in energy transport mechanisms of macroscopic systems (e.g. in the celebrated FMO complexes [158]), paving the way to determine universal thermodynamical constraints to the creation of QC and complexity in quantum systems (if any), which will be again addressed with OSQIT techniques.

5.2.5 Motivation

These projects seem to me timely and novel in both vision and methodology, proposing to walk unconventional lines of thinking. We will tackle well-posed, wide scope open problems, taking into account a realistic, fixed amount of

mixedness, and deem QC as a mere conceptual tool, which gives access to a privileged general framework for understanding a given issue and providing a solution. Also, *Complexity* is usually seen as a "negative" feature of physical systems, a synonym of uncontrolled sensitivity to initial conditions and an impediment to model and understand them. We dispute this common belief, and enlighten the positive, useful properties encoded in organized systems. Regarding the methods, we remark that research on QC is usually limited to model-dependent settings: a certain dynamics is selected, a restricted class of initial available states are picked, and results with little or no generality are derived. The proposal here outlined appear to be more solid. We expect to overcome technical difficulties related to quantum dynamics modelling by adopting techniques from information geometry, treating density matrices and channels as geometric entities. Differential geometry techniques will be essential to translate into a coordinate-free geometric language.

Also, the projects will deliver results of relevance for researchers in quantum metrology, open quantum system/quantum biology and complexity science. The contributions would be twofold. First, to lead to the full-fledged characterisation of quantum correlations in multipartite systems. In spite of the theoretical flavour of the project, by bridging the gap between theory and experiments will ensure a solid ground for the next generation of quantum-enhanced devices. Second, to uncover elusive connections between quantum mechanics and complexity, which will be of interest for complex system and information geometry researchers, due to the proposed lines of investigations linking quantum statistics and complexity in a coherent fashion. In conclusion, we expect that novel ways of manipulating and distributing information for metrology and communication will be devised using QC, motivated by the potential future findings of the line of research detailed in this Section. On a more speculative side, these proposals anticipate future courses of action that quantum researchers might undertake. Only 30 years ago it would have been hard to claim that quantum mechanics helps to improve communication or crypto graphic protocols. Now, we see as a strategic priority to explore new, alterna-

tive resources for quantum technology and the ultimate range of applicability of quantum mechanics. In his last work, E. Majorana argued that quantum mechanics could be the key to describe efficiently social and economic systems [175], and a celebrated Schrödinger's opera inspired the quest for a full understanding of Life mechanisms [176]. On a 10-50 years timescale, a question to address is whether *quantum* probabilistic models, where amplitudes replace probabilities, are intrinsically, universally more efficient than classical ones, and definitely if biologists, engineers, economists and social scientists should study quantum mechanics. On this hand, QC are more general, flexible quantum features than entanglement, so more appealing building blocks for such models.

References

[DG1] D. Girolami, M. Paternostro, and G. Adesso, J. of Phys. A 44, 352002, (2011) 3, 32, 40

[DG2] D. Girolami and G. Adesso, Phys. Rev. A 83, 052108, (2011) 3, 40

[DG3] D. Girolami and G. Adesso, Phys. Rev. A 84, 052110 (2011) 3, 40

[DG4] D. Girolami and G. Adesso, Phys. Rev. Lett. 108, 150403 (2012) 4, 81, 87, 95

[DG5] D. Girolami, R. Vasile, and G. Adesso, Int. J. Mod. Phys. B 27, 1345020 (2012) 4, 81

[DG6] I. Almeida-Silva, *et al.*, Phys. Rev. Lett. 110, 140501 (2013) 4, 81, 100

[DG7] D. Girolami, T. Tufarelli and G. Adesso, arXiv:1212.2214, submitted to Phys. Rev. Lett. 4, 32, 109, 133, 139

[DG8] L. Mista, R. Tatham, D. Girolami, N. Korolkova, and G. Adesso, Phys. Rev. A 83, 042325, (2011) 4, 78

[DG9] G. Adesso and D. Girolami, Int. J. Quant. Inf. 9, 1773 (2011) 4

[DG10] T. Tufarelli, D. Girolami, R. Vasile, S. Bose, and G. Adesso, Phys. Rev. A 86, 052326 (20012) 4, 52, 89

[DG11] G. Adesso, S. Ragy, and D. Girolami, Class. Quant. Grav. 29, 224002 (2012) 4

[DG12] G. Adesso, D. Girolami, and A. Serafini, Phys. Rev. Lett. 109, 190502 (2012) 5

[DG13] G. Adesso and D. Girolami, Nature Phot. - News and Views 6, 579 (2012) 5

[DG14] T. Tufarelli, T. MacLean, D. Girolami, R. Vasile, and G. Adesso, arXiv:1301.3526, submitted to J. of Phys. A 5, 32

[15] R. P. Feynman, R. B. Leighton, and M. Sands, *The Feynman lectures on physics, Vol. 3*, Addison Wesley (1971); J. J. Sakurai, *Modern Quantum Mechanics*, Addison Wesley (1993) 6

[16] J. von Neumann, *Mathematical foundations of Quantum Mechanics*, Princeton landmarks in Mathematics & Physics (1955) 6

[17] M. A. Nielsen and I. L. Chuang, *Quantum Computation and Quantum Information*, Cambridge University Press (2000) 6, 11, 15, 21, 22, 36, 39, 66, 83, 88, 97, 98, 101, 102, 140, 141, 142, 147

[18] H.-P. Breuer and F. Petruccione, *The Theory of Open Quantum Systems*, Oxford University Press (2007) 10, 84, 141, 143

[19] E. Schrödinger, Proc. Cam. Phil. Soc. 31, 555 (1935); 32, 446 (1936) 15

[20] R. Horodecki, P. Horodecki, M. Horodecki, and K. Horodecki, Rev. Mod. Phys. 81, 865 (2009) 16, 19, 23, 24, 25, 33, 39, 56, 97, 110, 112, 114

[21] A. Einstein, B. Podolsky, and N. Rosen, Phys. Rev. 47, 777 (1935); J. S. Bell, Rev. Mod. Phys. 38, 447 (1966) 16, 17, 26

[22] A. Aspect, P. Grangier, and G. Roger, Phys. Rev. Lett. 47, 460 (1981); A. Aspect, J. Dalibard, and G. Roger, Phys. Rev. Lett. 49, 1804 (1982) 17

[23] D. F. Walls and G. H. Millburn, *Quantum Optics*, Springer-Verlag (2008) 18

[24] J. F. Clauser, M. A. Horne, A. Shimony, and R. A. Holt, Phys. Rev. Lett. 23, 880 (1969) 18

[25] R. F. Werner, Phys. Rev. A 40, 4277 (1989) 19

[26] N. Brunner, D. Cavalcanti, S. Pironio, V. Scarani, and S. Wehner, arXiv:1303.2849 19, 35

[27] G. Gabrielse, D. Hanneke, T. Kinoshita, M. Nio, and B. Odom, Phys. Rev. Lett., 97, 030802 (2006), ibid. 99, 039902 (2007) 20

[28] C. E. Shannon, Bell Syst. Tech. J. 27, 379 (1948) 20

[29] A. Wehrl, Rev. Mod. Phys. 50, 221 (1978) 23

[30] C. H. Bennett, G. Brassard, C. Crépeau, R. Jozsa, A. Peres, W. K. Wootters, Phys. Rev. Lett. 70, 1895 (1993) 23

[31] V. Vedral, and M. B. Plenio, Phys. Rev. A 57, 1619 (1998) 25

[32] C. H. Bennett, D. P. DiVincenzo, J. A. Smolin, and W. K. Wootters, Phys. Rev. A 54, 3824 (1996) 25

[33] S. Kullback and R. A. Leibler, Ann. Math. Stat. 22, 79 (1951) 28

[34] V. Vedral, Rev. Mod. Phys. 74, 197 (2002) 28

[35] H. Ollivier and W. H. Zurek, Phys. Rev. Lett. 88, 017901 (2001) 29, 30, 32, 39, 52, 69, 90, 112, 116

[36] W. H. Zurek, Annal. der Phys. 9, 855 (2000) 30

[37] L. Henderson and V. Vedral, J. of Phys. A 34, 6899 (2001) 30, 32, 39, 90, 112

[38] A. Ferraro, L. Aolita, D. Cavalcanti, F. M. Cucchietti, and A. Acin, Phys. Rev. A **81**, 052318 (2010) 31, 32, 35, 57, 82, 110

[39] M. Piani, P. Horodecki, and R. Horodecki, Phys. Rev. Lett. 100, 090502 (2008) 31, 35, 50, 69, 70, 76, 77, 80

[40] B. M. Terhal, M. Horodecki, D. W. Leung, and D. P. DiVincenzo, J. Math. Phys. 43, 4286 (2002); D. P. DiVincenzo, M. Horodecki, D. Leung, J. Smolin, and B. M. Terhal, Phys. Rev. Lett. 92, 067902 (2004); A. K. Rajagopal and R. W. Rendell, Phys. Rev. A 66, 022104 (2002); S. Wu, U. V. Poulsen, and K. Mølmer, Phys. Rev. A 80, 032319 (2009); R. Rossignoli, N. Canosa, and L. Ciliberti, Phys. Rev. A 82, 052342 (2010); M. D. Lang, C. M. Caves, and A. Shaji, Int. J. Quant. Inf. 9, 1553 (2011) 32, 70, 76, 79, 90

[41] S. Luo, Phys. Rev. A 77, 022301 (2008) 69, 70, 76, 82

[42] J. Oppenheim, M. Horodecki, P. Horodecki, and R. Horodecki, Phys. Rev. Lett. 89 180402 36

[43] B. Dakić, C. Brukner, and V. Vedral, Phys. Rev. Lett. 105, 190502 (2010) 33, 37, 41, 50, 51, 52, 61, 63, 79, 84

[44] K. Modi, T. Paterek, W. Son, V. Vedral, and M. Williamson, Phys. Rev. Lett. 104, 080501 (2010) 32, 33, 36, 57

[45] K. Modi, A. Brodutch, H. Cable, T. Paterek, and V. Vedral, Rev. Mod. Phys. 84, 1655-1707 (2012) 32, 39, 41, 42, 52, 57, 112, 115, 116

[46] W. H. Zurek, Phys. Rev. A 67 012320 (2003); V. Madhok and A. Datta, Phys. Rev. A 83, 032323 (2011) 32, 35

[47] S. Yu, C. Zhang, Q. Chen, and C.H. Oh, arXiv:1112.5700 33

[48] F. Ciccarello and V. Giovannetti, Phys. Rev. A 85, 022108 (2012) 33

[49] P. Perinotti, Phys. Rev. Lett. 108, 120502 (2012) 34, 111

[50] W. H. Zurek, Rev. Mod. Phys. 75, 715 (2003) 34

[51] M. Piani, S. Gharibian, G. Adesso, J. Calsamiglia, P. Horodecki, and A. Winter, Phys. Rev. Lett. 106, 220403 (2011) 34, 36, 40, 57, 65, 84, 88, 141

[52] J. Maziero, L. C. Celeri, R. M. Serra, and V. Vedral, Phys. Rev. A 80, 044102 (2009); L. Mazzola, J. Piilo, and S. Maniscalco, Phys. Rev. Lett. 104, 200401 (2010); B. You and L.-X. Cen, Phys. Rev. A 86, 012102 (2012) 34, 52, 84, 107, 108

[53] J.-S. Xu, X.-Y. Xu, C.-F. Li, C.-J. Zhang, X.-B. Zou, and G.-C. Guo, Nat. Comm. 1, 7 (2010) 70, 80, 82

[54] R. Dillenschneider, Phys. Rev. B 78, 224413 (2008); C. A. Rodriguez-Rosario, K. Modi, A. Kuah, A. Shaji, and E. C. G. Sudarshan, J. of Phys. A 41, 205301 (2008); A. Shabani and D. A. Lidar, Phys. Rev. Lett. 102, 100402 (2009); M. S. Sarandy, Phys. Rev. A 80, 022108 (2009); T. Werlang, S. Souza, F. F. Fanchini, and C. J. Villas-Boas, Phys Rev. A 80, 024103

(2009); B. Bylicka, and D. Chruscinski, Phys. Rev. A 81, 062102 (2010); L. C. Celeri, A. G. S. Landulfo, R. M. Serra, and G. E. A. Matsas, Phys. Rev. A 81, 062130 (2010); A. Brodutch, and D. R. Terno, Phys. Rev. A 81, 062103 (2010); M. D. Lang and C. M. Caves, Phys. Rev. Lett. 105, 150501 (2010); T. Werlang, C. Trippe, G. A. P. Ribeiro, and G. Rigolin, Phys. Rev. Lett. 105, 095702 (2010); F. F. Fanchini, L. K. Castelano, and A. O. Caldeira, New J. Phys. 12, 073009 (2010); B. Wang, Z. Xu, Z. Chen, M. Feng, Phys. Rev. A 81, 014101 (2010); D. O. Soares-Pinto, L. C. Celeri, R. Auccaise, F. F. Fanchini, E. R. deAzevedo, J. Maziero, T. J. Bonagamba, and R. M. Serra, Phys. Rev. A 81, 062118 (2010); K. Bradler, M. M. Wilde, S. Vinjanampathy, and D. B. Uskov, Phys. Rev. A 82, 062310 (2010); A. Datta, arXiv:1003.5256; M. F. Cornelio, M. C. de Oliveira, and F. F. Fanchini, Phys. Rev. Lett. 107, 020502 (2011); F. F. Fanchini, M. F. Cornelio, M. C. de Oliveira, A. O. Caldeira, Phys. Rev. A 84, 012313 (2011); A. Brodutch and D. R. Terno, Phys. Rev. A 83, 010301 (2011) 34, 106

[55] R. Jozsa and N. Linden, Proc. R. Soc. Lond. A 8, 2036 (2003) 35

[56] D. Cavalcanti, L. Aolita, S. Boixo, K. Modi, M. Piani, and A. Winter, Phys. Rev. A 83, 032324 (2011) 35

[57] A. Streltsov, H. Kampermann, and D. Bruss, Phys. Rev. Lett. 106, 160401 (2011) 36, 40, 57, 88

[58] M. Gu, *et al.*, Nature Phys. 8, 671 (2012) 36

[59] B. Dakić, *et al.*, Nature Phys. 8, 666 (2012) 36

[60] A. Streltsov, H. Kampermann, and D. Bruss, Phys. Rev. Lett. 108, 250501 (2012); K. Chuan, *et al.*, Phys. Rev. Lett. 109, 070501 (2012) 36

[61] E. Knill and R. Laflamme, Phys. Rev. Lett. 81, 5672 (1998) 36, 37, 98, 115

[62] A. Datta, S. T. Flammia, and C. M. Caves, Phys. Rev. A 72, 042316 (2005); A. Datta and G. Vidal, Phys. Rev. A 75, 042310 (2007); A. Datta, A. Shaji, and C. M. Caves, Phys. Rev. Lett 100, 050502 (2008); B. P. Lanyon, M. Barbieri, M. P. Almeida, and A. G. White, Phys. Rev. Lett. 101, 200501 (2008) 36, 37, 80, 116, 123

[63] G. Passante, O. Moussa, D. A. Trottier, and R. Laflamme, Phys. Rev. A 84, 044302 (2011) 82, 89, 99

[64] G. Passante, O. Moussa, and R. Laflamme, Phys. Rev. A 85, 032325 (2012) 36, 89, 91, 99

[65] G. Adesso and A. Datta, Phys. Rev. Lett. 105, 030501 (2010); P. Giorda and M. G. A. Paris, *ibid.* 105, 020503 (2010) 36, 41, 57

[66] A. Datta, *Studies on the Role of Entanglement in Mixed-state Quantum Computation*, PhD Thesis (University of New Mexico, 2008), arXiv:0807.4490 37, 42

[67] B. Eastin, arXiv:1006.4402 38

[68] K. Modi, H. Cable, M. Williamson, and V. Vedral, Phys. Rev. X 1, 021022 (2011) 38, 127, 128, 138, 140

[69] M. Piani and G. Adesso, Phys. Rev. A 85, 040301(R) (2012) 40, 57, 88, 137

[70] M. Shi, W. Yang, F. Jiang, and J. Du, J. of Phys. A 44, 415304 (2011) 41

[71] S. Luo, Phys. Rev. A 77, 042303 (2008) 41, 42, 43, 70, 76, 77

[72] M. Ali, A. R. P. Rau, and G. Alber, Phys. Rev. A 81, 042105 (2010); see also the Erratum, Phys. Rev. A 82, 069902(E) (2010) 42, 44, 46, 70, 72, 73, 76, 77

[73] Q. Chen, C. Zhang, S. Yu, X.X. Yi, and C. H. Oh, Phys. Rev. A 84, 042313(2011) 42, 46

[74] X.-M. Lu, J. Ma, Z. Xi, and X. Wang, Phys. Rev. A 83, 012327 (2011) 41, 45

[75] T.-C. Wei, K. Nemoto, P. M. Goldbart, P. G. Kwiat, W. J. Munro, and F. Verstraete, Phys. Rev. A 67, 022110 (2003) 42, 53, 70, 71, 72, 74

[76] F. Bloch, Phys. Rev. 70, 460 (1946) 42, 99

[77] U. Fano, Rev. Mod. Phys. 29, 74 (1957) 42, 99

[78] F. Verstraete, *A study of entanglement in quantum information theory*, PhD Thesis (Katholieke Universiteit Leuven, 2002) 43, 60, 61

[79] S. Luo and S. Fu, Phys. Rev A, 82, 034302 (2010) 51, 66, 82

[80] S. Gharibian, Phys. Rev. A 86, 042106 (2012) 51, 116

[81] M. Piani, Phys. Rev. A 86, 034101 (2012) 52

[82] R. Auccaise, *et al.*, Phys. Rev. Lett. 107, 140403 (2011) 52, 84, 99, 106

[83] A. Al-Qasimi and D. F. V. James, Phys. Rev. A 83, 032101 (2011) 54, 55, 70, 71, 72, 74, 75

[84] F. Galve, G. L. Giorgi, and R. Zambrini, Phys. Rev. A 83, 012102 (2011) 55

[85] M. B. Plenio and S. Virmani, Quant. Inf. Comp. 7, 1 (2007) 56

[86] C. H. Bennett, D. P. DiVincenzo, J. A. Smolin, and W. K. Wootters, Phys. Rev. A 54, 3824 (1996) 57

[87] V. Vedral, M. B. Plenio, M. A. Rippin, and P. L. Knight, Phys. Rev. Lett. 78, 2275 (1997) 57

[88] G. Vidal and R. F. Werner, Phys. Rev. A 65, 032314 (2002) 58, 59, 60, 65, 66, 79

[89] A. Peres, Phys. Rev. Lett. 77, 1413 (1996); R. Horodecki, P. Horodecki, and M. Horodecki, Phys. Lett. A 210, 377 (1996) 58, 60, 68

[90] R. Simon, Phys. Rev. Lett. 84, 2726 (2000); R. F. Werner and M. M. Wolf, Phys. Rev. Lett. 86, 3658 (2001) 59

[91] M. Horodecki, P. Horodecki, and R. Horodecki, Phys. Rev. Lett. 80, 5239 (1998) 59

[92] K. Życzkowski, P. Horodecki, A. Sanpera, and M. Lewenstein, Phys. Rev. A 58, 883 (1998) 59

[93] V. Coffman, J. Kundu, and W. K. Wootters, Phys. Rev. A 61, 052306 (2000); Y.-C. Ou, Phys. Rev. A 75, 034305 (2007); Y.-C. Ou and H. Fan, Phys. Rev. A 75, 062308 (2007) 59

[94] R. A. Horn and C. R. Johnson, *Topics in Matrix Analysis*, Cambridge University Press (1985) 61

[95] M. M. Sinolecka, K. Życzkowski, and M. Kus, Act. Phys. Pol. B 33, 2081 (2002) 65, 67

[96] S. Luo and S. Fu, Phys. Rev. Lett. 106, 120401 (2011) 66

[97] K. Chen, S. Albeverio, and S.-M. Fei, Phys. Rev. Lett. 95, 040504 (2005) 66

[98] S. Vinjanampathy and A. R. P. Rau, J. Phys. A 45, 095303 (2012) 68, 88

[99] S. Rana and P. Parashar, arXiv:1207.5523 68

[100] G. Adesso, S. Campbell, F. Illuminati, and M. Paternostro, Phys. Rev. Lett. 104, 240501 (2010) 70, 78

[101] F. Mintert and A. Buchleitner, Phys. Rev. Lett. 98, 140505 (2007) 82, 93, 107

[102] S. P. Walborn, P. H. Souto Ribeiro, L. Davidovich, F. Mintert, and A. Buchleitner, Nature 440, 1022 (2006); F. A. Bovino, G. Castagnoli, A. Ekert, P. Horodecki, C. M. Alves, and A. V. Sergienko, Phys. Rev. Lett. 95, 240407 (2005) 82, 93, 107

[103] R. Auccaise, J. Maziero, L. Celeri, D. Soares-Pinto, E. deAzevedo, T. Bonagamba, R. Sarthour, I. Oliveira, and R. Serra, Phys. Rev. Lett. 107, 070501 (2011) 82, 99, 106

[104] A. Abragam, *The Principles of Nuclear Magnetism*, Oxford University Press, (1978); R. R. Ernst, G. Bodenhausen, A. Wokaum, *Principles of Nuclear Magnetic Resonance in One and Two Dimensions*, Oxford University Press (1987); I. S. Oliveira, T. J. Bonagamba, R. S. Sarthour, J. C. C. Freitas, and E. R. deAzevedo, *NMR Quantum Information Processing*, Elsevier (2007) 83, 97, 98, 101, 102

[105] T. Nakano, G. Adesso, and M. Piani, arXiv:1211.4022 84, 103, 106

[106] R. Lo Franco, *et al.*, in preparation 84, 107

[107] B. Aaronson, R. Lo Franco, and G. Adesso, arXiv:1304.1163 84, 106

[108] M. Abramowitz and I. A. Stegun, *Handbook of Mathematical Functions with Formulas, Graphs, and Mathematical Tables*, Dover (1964) 85

[109] J.-S. Jin, F.-Y. Zhang, C.-S. Yu, and H.-S. Song, J. Phys. A 45, 115308 (2012) 86, 92, 95, 96, 107

[110] J. P. Paz and A. Roncaglia, Phys. Rev. A 68, 052316 (2003); T. A. Brun, Quant. Inf. and Comp. 4, 401 (2004) 86, 91, 92, 93

[111] A. K. Ekert, C. M. Alves, D. K. L. Oi, M. Horodecki, P. Horodecki, and L. C. Kwek, Phys Rev. Lett. 88, 217901 (2002); R. Filip, Phys. Rev. A 65, 062320 (2002) 93

[112] M. Hendrych, M. Dusek, R. Filip, and J. Fiurasek, Phys. Lett. A 310, 95 (2003); M. S. Leifer, N. Linden, and A. Winter, Phys. Rev. A 69, 052304 (2004) 93

[113] P. Horodecki and A. K. Ekert, Phys Rev. Lett. 89, 127902 (2002); P. Horodecki, Phys. Rev. A 67, 060101(R) (2003); P. Horodecki, R. Augusiak, and M. Demianowicz, Phys. Rev. A 74, 052323 (2006); R. Augusiak, M. Demianowicz, and P. Horodecki, Phys. Rev. A 77, 030301(R) (2008) 86, 92, 93

[114] G. Passante, O. Moussa, C. A. Ryan, and R. Laflamme, Phys. Rev. Lett. 103, 250501 (2009) 89

[115] A. Barenco, *et al.*, Phys. Rev. A 52, 3457 (1995); D. P. DiVincenzo, Phys. Rev. A 51, 1015 (1995) 92, 93

[116] C. Isham, N. Linden, and S. Schreckenberg, J. Math. Phys. 35, 6360 (1994) 94

[117] C.-F. Li, private communication 97

[118] Y.-F. Huang, *et al.*, Phys. Rev A 79, 052338 (2009) 97

[119] C.-J. Zhang, Y.-X. Gong, Y.-S. Zhang, and G.-C. Guo, Phys. Rev. A 78, 042308 (2008) 97

[120] D. O. Soares-Pinto, R. Auccaise, J. Maziero, A. Gavini-Viana, R. M. Serra, and L. C. Celeri, Phil. Trans. R. Soc. A 370, 4821 (2012); J. Maziero, R. Auccaise, L. C. Celeri, D. O. Soares-Pinto, E. R. deAzevedo, T. J. Bonagamba, R. S. Sarthour, I. S. Oliveira, and R. M. Serra, Braz. J. Phys. 43, 86 (2013) 97, 99, 101, 102

[121] L. M. K. Vandersypen, S. M. G. Breyta, C. S. Yannoni, M. H. Sherwood, and I. L. Chuang, Nature 414, 883 (2001) 98

[122] P. Huang, J. Zhu, X. Qi, G. He, and G. Zeng, Quant. Info. Proc. 11, 1845 (2012) 101

[123] G. L. Long, H. Y. Yan, and Y. Sun, J. Opt. B: Quantum Semiclass. Opt. 3, 376 (2001) 103

[124] J. Teles, E. R. deAzevedo, R. Auccaise, R. S. Sarthour, I. S. Oliveira, and T. J. Bonagamba, J. Chem. Phys. 126, 154506 (2007) 103

[125] V. Giovannetti, private communication (2012) 106

[126] W. Heisenberg, Z. Phys. 43, 172 (1927) 110, 111, 130

[127] J. Oppenheim and S. Wehner, Science 330, 1072 (2010) 110

[128] M. Berta, M. Christandl, R. Colbeck, J. M. Renes, and R. Renner, Nature Phys. 6, 659-662 (2010) 111

[129] P. J. Coles, R. Colbeck, L. Yu, and M. Zwolak, Phys. Rev. Lett. 108, 210405 (2012) 110, 111

[130] E. P. Wigner and M. M. Yanase, Proc. Natl. Acad. Sci. U.S.A. 49, 910 (1963) 111, 112, 116

[131] S. Luo, Phys. Rev. Lett. 91, 180403 (2003) 111, 128

[132] S. Luo, S. Fu, and C. H. Oh, Phys. Rev. A 85, 032117 (2012) 116, 125

[133] D. C. Brody, J. Phys. A 44, 252002 (2011); P. Gibilisco and T. Isola, J. Math. Phys. 44, 3752 (2003) 129

[134] F. Hansen, Proc. Natl. Acad. Sci. U.S.A. 105, 9909 (2008) 111

[135] P. J. Coles, Phys. Rev. A 85, 042103 (2012) 114

[136] A. Monras, G. Adesso, S. M. Giampaolo, G. Gualdi, G. B. Davies, and F. Illuminati, Phys. Rev. A 84, 012301 (2011) 116

[137] S. M. Giampaolo, A. Streltsov, W. Roga, D. Bruss, and F. Illuminati, Phys. Rev. A 87, 012313 (2013) 116

[138] I. Bengtsson and K. Zyczkowski, *Geometry of quantum states: An Introduction to Quantum Entanglement*, Cambridge University Press (2006) 116

[139] S. Luo and Q. Zhang, Phys. Rev. A 69, 032106 (2004) 116

[140] V. Giovannetti, S. Lloyd, and L. Maccone, Nature Photon. 5, 222 (2011) 123, 126, 127, 128, 129, 138

[141] C. W. Helstrom, *Quantum detection and estimation theory*, Academic Press (1976); A. S. Holevo, *Probabilistic and statistical aspects of quantum theory*, North-Holland (1982) 123

[142] H. Cramér, *Mathematical Methods in Statistics*, Princeton University Press, Princeton (1946); C. R. Rao, Bull. of Calc. Math. Soc. 37, 81 (1945) 125

[143] M. G. A. Paris, Int. J. Quant. Inf. 7, 125 (2009) 126

[144] S. L. Braunstein and C. M. Caves, Phys. Rev. Lett. 72, 3439-3443 (1994) 126, 127

[145] D. Petz and C. Ghinea, arXiv:1008.2417 126

[146] U. Dorner *et al.*, Phys. Rev. Lett. 102, 040403 (2009); R. Demkowicz-Dobrzanski, J. Kolodynski, and M. Guta, Nature Commun. 3, 1063 (2012) 126, 127

[147] B. M. Escher, R. L. de Matos Filho, and L. Davidovich, Nature Phys. 7, 406 (2011) 126, 127, 140

[148] S. Luo, Proc. Amer. Math. Soc. 132, 885 (2003) 128

[149] L. Pezzé and A. and Smerzi, Phys. Rev. Lett. 102, 100401 (2009) 128

[150] S. Boixo, S. T. Flammia, C. M. Caves, and J. M. Geremia, Phys. Rev. Lett. 98, 090401 (2007) 128

[151] C. Vaneph, T. Tufarelli, and M. G. Genoni, arXiv:1211.7224v2 128

[152] G. Wick, A. S. Wightman, and E. P. Wigner, Phys. Rev. 88, 101 (1952) 131

[153] S. D. Bartlett and H. M. Wisemann, Phys. Rev. Lett. 91, 097903 (2003) 131

[154] A. S. Wightman, Il Nuovo Cimento 110 B, (1995) 131

[155] S. D. Bartlett, T. Rudolph, and R. W. Spekkens, Rev. Mod. Phys. 79, 555 (2007) 131

[156] S. Boixo and C. Heunen, Phys. Rev. Lett. 108, 120402 (2012) 139

[157] R. Chaves, J. B. Brask, M. Markiewicz, J. Kolodynski, and A. Acin, arXiv:1212.3286 140

[158] N. Lambert, Y.-N. Chen, Y.-C. Cheng, C.-M. Li, G.-Y. Chen, and F. Nori, Nature Phys. 9, 10 (2013); M. Sarovar, A. Ishizaki, G .R. Fleming, and K. B. Whaley, Nature Phys. 6, 462-467 (2010) 141, 147

[159] A. Olaya-Castro, A. Nazir, and G. R. Fleming, Phil. Trans. R. Soc. A 370, 3613 (2012) 141

[160] S.-I. Amari, O.E. Barndorff-Nielsen, R.E. Kass, S.L. Lauritzen, and C.R. Rao, *Differential geometry in statistical inference*, Lecture Notes-Monograph Series, Institute of Mathematical Statistics (1987) 142

[161] P. Zanardi, P. Giorda, and M. Cozzini, Phys. Rev. Lett. 99, 100603 (2007) 142

[162] A. W. Chin, S. F. Huelga, and M. B. Plenio, Phys. Rev. Lett. 109, 233601 (2012) 142

[163] B. Bylicka, D. Chruschinski, and S. Maniscalco, arXiv:1301.2585 142

[164] A. Ishizaki and G. R. Fleming, Proc. Nat. Acad. USA 106, 17255 (2009) 143

[165] J. Wu, *et al.*, New. J. of Phys. 12, 105012 (2010) 143

[166] S. Gangulia, D. Huhc, and H. Sompolinskyd, Proc. Nat. Acad. USA 105, 18970 (2008) 144

[167] S. Lloyd, *Measures of Complexity, a non-exhaustive list*, `http://web.mit.edu/esd.83/www/notebook/Complexity.PDF` 144

[168] A. N. Kolmogorov, Probl.Inf. Transm. 1, 3 (1965) 144

[169] R. Badii and A. Politi, *Complexity: Hierarchical Structure and Scaling in Physics*, Cambridge University Press (1997) 144, 147

[170] J. P. Crutchfield and K. Young, Phys. Rev. Lett. 63, 105 (1989) 144, 145, 147

[171] M. Gu, K. Wiesner, E. Rieper, and V. Vedral, Nature Commun. 3, 762 (2012) 145

[172] C. R. Shalizi, K. L. Shalizi, and R. Haslinger, Phys. Rev. Lett. 93, 118701 (2004) 146

[173] W. R. Ashby, *An Introduction to Cybernetics*, Chapman & Hall (1956) 146, 147

[174] H. Touchette and S. Lloyd, Phys. Rev. Lett. 84, 1156 (2000) 146

[175] E. Majorana, *E. Majorana: Scientific Papers*, edited by G.F. Bassani, Springer (2007) 149

[176] E. Schrödinger, *What is life?*, Cambridge University Press (1944) 149